Charles University in Prague

Faculty of Science

PhD. programme: Developmental and Cell Biology

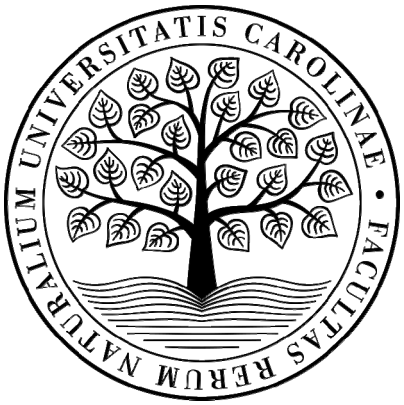

Molecular basis of clonal heterogeneity of hematological diseases

Ph.D. thesis

M.Sc. Oľga Babošová

Supervisor: Ing. Lucie Láníková, Ph.D.

Laboratory of Cell and Developmental Biology

Institute of Molecular Genetics of the ASCR

Prague 2018

Declaration

I hereby declare that this thesis is a presentation of my original research work. Wherever contributions of others are involved, every effort is made to indicate this clearly, with due reference to the literature and acknowledgement of collaborative research and discussions. This thesis contains no material that has been submitted previously, in whole or in part, for the award of any other academic degree or diploma.

Prague, 26 October 2018

Signature:

Acknowledgement

My special thanks belongs to Dr. Lucie Láníková for the opportunity to become a part of her team, for guiding and supporting me. Her excellent ideas are the cornerstones of my work. I would like to thank Dr. Vladimír Kořínek for the opportunity to be part of his team and for his great scientific input. I thank Dr. Vladimír Divoký from the Faculty of Medicine and Dentistry, Palacky University, Olomouc, for excellent cooperation and support.

The accomplishment of this thesis would not be possible without the members of our team of Laboratory of Cell and Developmental Biology at IMG and friends from the PhD programme. I am very grateful for the support from my partner Libor Riška and my family. Thank you.

Abstract

Tumor heterogeneity has been recognized for decades. The molecular mechanisms impacting clonal heterogeneity in hematological diseases, specifically myeloproliferative neoplasms (MPN) and mantle cell lymphoma, with the focus on several inherited genetic factors, inflammation, the protective mechanisms of DNA damage response (DDR) in the leukemic transformation and the treatment strategies are the focus of this thesis.

Firstly, I focus on studying germline *JAK2* variants and how these may influence the initiation and progression of MPN diseases, and even contribute to further genomic alterations in the mutated clone. A study performed by our cooperating lab in Utah, USA,[1] analyzing the mutational landscape of 31 *JAK2* V617F-positive polycythemia vera (PV) patients identified two novel germline mutations in *JAK2* gene, *JAK2* T108A and *JAK2* L393V. Another study[2], performed by our cooperating lab in Olomouc, Czech Republic, characterized two germline *JAK2* mutations, E846D and R1063H, in a case of hereditary erythrocytosis accompanied by megakaryocytic atypia. The *JAK2* R1063H variant was initially described in 3 out of 93 PV patients that were *JAK2* V617F-positive.[3] Our aim was to identify the role of selected inherited mutations in *JAK2* gene in the initiation and progression of myeloproliferative neoplasms. We show that the mutations *JAK2* T108A and L393V are weakly activating, they give rise to a kinase hypersensitive to erythropoietin, which could predispose cells carrying these mutations to proliferate at higher rate in physiological conditions. It is therefore possible that these two variants could precede the acquisition of *JAK2* V617F mutation in the course of the disease and contribute to further genomic alterations in the mutated clone and perhaps even leukemic transformation. We further characterized the double mutant *JAK2* V617F/R1063H in a cohort of MPN patients from Belgium and Romania. The two mutations are shown to cooperate to further increase JAK-STAT signaling characteristic of the single mutant JAK2 V617F. MPN patients with these two mutations present with higher amounts of white blood cells, and consequently higher amounts of neutrophils, which could be linked to increased biochemical association of the JAK2 R1063H mutant to granulocyte colony-stimulating factor receptor (G-CSFR).

Secondly, I focus on deciphering the protective role of KAP1 protein in the progression of myeloproliferative neoplasms. We hypothesize that a similar process of activating DRR

components as described in solid tumors underlines the course of MPNs and that the activation of a tumor suppressor barrier counteracts the progression to acute leukemia. In order to characterize the role of KAP1 protein in DDR of *JAK2* V617F-positive cells we generated HEL cell line (human erythroleukemia, *JAK2* V617F-positive) carrying either *JAK2* WT or *JAK2* V617F allele and consequently we knocked-out *KAP1* gene in these cells. KAP1 will further be studied in this setting, its role in cell proliferation upon induced DNA damage, differentiation and its impact on genomic instability will be characterized.

Thirdly, I focus on identifying the role of prolyl hydroxylase 1 (*EGLN2*/PHD1) and FOXO3A transcription factor in mantle cell lymphoma (MCL). It has been previously[4] reported that an inability of PHD1 to hydroxylate FOXO3A promotes its accumulation in cells, which in turn suppresses *cyclin D1* expression by a yet unknown mechanism. Cyclin D1 is overexpressed in MCL and it is therefore of interest whether iron chelation, which inhibits the function of PHD1, would be beneficial in downregulating cyclin D1 in MCL cells. It was indeed shown that iron chelation decreases cyclin D1 mRNA and protein levels in MCL cell lines[5], the molecular mechanism, however, remains unknown. Iron chelation has been previously reported to promote cyclin D1 proteasomal degradation by a ubiquitin-independent mechanism.[6] In our study we show that in MCL cell lines iron chelation is effective in inhibiting proliferation, inducing apoptosis and cell cycle arrest by means of regulating cyclin D1 levels. We also show that the overexpression of cyclin D1 in these cells makes them more susceptible to chelation treatment. We found out that cyclin D1 in MCL cells escapes PHD1 – FOXO3A regulation circuit and cyclin D1 downregulation upon iron depletion is regulated by a different yet unknown mechanism. We further studied the role of NQO1, previously shown to be involved in ubiquitin-independent proteasomal degradation, by employing NQO1 inhibitor dicoumarol to determine whether its unavailability could lead to destabilization of cyclin D1 protein in MCL cell lines. DIC-treated cells exhibited downregulation of *cyclin D1* mRNA and protein levels. It remains unclear whether the observed cyclin D1 repression is an outcome of NQO1 having a specific protective role in protein degradation or is a result of unspecific inhibition of its oxidoreductase activity.

Abstrakt

Nádorová heterogenita bola rozoznávaná už desiatky rokov. Predmetom tejto práce sú molekulárne mechanizmy ovplyvňujúce klonálnu heterogenitu hematologických ochorení, konkrétne myeloproliferatívnych neoplázií (MPN) a lymfómov z plášťových buniek so zameraním sa na niekoľko zdedených genetických faktorov, zápal, obranné mechanizmy poškodenia DNA (DDR) v procese leukemickej transformácie a liečebné stratégie.

V prvom rade sa venujem štúdiu dedičných mutácií v géne *JAK2,* ako tieto mutácie ovplyvňujú iniciáciu a progresiu MPN ochorení a ako môžu prispievať k ďalším genómovým zmenám v mutovanom klone. V štúdii, ktorú vykonalo naše spolupracujúce laboratórium v Utahu v USA[1], analyzovali mutačné rozpätie 31 pacientov s *JAK2* V617F-pozitívnym polycytémia vera ochorením. Identifikovali dve nové dedičné mutácie v géne *JAK2*, *JAK2* T108A a *JAK2* L393V. Ďalšia štúdia[2], ktorú vykonalo naše spolupracujúce laboratórium v Olomouci, charakterizovala dve zdedené mutácie *JAK2*, E846D a R1063H, v prípade dedičnej erytrocytózy sprevádzanej megakaryocytárnou atypiou. Mutácia *JAK2* R1063H bola spočiatku opísaná u 3 z 93 pacientov polycytémie vera, ktoré boli *JAK2* V617F-pozitívne.[3] Naším cieľom bolo identifikovať úlohu vybraných zdedených mutácií v géne *JAK2* pri iniciácii a progresii MPN ochorení. Ukazujeme, že mutácie *JAK2* T108A a L393V sú slabo aktivujúce, vedú k zvýšenej senzitivite na erytropoetin, ktoré môžu predurčovať bunky nesúce tieto mutácie na zvýšenie rýchlosti rastu (proliferácie) vo fyziologických podmienkach. Preto je možné, že tieto dva varianty môžu predchádzať získaniu mutácie *JAK2* V617F v priebehu ochorenia a prispievať k ďalším genómovým zmenám v mutovanom klone a prípadne aj k leukemickej transformácii. Ďalej sme charakterizovali dvojitý mutant *JAK2* V617F/R1063H v kohorte MPN pacientov z Belgicka a Rumunska. Ukázalo sa, že obe mutácie spolupracujú na zvyšovaní signalizácie JAK-STAT charakteristickej pre mutant JAK2 V617F. MPN pacienti s týmito dvoma mutáciami maju zvýšené množstvo bielych krviniek a následne zvýšené množstvo neutrofilov, čo by mohlo byť dôsledkom zvýšenej biochemickej asociácie mutantu JAK2 R1063H s receptorom faktora stimulujúceho kolónie granulocytov (G-CSFR).

V druhom rade sa sústredim na charakterizovanie ochrannej úlohy proteínu KAP1 v progresii MPN ochorení. Predpokladáme, že podobný proces aktivácie komponentov DRR, ako je opísaný v pevných nádoroch, sprevádza priebeh MPN a že aktivácia nádorovej supresorovej

bariéry pôsobí proti progresii akútnej leukémie. Na charakterizáciu úlohy proteínu KAP1 v DDR u buniek pozitívnych na *JAK2* V617F sme vytvorili HEL (ľudská erytroleukémia, *JAK2* V617F-pozitívne) bunkovú líniu nesúcu alelu *JAK2* WT a následne sme v týchto bunkách vyradili gén *KAP1*. KAP1 bude ďalej študovaný v tomto settingu, bude skúmaná jeho úloha v proliferácii buniek pri indukovanom poškodení DNA, diferenciácia a jeho vplyv na genómovú nestabilitu.

V treťom rade sa sústredím na identifikáciu úlohy prolylhydroxylázy 1 (*EGLN2*/PHD1) a transkripčného faktora FOXO3A v lymfóme z plášťových buniek (mantle cell lymphoma, MCL). Bol popisané[4], že neschopnosť PHD1 hydroxylovať FOXO3A podporuje jeho akumuláciu v bunkách, čo následne potláča expresiu cyklínu D1 ešte neznámym mechanizmom. Cyklín D1 je nadmerne exprimovaný v MCL a preto je zaujímavé, či by chelácia železa, ktorá inhibuje funkciu PHD1, bola prospešná pri downregulácii cyklínu D1 v bunkách MCL. Ukázalo sa, že chelácia železa vedie k zníženiu hladiny mRNA a proteínov cyklínu D1 v bunkových líniách MCL[5], molekulárny mechanizmus však zostáva neznámy. Chelácia železa bola predtým popísaná v proteázovej degradácii cyklínu D1 mechanizmom nezávislým od ubikvitínu.[6] V našej štúdii sme ukázali, že v bunkových líniách MCL je chelatácia železa účinná pri inhibícii proliferácie, indukcii apoptózy a zastavenia bunkového cyklu pomocou regulácie cyklínu D1. Ukazuje sa tiež, že nadmerná expresia cyklínu D1 v týchto bunkách spôsobuje, že sú náchylnejšie na chelatáciu. Zistili sme, že cyklín D1 v bunkách MCL uniká regulačnému okruhu PHD1 - FOXO3A a downregulácia cyklínu D1 pri deplecii železa je regulovaná iným neznámym mechanizmom. Ďalej sme skúmali úlohu NQO1 (o ktorom sa preukázalo, že sa podieľa na proteazomálnej degradácii nezávislej od ubikvitínu) použitím inhibítora NQO1 dicumarolu, aby sa zistilo, či jeho nedostupnosť môže viesť k destabilizácii proteínu cyklínu D1 v bunkových líniách MCL. Bunky ošetrené DIC vykazovali zníženie hladín mRNA a proteínu cyklínu D1. Nie je jasné, či sledovaná represia cyklínu D1 je výsledkom NQO1, ktorý má špecifickú ochrannú úlohu pri degradácii proteínov alebo je výsledkom nešpecifickej inhibície jeho oxidoredukčnej aktivity.

Contents

I. Theoretical Background

1 Introduction to clonal heterogeneity

Tumor heterogeneity has been observed pathologically for decades[7,8], the undergoing molecular mechanism, however, was first proposed in 1976 by Peter Nowell.[9] In order to understand the tumor's growth and increased aggressiveness observed in advanced tumors Nowell proposed a model of clonal evolution of cancer applying the Darwinian evolutionary model to tumor clonal heterogeneity. He proposed that the tumor evolution is driven by somatic cell mutations and subsequent subclonal selection.[9,10] The extent of genomic intratumor heterogeneity (ITH) is becoming apparent with the advent of next-generation sequencing studies. In a study by Johnson and colleagues[11] it was shown that the number of heterogeneous coding mutations within primary tumors or between primary tumors and recurrent sites can range between 0 to over 8,000.

Nowell's model is in line with modern cancer genomics that see the evolution of cancer as an evolution from a single cell which gains the proliferation advantage by obtaining mutations.[12] The aberrant genetic modifications accumulate and consequently differ in the subpopulations ultimately leading to the development of carcinoma.[13] This is induced by several factors which create the ideal environment for a cell to proliferate at high rate and gain more mutations predisposing it for better survival and maintained proliferation.

In the late 1990s Bonnet and Dick[14] introduced the concept of a cancer stem cell giving rise to ITH which they discovered in acute myeloid leukemia (AML). Cancer stem cell is a cell which is able to give rise to all the differentiated types of cells within the tumor and has a potential to metastasize. Such a cell possesses all the hallmarks of a normal stem cell, it has the ability to self-renew, cycle and give rise to several distinct cell types. According to the cancer stem cell model of ITH only a small proportion of cells have the capacity to form a tumor and thus give rise to heterogeneous populations found in tumor tissue. Although often the genetic and cancer stem cell models of cancer describing ITH were considered as mutually

exclusive they can be synchronized by considering the impact of genetics, epigenetics and the tumor microenvironment (TME) on the 'stemness' of tumor cells.[15]

The three facets genetics, epigenetics and the TME have a major impact on the cancer development and the tumor heterogeneity. The molecular mechanisms influencing clonal heterogeneity of selected hematological diseases will be discussed in this doctoral thesis with the focus on several inherited genetic factors, environmental factors like cell's microenvironment and inflammation, the protective mechanisms of DNA damage response (DDR) in the leukemic transformation and finally the treatment strategies based on the tumor heterogeneity.

1.1 Genetic factors

Genetic mutations in human body arise *de novo* at a certain rate, which varies among the cell types. The mutational rate is also influenced by environmental factors such as the UV light, smoking and carcinogens. Furthermore, mutations can be inherited, such as in the case of childhood leukemia[16] or acute myeloid leukemia.[17] The genetic factors affecting the initiation and progression of clonal hematopoiesis in myeloproliferative neoplasms, which have been shown to be affected both by somatic and inherited mutations, will be discussed in this thesis.

1.1.1 Myeloproliferative Neoplasms

Myeloproliferative neoplasms (MPN) are a group of hematopoietic disorders characterized by clonal division of a myeloid progenitor cell resulting in excessive production of differentiated blood cells, firstly recognized by Dameshek in the early 50's.[18], Philadelphia chromosome-negative classical MPNs are represented by polycythemia vera (PV), essential thrombocytosis (ET) and primary myelofibrosis (PMF). They are characterized by hyperplasia of at least one myeloid lineage in the bone marrow and an increased number of mature and entirely functional erythrocytes, platelets or leukocytes resulting in marrow fibrosis, respectively.[19] Chronic myeloid leukemia, also belonging to MPN group of diseases, is caused by the Philadelphia chromosome created by a translocation between chromosomes

9 and 22, which gives rise to a fusion gene called *BCR-ABL1*. This thesis focuses solemnly on Philadelphia chromosome-negative classical MPNs.

Many MPN patients (an estimate of about 50%) are asymptomatic at the time of diagnosis.[20] Besides the hematological phenotype resulting from the expansion of all myeloid blood cell types, patients with PV and ET most commonly suffer from hypertension and cardiovascular abnormalities, especially thromboses and hemorrhages.[21,22] In fact, some studies report thrombotic events as frequent as in 40 – 60% of PV patients.[23] Another common symptom PV patients report is erythromegalia, which is a burning feeling in extremities, redness and erythema of hands and feet, responding very well to low doses of aspirin.[24] PV and ET patients are in high risk of developing myelofibrosis and potentially leukemia.

Myelofibrosis is associated with poor prognosis, PMF patients have an average survival of less than 5 years.[25] Myelofibrosis arises from high rate of cell proliferation in the bone marrow accompanied by high level of inflammation. Bone marrow reaction appears to be an active process mediated by cytokines produced by megakaryocytes and monocytes, such as transforming growth factor β (TGF-β)[26,27], basic fibroblast growth factor (bFGF)[27,28], platelet-derived growth factor (PDGF)[29], and vascular endothelial growth factor (VEGF).[30] As a result, proliferation of fibroblasts and deposition of collagen gives rise to fibrosis in the bone marrow. Hematopoiesis is consequently forced to occur at other sites of the body, particularly the liver and spleen. This causes an enlargement of these organs, hepatomegaly and splenomegaly. Hematopoiesis in these organs is not sufficient to replace the bone marrow hematopoiesis contributing to thrombocytopenia and anemia, low amount of thrombocytes and erythrocytes.

Precise diagnosis of MPNs is often challenging and has been shown to occur years after the initiation of the disease (5–10–15 years).[31] MPN diseases seem not to be separate entities, but rather show a continuum where disease subtypes progress from ET to PV to MF, and eventually have a high risk of progression to an acute phase – acute myeloid leukemia.[32]

1.1.1.1 Myeloproliferative Neoplasms' background - Erythropoiesis

Hematopoiesis is the process by which all the blood cells are produced. In an adult human body hematopoiesis occurs in the bone marrow and originates from a hematopoietic stem cell (HSC). It is characterized by several commitment steps that influence cells' capacity to proliferate and differentiate.

A red blood cell, also called an erythrocyte, is produced by a process called erythropoiesis. In the bone marrow HSC differentiates into the common myeloid progenitor (CMP) and common lymphoid progenitor (CLP) giving rise to the myeloid and lymphoid lineage. CMP then differentiates into a common progenitor for erythrocytes and megakaryocytes the megakaryocyte–erythroid progenitor cell (MEP). The first committed erythroid progenitors are burst forming unit-erythroid (BFU-E) and colony forming unit-erythroid (CFU-E).[33] CFU-E differentiates into the first identifiable cell of erythroid lineage the pro-erythroblast, which then gives rise to the basophilic erythroblast, polychromatophilic erythroblast and the acidophilic erythroblast. Acidophilic erythroblast is the last nucleated cell of the erythrocytosis pathway. Its enucleation gives rise to the reticulocyte which then matures into erythrocyte. Erythropoiesis takes place in the bone marrow in so-called erythroblastic blood islands, in which a macrophage surrounds cells of all the different stages of maturation. Macrophage provides cells the needed microenvironment regulating their differentiation and proliferation.[34,35]

Erythropoiesis is a highly dynamic process with an estimated production of $2x10^{11}$ of erythrocytes daily.[36] The most immature erythroid progenitors BFU-Es, however, represent only about 0.03% of bone marrow hematopoietic cells and only about 40% of those are cycling. CFU-Es on the other hand represent about 0.3% of hematopoietic cells in the bone marrow and most of them are cycling.[37,38] Pro-erythroblasts and erythroblasts have high proliferative index giving rise to quantitatively the largest blood cell population. The cell cycle of pro-erythroblasts is estimated to be around 6 – 7 hours, which is unique in an adult human body.[39] These processes are tightly transcriptionally and environmentally regulated.

1.1.1.2 Myeloproliferative Neoplasms' background - Regulation of erythropoiesis

Blood is one of the most highly regenerative tissues in the human body with about a trillion (10^{12}) cells being produced daily.[40] This production needs to be tightly regulated in order to prevent disease formation. Erythropoiesis is regulated by the microenvironment and growth factors that control the cell survival, proliferation and differentiation of the progenitors. While for the early stages of erythropoiesis various growth factors are important, such as the stem cell factor (SCF), interleukin-3 (IL-3), thrombopoietin (TPO) and granulocyte-colony stimulating factor (G-CSF), from CFU-E stages erythropoietin (EPO) becomes the primary molecule controlling the erythrocyte production.

Erythropoietin acts by stimulating the erythropoietin receptor (EPOR). EPOR belongs to type I cytokine receptors, it has a single transmembrane domain and lacks the kinase domain.[41] EPOR is expressed from the early stages of BFU-Es, it, however, becomes crucial for survival only from the CFU-E stages.[42] In the cell EPOR is believed to exist in an unliganded dimeric state. Upon EPO binding it undergoes conformational change which brings the pre-bound Janus kinase 2 (JAK2) proteins to closer proximity allowing their cross-phosphorylation and activation. JAK2 in turn phosphorylates several cytoplasmic tyrosine residues of EPOR which serve as docking sites for Src homology 2 (SH2) domain-containing signaling proteins like signal transducer and activator of transcription 5 (STAT5), p85a regulatory subunit of PI 3-kinase (PI3K), growth factor receptor-bound protein 2 (GRB2), Src homology region 2 domain-containing phosphatase-1 and -2 (SHP-1, SHP-2) and suppressor of cytokine signaling (SOCS).[43] As a result signaling pathways important for erythroid proliferation, survival and differentiation are activated, JAK2/STAT5 signaling, a mitogen-activated protein kinase (MAPK) pathway and PI3K/protein kinase B (PKB/AKT) pathway. SHP-1 and SOCS, on the other hand, serve as negative regulators of EPOR activated signaling by either dephosphorylating JAK2 protein as such (SHP-1) or by inducing its degradation (SOCS; Figure 1).[44]

Transcription factors GATA-1 (GATA-binding factor 1) and KLF-1 (erythroid Krüppel-like factor 1) are lineage specific transcription factors crucial for activating many erythroid specific genes and for normal erythropoiesis. They control the transcription of genes encoding

for globin protein chains, heme biosynthesis, erythroid specific membrane proteins, and also coordinate the proliferation and anti-apoptotic pathways.[45–48]

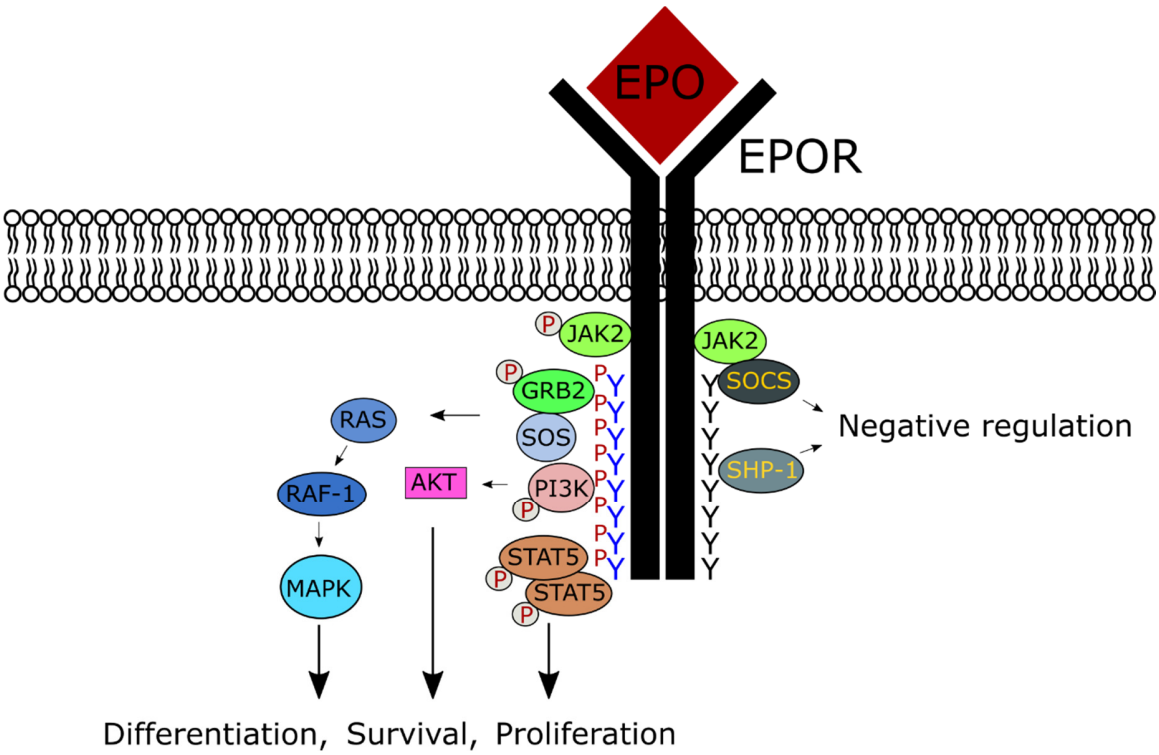

Figure 1. EPO activated EPOR signaling. Upon EPO binding the EPOR receptor becomes transphosphorylated by the pre-bound JAK2 kinase on 8 tyrosine (Y) residues. As a result adaptor proteins GRB2, PI3K, STAT5, and others get phosphorylated and activate the downstream signaling of PI3K/AKT pathway, JAK/STAT signaling and the MAPK pathway. Negative regulators, such as SOCS family of negative regulators of cytokine signaling and SHP-1, are transcriptional targets of EPOR signaling creating a negative feedback loop to inhibit the activation of JAK2. SHP-1 interacts with certain phosphorylated tyrosine residues and dephosphorylates the receptor as such (a simplified version adapted from ESH Handbook on Disorders of Iron Metabolism (2009)).[49]

1.1.2 Genetic background of Myeloproliferative Neoplasms

In general, MPN diseases arise from a single somatically mutated HSC that expands clonally and gives rise to all myeloid lineage cells. The expansion of the mutated clone is usually

accompanied by hyperplasia of a single lineage giving rise to phenotypically distinct manifestations of the disease. The progenitor cell is driven to proliferate at high rate by the so-called 'driver mutation' in genes important for normal myeloproliferation.

The identified activating driver mutations described in MPNs occur in three genes directly involved in clonal myeloproliferation: Janus Kinase 2 (*JAK2*), thrombopoietin receptor (*MPL/*TPOR) and calreticulin (*CALR*).[19,50] In addition to the driver mutations, loss-of-function or neomorph mutations in genes that code for epigenetic regulators and are shared with myelodysplastic syndromes (MDSs) and acute myeloid leukemia (AML) can act as disease modifiers in MPNs.[51] Besides somatic mutations other factors, such as germ line variants, can modulate the risk of MPN development, favor the acquisition of somatic mutations and influence the clinical course of the disease. Furthermore, several germ-line mutations have been described in hereditary erythrocytosis and hereditary thrombocytosis, benign conditions represented by polyclonal hematopoiesis that, clinically, can mimic MPNs and pose a difficulty in diagnosis and therapeutic management.[52]

The most frequently occurring acquired gain-of-function *JAK2* V617F mutation gives rise to a constitutively active JAK2 kinase driving the JAK/STAT signaling that leads to excessive proliferation and survival of myeloid progenitor cells. Since the JAK2 V617F mutation has been described, more JAK2 mutations contributing to MPN phenotype are being discovered (described in detail below, chapter 1.1.3).[3,53]

Activating mutations in myeloproliferative leukemia virus gene (*MPL),* a gene encoding for thrombopoietin (TPO) receptor (TPOR), can be either germline, such as in rare cases of familial essential thrombocytosis (*MPL* S505N)[54], or somatic. Surprisingly, *MPL* S505N mutation has also been reported to be acquired in some rare cases of ET.[55] The most frequent somatic mutation in *MPL* is a mutation of the tryptophan residue at the position 515 (*MPL* W515).[56,57] The mechanism these mutations alter TPOR signaling is modifying the geometry of the TPOR dimers thus leading to transphosphorylation of the pre-bound JAK2 proteins. A result is constitutively active JAK2/STAT signaling initiated through TPOR.[58,59]

Calreticulin is a multifunctional protein. It plays a role in calcium homeostasis as it binds calcium ions rendering them inactive. Calreticulin also serves as a chaperone in endoplasmic

reticulum. The last four amino acids of calreticulin contain the endoplasmic reticulum–retention signal, KDEL. This signal is absent in all the mutated forms of calreticulin subsequently altering its subcellular localization.[60] The role of mutated calreticulin gene (*CALR*) in the pathogenesis of MPN was proposed by Stefan Constantinescu.[19] It was suggested that it participates in folding the TPOR/*MPL* in the endoplasmic reticulum and when mutated it remains attached to the TPOR, and is transferred to the plasma membrane together with the receptor, leading to its activation and downstream signaling. A result is the activation of JAK/STAT signal downstream of TPOR, similar to *MPL* mutations.[19,61,62]

Additionally, mutations in granulocyte-colony stimulating factor (G-CSF) receptor (*GSF3R*) gene have also been reported. These are associated with familial neutrophilia[63] and with sporadic chronic neutrophilic leukemia (CNL)[64] and also result in constitutive phosphorylation of JAK2 kinase and activation of its downstream signaling.

It has been proposed that about 95-98% of PV patients carry a mutation in *JAK2* gene, the occurrence in ET patients is about 60% and in PMF patients about 58%.[65] Somatic mutation *MPL* W515 occurs in 3 – 8% of patients with ET and PMF. Mutations in *CALR* occur in 20 – 35% patients with ET and PMF.[50] Noticeably, the activation of TPOR leads to a phenotype of ET and PMF, not the PV phenotype. There are also MPN patients who do not carry any of the aforementioned mutations, so-called 'triple negative' MPN patients.

Triple negative patients either carry a mutation that is yet unknown and remains to be elucidated, or are influenced by another factor affecting their hematopoietic stem cell progenitors. In fact, it has been shown that acquiring a somatic driver mutation is rather a late event in the disease process and other factors, such as chronic inflammation, can predispose patients' cells to MPN transmission.[66–68] Additionally, polymorphisms in genes involved in DNA damage response and in JAK/STAT pathway may increase the risk of MPN development. This includes the polymorphisms in *JAK2* gene known as the JAK2 46/1 haplotype. 46/1 haplotype was discovered by a genome-wide association study, and is a 280 Kb-long region of chromosome 9p that includes three genes in their entity: *JAK2* gene, insulin like 4 (*INSL4*) and insulin like 6 (*INSL6*). Surprisingly, *INSL4* and *INSL6* genes are not expressed in hemopoietic cells. There seems to be strong association between the 46/1

haplotype and the occurrence of *JAK2* V617F mutation, however, the precise mechanism remains to be elucidated.[19,69–71]

There are other acquired mutations often reported in MPN patients. These are not restricted to MPNs and frequently occur in MDSs and AML. They do not directly drive the clonal proliferation, nevertheless, they influence the course and progression of the disease and thus contribute to heterogeneity of MPNs. Among the most frequently reported ones are mutations in epigenetic regulators, splicing factors, and transcription factors, such as the tumor protein 53 (*TP53*). Out of these the most frequently mutated are epigenetic regulators TET methylcytosine dioxygenase 2 (*TET2*) and DNA (cytosine-5)-methyltransferase 3A (*DNMT3A*). Mutations in epigenetic regulators enhancer of zeste homolog 2 (*EZH2*), additional sex combs like 1 (*ASXL1*), and a splicing factor, arginine/serine-rich 2 (*SRSF2*) are associated with poor prognosis and risk of AML transformation.[19]

1.1.3 JAK2 gene

As described above, all the driver mutations in the three described genes lead to hyperactivation of JAK2 signaling. JAK2 therefore appears to be the main driving force in the pathogenesis of MPN passing the signaling from all three receptors involved in the MPN pathogenesis, EPOR, TPOR and G-CSFR.

JAK2 gene encodes for a tyrosine kinase Janus kinase 2 (JAK2) responsible for mediating a signal from hematopoietic cytokines and hormones, such as erythropoietin (EPO), thrombopoietin (TPO), granulocyte-colony stimulating factor (G-CSF), interferon-γ (IFN-γ), a growth hormone and several interleukins. It was first discovered in a large PCR-based screen of tyrosine kinases together with JAK1[72], when they were named ‘Just another kinases’, or JAK kinases. They were later given name JAnus Kinase (JAK) which refers to Roman god Janus, who is a two-faced gate keeper of heaven, as JAKs have two homologous kinase-like domains in tandem. JAK family of kinases include JAK1, JAK2, JAK3 and TYK2.[44,73–75]

JAK2 has seven regions of sequence similarities shared with other members of the JAK family of proteins, these are called the JAK homology domains (JH domains). It lacks the scr homology domains (SH domains), however, it was shown that the JH4 domain bears a remarkable similarity to the core element of the SH2 domain. The N terminus contains an N-terminal Band 4.1, ezrin, radixin, moesin (FERM) domain important for the association with the receptor and the relief of the inhibitory conformation of kinase domain which leads to JAK2 activation.[76,77] JH1 and JH2 domains are homologous kinase-like domains. JH1 is kinetically active, while the JH2 is not, it is therefore referred to as a 'pseudokinase' domain. This domain was thought not to have a kinase activity, however, as shown by Ungureanu and colleagues it is kinetically active as it phosphorylates two negative regulatory sites in JAK2, Ser523 and Tyr570.[78] Silvennoinen and Hubbard[79] proposed a model which predicts that in the absence of ligand the cytokine receptor is kept in an inactive state by a tight interaction of JH1 and JH2 domain. This inactive state is in equilibrium with partially active state, in which the JH1 domain is released and is in closer proximity to the JH1 domain of the second JAK2 thus enabling its transphosphorylation (Figure 2).

Interestingly, the most frequently occurring driver mutation in MPN the *JAK2* V617F mutation was first described independently by three research groups in 2005.[53,80,81] *JAK2* V617F mutation is a point mutation (c.1849G>T) that causes a single amino-acid change from valine to phenylalanine in the JH2 domain of the JAK2 protein. The precise mechanism of action of *JAK2* V617F mutation is not known, although it is currently believed that specific regions of the pseudokinase domain negatively regulate the activity of the JH1 or kinase domain. This is supported by the fact that pseudokinase domain can phosphorylate two negative regulatory sites in JAK2, Ser523 and Tyr570.[78] In the model proposed by Silvennoinen and Hubbard, JAK2 V617F favors the partially active kinase state leading to a shift in the equilibrium resulting in active JAK2.[79] Concurrently, disrupting the adenosine triphosphate (ATP) binding site in the pseudokinase domain had only little effect on the kinase activity of wild-type (WT) JAK2, but the same disruption had a major effect on JAK2 V617F activity.[82] One amino acid, F595, in the pseudokinase domain was shown to be important in the JAK V617F pathogenesis but is dispensable for the activity of JAK2 WT.[83] Furthermore, FERM domain was also shown to play a role in regulating the JAK2 V617F signaling by lowering the *Km* of the kinase domain towards substrates.[76] Additionally, JAK2

V617F may allow for escape of the negative regulation of signaling by SOCS3.[84] Active JAK2 in turn activates the downstream signaling (Figure 1), giving the hematopoietic cell with this mutation a clonal advantage.

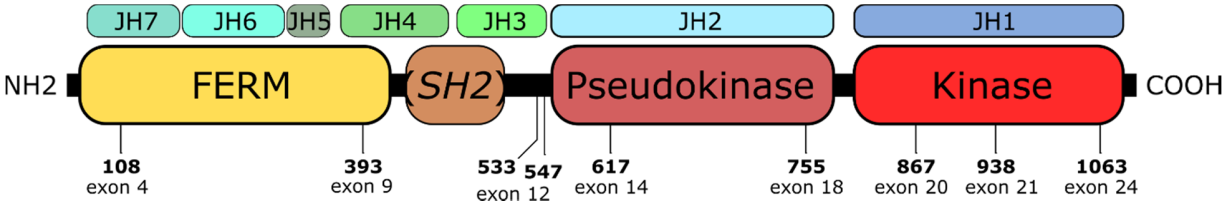

Figure 2. Graphical structure of JAK2 kinase protein. JAK2 protein contains 7 JH domains JH1 – JH7. JH1 domain has kinase activity, JH2 domain is also called a pseudokinase domain. Other parts of the protein are also the FERM and SH2-like domains. Depicted are numbers of amino acids (and the corresponding exons) frequently substituted/mutated and associated with MPN pathogenesis.

Since the *JAK2* V617F mutation has been described, more *JAK2* mutations contributing to MPN phenotype are being discovered. Exon 12 of the *JAK2* gene is frequently (about 1 – 2% of patients with PV) mutated in patients that are *JAK2* V617F negative. These mutations lead to PV phenotype and include non-synonymous substitutions, deletions and duplications, all affecting a region adjacent to the pseudokinase domain located between F533 and F547.[85,86] Other germline mutations were identified both in the pseudokinase (V617I, R564Q S755R) and in the kinase (R867Q, R938Q) domain[87–89] giving rise to thrombocytosis phenotype. In some cases, the germline *JAK2* mutations were found to co-exist with *JAK2* V617F, further enhancing its signaling and likely predisposing the progenitor cells for the acquisition of *JAK2* V617F.[90] Recently, two germline *JAK2* mutations, E846D and R1063H, were described in a case of hereditary erythrocytosis accompanied by megakaryocytic atypia[2], R1063H being initially described in 3 out of 93 polycythemia vera patients that were positive for *JAK2* V617F.[3]

More non-canonical roles have been discover for JAK2 which may be affected by the mutations. JAK2 localizes in the nucleus where it phosphorylates tyrosine 41 on histone H3, which has been implicated in leukemogenesis.[91] The expression of *JAK2* V617F *in vitro* has

also been associated with the activation of DNA repair mechanisms of homologous recombination and aneuploidy.[92] Furthermore, there is an evidence that *JAK2* V617F can increase the production of reactive oxygen species, promote the G1/S transition[93] and is involved in regulating DNA damage response (DDR) mechanisms (described below, see chapter 1.3).

Seeing as the *JAK2* V617F mutation can drive the pathogenesis of all three classical MPNs, a question arises of how the progression of the disease differs in people with the same mutation. A correlation between the level of expression and the phenotype has been found: low expression being associated with an ET-like phenotype and higher expression (70% of *JAK2* V617F or more) with a PV-like phenotype.[19] This is supported by the fact that *JAK2* exon 12 mutations exclusively lead to PV phenotype and have been shown to activate STAT5 to a greater extend.[94] Secondly, uniparental disomy (UPD) of chromosome 9 giving rise to *JAK2* V617F homozygosity is associated with polycythemia and only rarely with thrombocytopenia.[95,96] This theory is also supported in knock-in mouse models, in which the ratio of mutant to WT *JAK2* correlates with the degree of erythrocytosis.[97,98] On the top of this, ET patients that show greater *JAK2* V617F allele burdens are associated with a higher degree of erythrocytosis and leukocytosis.[99]

Although rare, there are, however, still cases when *JAK2* V617F homozygosity occurs in subclones of ET patients and on the other hand PV patients with very low JAK V617F allele burden.[100] These findings suggest that other factors contribute to the pathogenesis of MPNs. *JAK2* V617F associates with all three receptors involved in the pathogenesis of MPNs, EPOR, TPOR and G-CSFR. In cases of familial MPNs exhibiting hereditary thrombocytosis and triple-negative MPNs it is proposed that the inherited *JAK2* mutations signal through the TPOR rather than EPOR.[88,89] Differential signaling of STATs might induce differential clinical phenotype; thrombocytosis being induced by TPOR/STAT1 signaling and erythrocytosis by EPOR/STAT5.[19,89,101,102] Furthermore, the acquisition of somatic mutations in disease modifiers also influence the course of the disease. Interestingly, even the order of the mutation acquisition matters.[103] Finally, the fact that the clonal architecture, microenvironment and the mutational profile changes in a given patient over time resulting in different phenotypes supports the idea that MPNs are not distinct biological entities but

rather a continuum in which ET transforms to PV, or chronic phase disease to accelerated phase to acute leukemia.[86]

Mutations in *JAK2* have been found to occur in all the cells of the hematopoietic tree starting from the HSC population including not only myeloid but also lymphoid lineage.[104] Several studies point to the fact that *JAK2* V617F does not provide the HSCs population a proliferation advantage.[105–108] Patient JAK2-mutant xenografts in immunodeficient animal models suggest that *JAK2* mutations do not result in self-renewal advantage. Instead, rather than enhanced self-renewal *JAK2* V617F-positive cells expand at the progenitor level. These observations suggest that *JAK2* V617F mutation alone is not sufficient to initiate MPN diseases and that additional factors are required.[97,109] This is consistent with fact that *JAK2* V617F mutations occurs in normal population, too.[110,111] An alternative plausible explanation would be that the expansion of the progenitor pool, rather than the stem cell pool, driven by the *JAK2* mutations is sufficient to induce the pathogenesis of MPNs. This theory is supported by recent studies researching the native clonal hematopoiesis showing that a pool of long-term multipotent progenitors are the main drivers of adult hematopoiesis.[112]

1.2 Inflammation

Inflammation has been recognized as one of the hallmarks of cancer.[113] Indeed it has been demonstrated that it drives the progression of various types of tumors. The fact that chronic inflammation accompanies MPN and that the reduction of inflammatory symptoms is beneficial for patients has been recognized for a while.[114] It has only recently been proposed, though, that inflammation might actually precede and initiate the disease. The selective pressure of chronic inflammation on the normal HSCs might define the selective advantage of mutant clones to the expense of normal cells. Inflammation might not only drive the development of mutant stem cells, it may promote the progression of the disease and worsen the symptoms.[115] Hasselbalch and Bjørn argue for the MPNs to be considered as chronic inflammatory diseases.[31]

1.2.1 Clinical concern of inflammation in Myeloproliferative Neoplasms

Overproduction of cytokines is a shared characteristic of many hematological malignancies. Pro-inflammatory as well as anti-inflammatory cytokines can be detected, the balance of which often determines the immune response. Some are uniquely elevated in certain diseases suggesting a role in the pathogenesis of that respective disease. The most commonly overproduced cytokines are tumor necrosis factor alpha (TNFα) and interleukin 6 (IL-6). Furthermore, elevated levels of cytokines are associated with worse prognosis in MPN.[115,116]

Inflammatory diseases may precede the development of MPNs. A link to MPNs and autoimmune diseases (AID) has been made by several studies which show that patients with AID, for instance Crohn's disease, rheumatoid arthritis and polymyalgia rheumatic, are in significantly higher risk of developing MPNs.[114,117] Higher levels of pro-inflammatory cytokines in the serum of patients with AID can be detected, which play a critical role in the pathogenesis of AID and may also aid in tumorigenesis. Importantly, increased frequency of *JAK2* V617F mutation and the JAK2 46/1 haplotype has been associated with inflammatory diseases, particularly Crohn's disease.[118,119] It has been proposed that the 46/1 haplotype results in augmented response to cytokine stimulation consequently leading to increased inflammation.[120]

Last but not least, inflammation worsens the symptom burden in MPNs. The elevated levels of pro-inflammatory cytokines are associated with lethargy, depression, cognitive impairment and decreased social interaction.[121] As MPNs are chronic diseases, many current therapies use regiments that control the blood cell count with a so-called 'watch and wait' management. This approach is now being challenged by the introduction of interferon-alpha (IFNα). IFNα is an inflammatory cytokine and it has been proposed that it induces cell cycle activation of mutant HSCs driving their differentiation in erythroid lineage consequently leading to their depletion.[122] More therapeutic strategies are discussed in chapter 1.4.

1.2.2 Inflammation drives the onset and progression of Myelopreoliferative Neoplasms

Substantial research has demonstrated that chronic inflammation correlates with myeloid malignancies, moreover, some evidence shows that chronic inflammation can promote clonal

hematopoiesis. Clonal hematopoiesis is associated with higher age as it was shown in more than 10% of people over the age of 70 without a phenotype of hematopoietic malignancy. It is, however, correlated with higher incidence of non-hematological cancers and atherosclerosis.[123,124] Given the frequency of clonal hematopoiesis in higher age it might be an inevitable consequence of aging. The level of pro-inflammatory cytokines is also increasing with age and inflammation likely contributes to the onset of clonal hematopoiesis and the initiation of MPN, although the mechanism is not yet clear.[115]

Aspects of immune reaction which are not attributable to clonal myeloproliferation have been discovered. It has been shown that *JAK2* V617F mutation induces leukocyte and platelet activation and can be a thrombogenic factor in MPNs.[125–128] Furthermore, mice injected with Ba/F3 cells expressing *JAK2* V617F display elevated production of inflammatory cytokines including TNFα and IL-6, but the Ba/F3 *JAK2* V617F cells are not the source of these cytokines.[129] Additionally, it has been shown that the levels of C-reactive protein (CRP) are elevated in MPN patients and that these levels correlate with the *JAK2* V617F allele burden and also increase with the progression to acute phase.[130] MPN patients are also in higher risk of second cancers, which with a high probability are inflammation-mediated.[131,132] Interestingly, higher risk of second cancers has been recorded prior to MPN diagnosis. As mentioned previously, MPNs may have a long pre-diagnostic period accompanied by chronic inflammation which promotes mutagenesis and immune deregulation.[133–135]

In the context of association between inflammation and MPNs, inflammation might be considered as a secondary event brought on by clonal cells. It is, however, likely that inflammation precedes the acquisition of somatic mutations and the development of the disease, which is also supported by the fact that there is significantly higher frequency of MPNs in patients with autoimmune and autoinflammatory conditions.[31] Furthermore, inflammation drives the progression of MPNs. In MF patients, for instance, the deposition of immune complexes in the bone marrow can be detected in early stages of the disease followed by the activation of complement and local immune reaction leading to immune-mediated damage in the early phase of the disease followed by the fibrotic stage, or the 'burned out' phase of the disease.[31]

Several gene studies have unraveled the molecular evidence of inflammation being the driving aspect of clonal evolution in MPNs. They all show that MPNs exhibit an immense upregulation of immune and inflammation related genes, TNF-related genes, especially interferon-inducible (IFI) gene *IFI27*, and others. The increase in gene expression was detected in the biological continuum from ET over PV to myelofibrosis. The deregulation of IFI genes likely reflects hyperstimulated immune system including enhanced IFN gamma expression, and at the same time its antitumor incompetence. This hyperactivated immune system may also contribute to the increased risk of autoimmune diseases in MPN patients.[136–139]

In summary, the current data suggest that the mutated or neoplastic clone may induce an immune reaction mediated by the nonneoplastic host cells and that this reaction is a key player in the MPN pathogenesis. In mouse models both the innate and the adaptive immune cells contribute to the MPN pathology further favoring the notion that some pathologic features are a consequence of the host's immune reaction to the neoplastic clone rather than the reaction caused by the clone itself. It is possible that the phenotype brought on by the *JAK2* V617F mutation is modulated by the immune reaction to the mutated clone resulting in different conditions caused by the same mutation. In case of absent immune reaction *JAK2* V617F mutation could only lead to clonal hematopoiesis observed in elder people, which is also supported by the prevalence of *JAK2* V617F mutation in older population without the MPN phenotype. In addition, the theory that chronic inflammation can promote the formation of the *JAK2* V617F mutation is supported by the fact that unlike normal HSCs the *JAK2* V617F-positive cells are resistant to the inflammatory cues and are likely to emerge under inflammatory stress to sustain the hematopoiesis.[140]

1.3 DNA damage response

DNA damage response is a complex of mechanisms and signaling cascades that take place upon DNA damage. In the early phase of DNA double stranded breaks (DSBs) a protein kinase ataxia telangiectasia mutated (ATM) recognizes this damage and becomes activated, consequently phosphorylating several key players in the DNA repair machinery, one of which

is a histone variant H2AX at serine 139 - γH2AX.[141] There are two mechanisms, by which a double stranded break can be repaired, non-homologous end joining (NHEJ) and homologous recombination (HR). HR takes place during the replicative and post-replicative cell cycle state (S/G2) when a sister chromatid is present. RAD51 is a molecule representative of HR as it is involved in search for homology. It binds ssDNA and is present during strand pairing stages of the HR process.[142] Together, γH2Ax and RAD51 represent common markers for DNA damage in eukaryotic cells.

It was shown that abnormally proliferating cells of myeloid lineages activate ATM-p53-p21 pathway which leads to a barrier-like mechanism against leukemic transformation. Takacova and colleagues[143] have described DDR mechanisms creating a barrier to mixed-lineage leukaemia (MLL). They identified ataxia telangiectasia and Rad3-related protein – checkpoint kinase 1 (ATR-Chk1) pathway to be activated in the early proliferative phase of MLL. The activation of this pathway was accompanied by the activation of ATM, which is a protein required for an effective activation of the p53/p21^{cip1} pathway. Interestingly, they observed a different phenotype in bone marrow (BM) and spleen of the affected mice. In BM the ATM-p53-p21^{cip1} pathway was prominent which correlated with pronounce senescence phenotype and proliferation arrest. In spleen, however, they noted exclusive ATR signaling, which led to a state of partial proliferation and partial senescence. They further identified that the upregulation of the transcription of several inflammatory factor genes, such as *Cxcl2* and *Ccl3*, serve as a feedback loop to further boost the p53-p21 checkpoint response leading to cell cycle arrest. The inflammatory response and their feedback loop with DDR balance the response to oncogene-induced DNA damage. All in all, tumorigenesis barrier was shown to form a failsafe mechanism not only in solid tumors[144] but also in hematological malignancy preventing further leukemic progression.[143]

It has been demonstrated that in MPN diseases *JAK2* V617F-positive cells are in high risk of accumulating DNA damage. Firstly, the replication fork was shown to be stalled in the intra-S checkpoint in erythroblasts from PV patients leading to increased DNA damage in these cells.[145] Secondly, CD34+ hematopoietic cells obtained from MPN patients positive for *JAK2* V617F were shown to contain RAD51 positive loci, which are indicative of DSB repair.[92] Thirdly, both in cell cultured cells, Ba/F3 over-expressing *JAK2* V617F[146], and in primary

cells of 6-month old *JAK2* V617F-heterozygous knock-in (KI) mice[147] the cells positive for the *JAK2* mutation were shown to accumulate γH2Ax-marked double-strand breaks. Moreover, a profound increase of reactive oxygen species (ROS) with subsequent oxidative DNA damage and DNA DSBs were detected in the hematopoietic stem cell compartment of a KI mouse model and in patients with *JAK2* V617F MPNs.[146,147] Intriguingly, it was shown that treatment with antioxidant significantly reduces the ROS-mediated DNA damage and might prevent the development of *JAK2* V617F-driven MPN further proving that ROS is a mediator of *JAK2* V617F-induced DNA damage that promotes the disease progression.[146] All in all, there is indication that *JAK2* V617F-positive cells are in high risk of DNA damage induced by the mutated kinase itself.

There is not only high amount of DNA damage detected in *JAK2* mutated cells, the response to DNA damage in the mutated clones was shown to be impaired as well. DNA damage in normal conditions increases the activity of the amiloride-sensitive sodium-hydrogen exchanger isoform 1 (NHE-1) thus raising the internal pH which ultimately leads to deamidation of B-cell lymphoma extra-large (BCL-X_L, an anti-apoptotic mitochondrial transmembrane molecule) and subsequent apoptosis. The BCL-X_L deamidation pathway, however, appears to be inhibited in *JAK2* V617F-positive cells.[148] This inhibition was shown to be mediated by PI3K/AKT signaling which promotes cytoplasmic sequestration of forkhead box O 3A (FOXO3A) leading to elevated levels of ROS and impaired BCL-X_L deamidation pathway. The precise link between the ROS levels and BCL-X_L deamidation remains to be elucidated, although it has been suggested that pro-oxidative state inactivates the AP2 transcription factor (activating enhancer binding protein 2 alpha) implicated in controlling the expression of NHE-1.[149] Additionally, p53 signaling appears to be also affected in cells exhibiting *JAK2* V617F mutation. This is due to enhanced expression of the La autoantigen resulting in increased translation of mouse double minute 2 homolog (MDM2, E3 ubiquitin ligase important for negative regulation of p53).[150] Functional inactivation of p53 augments the cells response to DNA damage. As a result of impaired BCL-X_L deamidation pathway and deregulated p53 response *JAK2* V617F-positive cells display reduced apoptosis and thus accumulate mutations over time. Accumulated DNA damage is also connected with senescence, which has been suggested to provide a barrier to neoplastic progression *in vivo*.[147]

Given the evidence described above, *JAK2* V617F-positive patients would be expected to have an accelerated disease progression caused by the DNA damage accumulation, but in fact this does not hold true. On the contrary, cytogenetic abnormalities are thought to be rare in MPN chronic phase patients.[151] Moreover, recent longitudinal studies of MPN progression indicate that PV and ET patients below 60 years of age have a delayed disease progression and usually remain clinically stable over many years/decades.[152] Furthermore, triple-negative PMF patients were shown to have worse median survival than *JAK2* V617F-positive PMF patients.[152] The presented data indicate the existence of a protective mechanism of DDR in *JAK2* V617F-positive cells, the failure of which would allow the leukemic progression.

1.3.1 The role of RecQ Like Helicase 5 in the progression of Meyloproliferative Neoplasms

Chen and colleagues[153] recently identified DNA repair helicase RecQ Like Helicase 5 (RECQL5) to be upregulated in *JAK2* V617F-positive cells and to be employed in the suppression of induced replication stress and genomic instability in these cells. RECQL5 was not only found to protect *JAK2* V617F cells from endogenous stress, it was also shown that the depletion of RECQL5 sensitizes these cells to replication stress and increases the severity of replication fork stalling. They also showed that the upregulation of RECQL5 is driven through JAK2-PI3K signaling, however, the precise mechanism of this upregulation is unknown. They propose that a direct transcriptional mechanism, possibly by modulating the activity of FOXO family of transcription factors, might play a role.[153] As described above, it has been shown that *JAK2* V617F mutation mediates FOXO3A translocation from nucleus to cytoplasm making these cells resistant to DNA-damage induced apoptosis.[149] The specific role of helicase RECQL5 and its protective mechanisms in MPN remain to be elucidated.

1.3.2 The role of KAP1 in the progression of Meyloproliferative Neoplasms

It is of interest whether a DRR response mechanism, such the one described in MLL involving ATM-p53-p21^{cip1} pathway, serves as a barrier for the neoplastic *JAK2* V617F-positive clones to progress to acute leukemia. Tripartite motif-containing 28 (TRIM28), also known as KRAB-associated protein-1 (KAP1) is one of the proteins phosphorylated by ATM upon DNA damage and this phosphorylation was shown to be necessary for proper DNA repair.[154]

Its role in hematopoiesis was studied by Barde and colleagues[155] who demonstrate that KAP1-deleted erythroblasts accumulate mitochondria that in a mouse animal model leads to severe hypoproliferative anemia. This is due to deregulated expression of microRNAs that target mitophagy transcripts, which itself is a result of failed repression by KAP1 associated with specific Krüppel-associated box domain zinc finger proteins (KRAB-ZFPs). Thus, KAP1 appears to play a substantial role in hematopoiesis.

The role of KAP1 has been explored in several systems discovering it is indeed a crucial multifunctional protein. It is ubiquitously expressed throughout development, and it localizes in the nucleus. KAP1 was first discovered as a protein interacting with KRAB-ZFPs and it appears that many of its functions are being mediated through this interaction. It is considered to be a critical transcriptional co-repressor as it binds to the conserved repression domain of KRABs in many transcription factors.[156,157] Interestingly, it has been shown that it can be recruited to the chromatin even by a mechanism independent of KRAB-ZFPs, although the factor that recruits KAP1 to promoters has not yet been identified. Its function is modulated by post-translational modifications that determine its activity. Phosphorylation and sumoylation act as modifications important for transcriptional modulation and chromatin remodeling. The function of KAP1 has been implied in DDR, cell differentiation, immune response, virus replication and tumorigenesis. It is also important in normal development, maintaining pluripotency and erythroid differentiation. All things considered, it is no wonder KAP1 has been called the 'enigmatic master regulator of the genome'.[158,159]

Upon DNA damage heterochromatin needs to be decompacted – a process which is most likely controlled by KAP1. Phosphorylation of KAP1 induced by DNA damage-inducing agents is primarily performed by phosphoinositide 3 kinase-like protein kinases (PIKKs), including ATM and ATR. The specific phosphorylation of KAP1 at serine 824 co-localizes with DNA repair factors like γH2AX, implicating its role in DNA repair processes.[160] It was further shown that this phosphorylation is responsible for activating DNA damage checkpoints and ATM-mediated relaxation of chromatin.[161] In fact, it has been proposed that KAP1 is a direct downstream effector of the ATM-mediated DSB repair in heterochromatin.[162] Chromatin remodeling is also accompanied by KAP1 desumoylation as S824 KAP1 phosphorylation perturbs SUMO-dependent (SUMO - Small Ubiquitin-like

Modifier proteins) interaction of KAP1 with other factors resulting in decondensation of heterochromatin.[163,164] Phosphorylation of serine-473 was shown to be involved in cell survival upon DNA damage and efficient DNA repair.[165–167] Several studies point that KAP1 in DSB repair may be associated with the chromatin complexity and cell cycle status. Taken together, one of the major functions of KAP1 could be chromatin remodeling during the DSB repair, and possibly even recruitment of other factors of DNA repair machinery. The deregulation of a balance of KAP1 will disturb the process of DNA repair and might create a situation where cells are more prone to DNA damage and subsequent genomic instability.[154,159]

1.4 Treatment strategies based on the tumor heterogeneity

As hematologic malignancies are heterogeneous diseases the treatment strategies need to be adjusted accordingly. The major purpose of PV and ET therapy is reduction of vascular risks and a risk of evolution to PMF and acute leukemia. The most frequent strategy in treating PV is reducing hematocrit to sex-specific levels, usually performed by phlebotomy. Phlebotomy also prevents thrombosis which is a major complication in PV patients. Aspirin is often used for the prevention of erythromegalia and ocular migrane. The use of chemotherapy in MPN patients is ineffective in eradicating the disease and often increases the risk of progression to acute leukemia, nevertheless, hydroxyurea (HU) is a recommended drug of choice for treating PV. The use of HU, a common cytoreductive agent also known as hydroxycarbamide, has not been backed up by any prospective study as it causes DNA copy number changes and impairs the function of p53. Furthermore, HU in combination with other therapies increases the risk of acute leukemia and dermal tumors. It should therefore be avoided in younger patents, but also elder patients given the higher frequency of naturally occurring mutations in older age. As a result, HU is preferably limited to situation of high levels of blood cells that need to be rapidly reduced.[115,168,169]

Other important therapeutic agents target JAK/STAT signaling. Ruxolitinib, a non-selective JAK1/2 inhibitor, has been shown to be effective in treatment of MPNs. It was demonstrated to alleviate the symptoms of PV, control splenomegaly and can also control the blood counts.

It appears to control the *JAK2* V617F allele burden, too, and to reduce multiple cytokines, including CRP, TNFα, and IL-6 in PMF patients, which also correlates with symptom improvement further proving a connection between the symptom burden in MPNs and inflammatory cytokines.[115] Its effect on HSCs is less effective than on progenitor cells and for un unknown reason Ruxolitinib is not effective in every patient.[168] It is speculated whether Ruxolitinib's effect in treatment of MPN is JAK2 specific, as a JAK1 inhibitor, Itacitinib, was demonstrated to have similar efficacy to Ruxolitinib in myelofibrosis. It has been proposed that the effect of both inhibitors is not the inhibition of signaling in the neoplastic cells, but rather an anti-inflammatory effect via reducing the immune reaction of non-neoplastic cells thus improving the MPN symptoms and decreasing leukemogenesis. This is yet another proof that *JAK2* V617F-positive cells have a proliferative advantage in inflammatory environment over the non-neoplastic progenitors and that MPN patients benefit from reduction of inflammation. Additionally, JAK inhibitors have proved to be efficient drugs in treatment not only of MPN diseases, but also in AIDs, such as alopecia areata, psoriasis and graft versus host disease.[115,140]

As inflammation appears to be a driving force in the pathogenesis of MPN the most appropriate therapy would seem to be to suppress it. Indeed, immunosuppression using INFα is currently the most promising MPN therapy.[170] INFα is a nonleukemogenic drug that has been used in treatment for PV for more than 20 years. It has not been, however, widely used because of its toxicity and cost. These are being overcome with the invention of pegylated (peg, polyethylene glycol) forms which were shown to be more tolerable and efficient in INFα-treated hepatitis patients. Phase 2 studies performed in PV and ET patients using peg-INFα are currently underway[169] and some of these trials combining Ruxolitinib and peg-INFα are proving to be very promising.[115] The results so far display reduction of neutrophil and HSC *JAK2* V617F allele burden (a complete molecular remission is obtained in approximately 20% of patients), lower toxicity, blunting of fibrosis, symptom reduction and reduced splenomegaly. Side effects seem to be comparable to recombinant INFα.[115,168] To sum up, increasing amount of studies demonstrate sustained complete hematological remission after long-term INFα treatment further demonstrating the importance of inflammation in the pathogenesis of MPN.

In other hematological malignancies iron chelation and prolyl hydroxylase inhibition, among others, were demonstrated to be effective. The fact that iron is an important element indispensable for cell proliferation has been known for decades.[171] Iron chelators have been, in fact, used for overload diseases and are also potent inhibitors of DNA synthesis *in vitro*.[172] They exert their anti-proliferative effects via targeting molecules critical in the cell cycle, such as cyclins, cyclin-dependent kinases, p53 and p21.[173] Iron chelation was further shown to induce apoptosis *in vitro* in breast cancer, renal carcinoma, neuroepithelioma and melanoma cell lines.[6] The inhibition of prolyl hydroxylases leads to hypoxia-inducible factor (HIF) stabilization that can very efficiently treat anemia.[174] The mechanisms of action of iron chelators and PHD inhibitors are discussed below.

1.4.1 Regulation of oxygen sensing

Both iron chelators and PHD inhibitors negatively regulate oxygen sensing. Sensing oxygen levels is a crucial mechanism required for normal EPO production and erythropoiesis. Animal studies have shown that the major site of production of EPO in adult body is the kidney, specifically peritubular interstitial fibroblasts. Besides kidneys, liver produces substantial amount of EPO especially in severe hypoxia/anaemia. The cells responsible for EPO production in liver are the hepatocytes and stellate cells. In fact, liver is the major producer of EPO during embryonic development and the EPO production pathway was first characterized in human hepatoma cell lines Hep3B and HepG2. In 1991 a hypoxia response enhancer (HRE) was identified in human and mouse genome lying approximately 120 bases 3' to the polyadenylation site of EPO gene.[175–177] Subsequently, the hypoxia-inducible factor (HIF) complex was identified and characterized.[178–180]

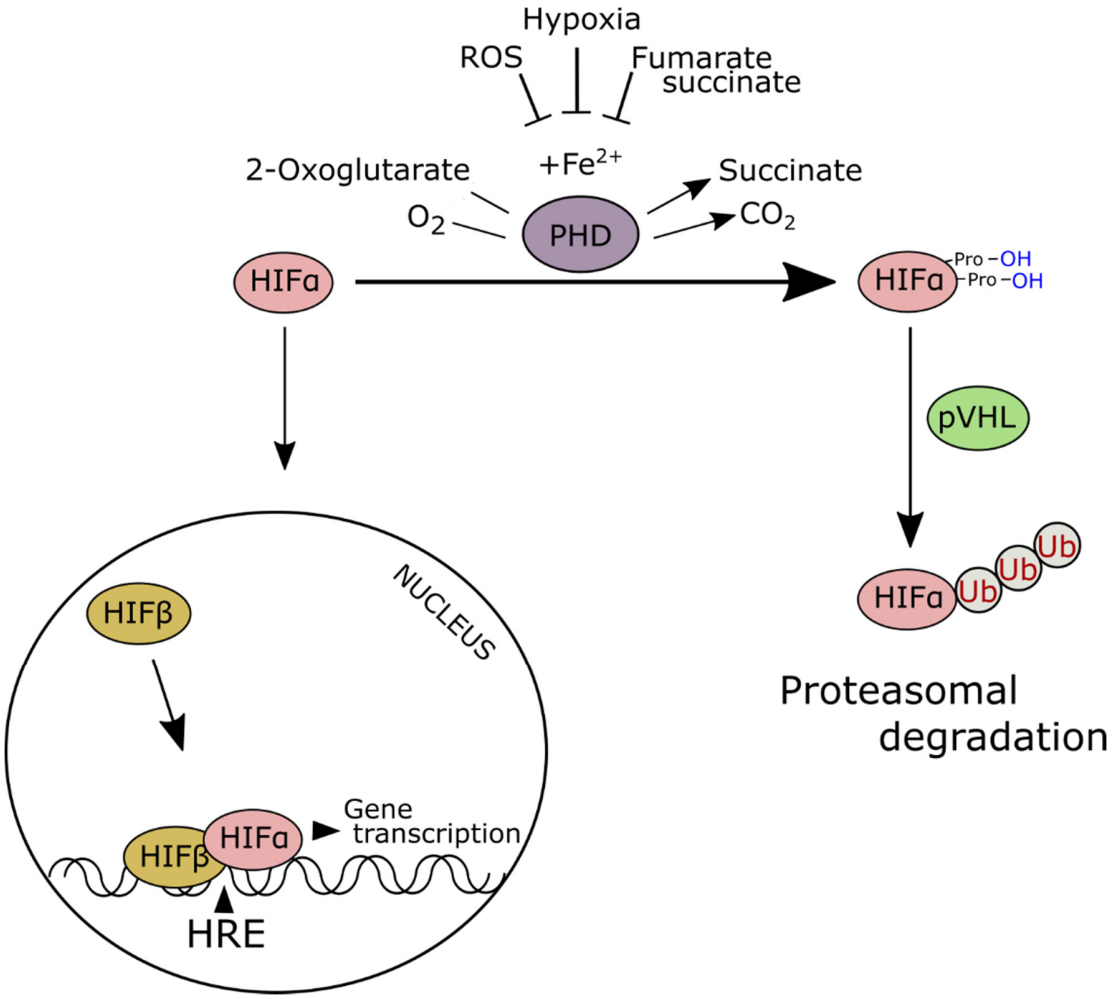

Figure 3. Regulation of HIFα by PHD hydroxylation. In normal conditions HIFα is hydroxylated (Pro402 and Pro564 in human HIF1α; Pro405 and Pro531 in human HIF2α) by prolyl hydroxylases PHDs in the presence of oxygen, using 2-oxoglutarate as a substrate and Fe^{2+} as a co-substrate. Upon hydroxylation HIFα is polyubiquitinated by pVHL followed by its recognition and degradation by the 26S proteasome. In situations when PHDs are inhibited, such as in hypoxia, iron deficiency or by 2-oxoglutarate competitors, HIFα is stabilized and translocated into nucleus where it forms a complex with HIFβ and activate gene transcription of HIF-target genes. Adapted from reviews by Yang et al.[181] and Fong et al.[182]

HIF complex regulates the response to low oxygen levels by transcriptional activation of HIF-target genes. There are two subunits of the HIF complex, HIFβ (also called aryl hydrocarbon receptor nuclear translocator - ARNT) and HIFα. There are in fact three subunits of HIFα (HIF-1α, HIF-2α and HIF-3α), HIF2α (also known as endothelial PAS domain protein 1 - EPAS1) being considered as major regulator of EPO synthesis in kidney. Both HIFα and

HIFβ are constitutively expressed, but while HIFβ is stable and located in the nucleus, HIFα is being degraded in the cytoplasm. Its degradation is mediated by its hydroxylation by prolyl hydroxylases (PHDs, for further detail see chapter 1.4.2) that allow capture by the E3-ubiquitin ligase von Hippel-Lindau (pVHL). Following its polyubiquitination HIFα is degraded by a proteasome (Figure 3).[183] HIFα is also hydroxylated by asparagine hydroxylase, factor inhibiting HIF (FIH), thus inhibiting its interaction with co-activators p300/CREB-binding protein (CBP).[184] When the oxygen levels drop FIH and PHDs are inhibited leading to the stabilization of HIFα. Consequently, HIFα translocates into the nucleus where it forms a complex with HIFβ followed by their association with transcriptional co-activators p300/CBP. As a result via binding to HRE they activate the transcription of HIF-target genes including *EPO*, vascular endothelial growth factor A (*VEGFA*), solute carrier family 2A (*SLC2A*), hexokinase-1 (*HK1*) and prolyl hydroxylases, too, as a form of negative feedback loop.[178,185–187]

1.4.2 Prolyl hydroxylases

The key oxygen sensors are the prolyl hydroxylases, three paralogues of the Egln (Egg laying nine) family termed as *EGLN1*/PHD2, *EGLN2*/PHD1 and *EGLN3*/PHD3. They are members of iron and 2-oxoglutarate-dependent dioxygenases. Their oxygen sensing function lies in their need of oxygen as a co-substrate in order to catalyze the hydroxylation of their substrate 2-oxoglutarate. In fact, 2 oxygen atoms are needed, one to convert 2-oxoglutarate to succinate and the second is added to a peptidyl proline to form hydroxyproline. PHDs use Fe^{2+} and ascorbate as co-factors (Figure 3).[188,189] The discovery of PHDs and their substrates provided an explanation for HIF-dependent increase of EPO in patients treated with iron chelators.[190] Likewise, 2-oxoglutarate competitors, also called PHD inhibitors, such as FG-4497, inhibit HIF hydroxylation leading to increased levels of EPO.[191]

PHDs are widely expressed, however, *PHD3* mRNA expression peaks in cardiac and smooth muscle and brain, while *PHD1* is highly expressed in testis.[192–196] In the cell, PHD1 was found to be exclusively present in the nucleus, PHD2 is mainly located in the cytoplasm and PHD3 protein is homogenously distributed throughout the cytoplasm and nucleus.[197,198]

Functionally, out of the three isoforms PHD2 is the most widely studied as it is largely responsible for hydroxylating HIFα (Pro402 and Pro564 in human HIF-1α; Pro405 and Pro531 in human HIF-2α). The importance of PHD2 in hypoxic response is clearly demonstrated by the fact that a mutation in *Egln1*/PHD2, which causes a decrease in its function, is associated with familial erythrocytosis.[199] PHD1 was also shown to inhibit HIF2α and a combined knockout of PHD3 and PHD1, and not only one of them, leads to erythrocytosis.[200,201] PHD3 was first described as a gene upregulated by growth factors or serum,[202,203] and was later found to play a role in prolonged hypoxic stress where it was shown to have a major effect on the HIF system.[185]

The function of PHD1 is less clear. The mouse homologue *Falkor* was identified as a DNA damage related growth regulator in mouse embryonic fibroblasts.[195] PHD1 was also demonstrated to inhibit NF-κB activity and its target genes, one of which is *cyclin D1* and thus the inhibition of PHD1 would ultimately lead to NF-κB induced *cyclin D1* expression and proliferation.[204] These data are contradictory to another report, which demonstrates that PHD1 inhibition leads to the inhibition of IL-1β–induced NF-κB and thus downregulation of its target genes.[205] A link between *EGLN2*/PHD1 polymorphisms and non-small cell lung and gastric cancer was reported in Chinese population.[206,207] Interestingly, in contrast to PHD2 and PHD3, PHD1 is not hypoxia-inducible and responsive to growth factors.[192,197,208] In breast cancer *EGLN2* mRNA was shown to accumulate in cells stimulated with estrogen and participate in estrogen-independent growth.[209]

The link between prolyl hydroxylases and cell cycle regulation was first described in drosophila. Drosophila PHD homologue Hif-1 prolyl hydroxylase (Hph) was shown to be a regulator of cellular growth and a key mediator for the drosophila cyclin-dependent protein kinase complex cyclin D/cyclin-dependent kinase 4 (CycD/Cdk4) as it readily suppressed the growth phenotype brought by CycD/Cdk4 overexpression.[202] Zhang et al.[4] later showed that the mammalian cyclin D1-dependant proliferation is regulated by PHD1 in a HIF-independent manner and that it regulates cyclin D1 on the transcriptional level.

1.4.3 Regulation of cyclin D1 by PHD hydroxylases in mantle cell lymphoma

As described above, iron chelators were shown to downregulate cyclin D1 resulting in cell cycle arrest and apoptosis. Cyclin D1 is overproduced in mantle cell lymphoma (MCL), it therefore affords a great system for studying molecular mechanisms of cyclin D1 inhibition by iron chelators. MCL is an incurable B-cell non-Hodgkin lymphoma which is a lymphoid neoplasm characterized by uncontrolled proliferation of mature B lymphocytes. In most of the patients lymphoma progresses to an aggressive form with poor prognosis. MCL represents a small portion of malignant lymphomas, but it accounts for a disproportionately large percentage of lymphoma-related mortality. The hallmark of the disease is a translocation that juxtaposes the *CCND1* gene on chromosome 11q13 (which encodes cyclin D1, CD1) and an immunoglobulin heavy chain gene promoter on chromosome 14q32.[210] Novel therapeutic approaches target several cellular pathways of MCL (CDK inhibitors, proteasome inhibitors, mTOR inhibitors, NFκB inhibitors and others) but so far have shown only modest effects on overall survival.[211] Vazana-Barad et al.[5] reported that MCL patients could also benefit from iron chelator agents.

Iron chelation has been demonstrated to be effective in inhibition of cell proliferation and induction of apoptosis *in vitro* in several cancer cell lines. Iron chelator deferasirox was shown to downregulate cyclin D1 which in turn leads to inhibition of retinoblastoma (Rb) phosphorylation and increase of the E2F/Rb complex levels ultimately leading to G1/S arrest.[5] The mechanism by which it does so has been suggested by Nurtjaha-Tjendraputra, et al[6] in a study that examined the ability of iron chelators to inhibit cell proliferation and induce apoptosis. It was postulated that iron chelation caused posttranslational proteasomal degradation of cyclin D1 which was ubiquitin independent in iron deplete conditions, while ubiquitination is important for cyclin D1 degradation in iron-replete cells.

In the last years the field of ubiquitin independent proteasomal degradation by 20S proteasomes has been further explored. 20S ubiquitin independent degradation was for a long time thought to be a remnant of the pre-ubiquitin world, but has recently been shown to play a considerable part in mammalian degradation as it was revealed to cleave more than 20% of all cellular proteins. It has been postulated that the disordered regions of proteins are

recognized by the 20S proteasome and cleaved to produce stable products containing structured domains.[212,213] Ubiquitin-independent protein degradation could in some cases provide optimal regulation and thus lead to protein homeostasis. This type of degradation is involving NAD(P)H-quinone oxidoreductase (NQO1) and antizyme. Antizyme, a small inhibitory protein, is shown to promote the ubiquitin-independent degradation of proteins such as ornithine decarboxylase (ODC)[214] and c-myc.[215] NQO1 is a 2-electron reductase of quinones to hydroquinones, the enzymatic activity of which prevents the one electron reduction of quinones linked to the production of radical species. NQO1 was previously reported to bind proteins, such as p53 and ODC, leading to their stabilization and consequently preventing their degradation.[216–220] Interestingly, iron depletion was shown to regulate cyclin D1 repressor p21 where it induces ubiquitin-independent degradation of the protein, whereas its mRNA levels are increased.[221,222] The precise mechanism has not been identified yet, although it has been proposed that it might be mediated via NQO1 or antizyme.[221,222] Another link between hypoxia and ubiquitin-independent degradation was made when antizyme 2 was shown to mediate c-Myc degradation in stress situations, such as hypoxia and glucose-free condition.[215] All things considered, ubiquitin-independent degradation plays a role in regulating proteins important for cell cycle control.

Another link to cyclin D1 downregulation mediated by iron deficiency was made by Zhang et al.[4] showing that the mammalian cyclin D1-dependant proliferation is regulated by PHD1 in a HIF-independent manner. Cyclin D1 was shown not to be a direct substrate for *EGLN2*/PHD1, but its effect on cyclin D1 was demonstrated to be rather influenced by FOXO3A transcription factor. FOXO3A is a transcription factor known to be involved in many cellular processes such as apoptosis[223–225], autophagy[226], oxidative stress[226] and DNA repair.[227] Interestingly, PHD1 was revealed to hydroxylate FOXO3A thereby blocking its interaction with the USP9x deubiquitinase and promoting its proteasomal degradation. Loss of *EGLN2*/PHD1 leads to accumulation of FOXO3A and consequently cyclin D1 is suppressed by FOXO3A.[228] It was therefore suggested that FOXO3A is the link between the regulation of cyclin D1 and prolyl hydroxylase PHD1.[229]

II. Original Research

2 Aims and Hypotheses

As I became a part of several projects during my PhD studies I will divide the chapters *Aims and Hypotheses* and *Results* into sections according to the projects. In *Materials and Methods* chapter the particular project that the method belongs to will be addressed as Project 1 (P1), P2 and P3.

2.1 JAK2 germline mutations predisposing patients to Myeloproliferative Neoplasms

In a study performed in our cooperating lab in Utah, US, the mutational landscape of 31 PV patients was analyzed using whole exome sequencing.[1] Two novel germline *JAK2* mutations, *JAK2* T108A and *JAK2* L393V, were identified. Functional analysis of these two mutations was performed in order to determine their impact on the JAK/STAT signaling and PV pathogenesis. – *Project P1i*

Recently, two germline *JAK2* mutations, E846D and R1063H, were described in a case of hereditary erythrocytosis accompanied by megakaryocytic atypia.[2] The *JAK2* R1063H variant was initially described in 3 out of 93 PV patients that were *JAK2* V617F-positive.[3] In this study, we assessed the presence of *JAK2* V617F and *JAK2* R1063 mutations in a cohort of 390 MPN patients from Romania and Belgium to characterize phenotypically the double mutation carriers and gain insight into the functional consequences of coexisting mutations on JAK2 signaling. We also searched for additional mutations in these samples. – *Project P1ii*

PhD thesis aims:

(1) Identify the role of inherited mutations in the JAK2 gene in the initiation and progression of myeloproliferative neoplasms

2.2 Protective molecular mechanisms preventing the progression of Myeloproliferative Neoplasms

Neoplastic transformation of MPNs is a multistep process involving accumulation of mutations that allow proliferation and survival of the neoplastic clone. In recent years it was shown that activated oncogenes in solid tumors induce DSBs as well as activate DDR.[144] We hypothesize that a similar process underlines the course of MPNs and that the activation of a tumor suppressor barrier counteracts the progression to acute leukemia. We also propose that an inactivation of certain tumor suppressor genes will abrogate this barrier, which ultimately leads to acquisition of more mutations and faster disease progression. - *Project 2*

PhD thesis aims:

(2) Identify the protective role of KAP1 protein in the progression of myeloproliferative neoplasms

2.3 The role of *EGLN2*/Proline hydroxylase 1 in regulation of cyclin D1 in mantle cell lymphoma

Cyclin D1 downregulation by iron chelation by means of regulating PHD1 and FOXO3A was previously studied in cancer cell lines (other than MCL cell lines) and in mouse mammary tissue. Cyclin D1 is overexpressed in mantle cell lymphoma and it is therefore of interest whether iron chelation would be beneficial in downregulating cyclin D1 in MCL cells. It was indeed shown that iron chelation leads to decreased *cyclin D1* mRNA and protein levels in MCL cell lines[5], the molecular mechanism, however, remains unknown. In our study we

further explore the role of PHD1 and its hydroxylation target transcription factor FOXO3A in the downregulation of cyclin D1 in mantle cell lymphoma. – *Project 3*

PhD thesis aims:

(3) Identify the role of EGLN hydroxylases/PHDs and FOXO3A transcription factor in mantle cell lymphoma

3 Materials and Methods

Methods and materials are divided into sections according to the methods. The particular projects the method has been applied for are depicted in margins, addressed as Project 1 (P1i and P1ii), P2 and P3.

3.1 Cell culture

Human cell lines HCT 116 (human colon cancer cell line), HEL (human erythroleukemia cell line), HEK 293 (human embryonic kidney cells) and U2-OS (human osteosarcoma cell line) were purchased from the American Type Culture Collection (ATCC, Manassas, VA). HCT 116 were maintained in Iscove's Modified Dulbecco's Medium (IMDM; Sigma-Aldrich),
P1 + P2 HEL cell in Roswell Park Memorial Institute (RPMI) 1640 Medium (RPMI; Sigma-Aldrich), HEK 293 and U2-OS cells in Dulbecco's Modified Eagle's Medium (DMEM; Sigma-Aldrich), all supplied with 10% fetal bovine serum and GlutaMAX (both ThermoFisher Scientific) and treated with streptomycin, penicillin, and gentamicin mix (Thermo Fisher Scientific) in a humidified atmosphere containing 5% CO_2 at 37°C. The treatments of the cells by RS-1, Brefeldin A and SCR7 (all from Sigma Aldrich) are indicated in the corresponding figures and legends.

Human MCL cell lines Jeko-1 and Mino were a kind gift from Dr. Jianguo Tao at the H. Lee Moffitt Cancer Center & Research Institute (Tampa, FL). The HBL-2 cell lines were a kind gift from Dr. Elliot Epner at Oregon Health and Science University. Cell lines SUDHL-6 (CRL-2959™) and DG-75 (CRL-2625™) were purchased from ATCC (Manassas, VA). All cell lines were maintained in RPMI medium 1640 with GlutaMAX (ThermoFisher
P3 Scientific), supplemented with 10% fetal bovine serum (ThermoFisher Scientific), and treated with 100 U/mL penicillin and 100 µg/mL streptomycin (both ThermoFisher Scientific) in a humidified atmosphere containing 5% CO_2 at 37°C. The treatments of the cells by desferrioxamine (DFO, Sigma Aldrich), dimethyloxalylglycine (DMOG, Sigma Aldrich), FG-4497 (FibroGen, Inc), dicumarol (DIC, Sigma Aldrich), cycloheximide (CHX, Sigma Aldrich) or MG-132 (Sigma Aldrich) are indicated in the corresponding figures and legends.

3.2 RNA isolation, quantitative RT-PCR and digital droplet PCR

RNA was isolated using TRI reagent (Sigma Aldrich) and 1000 ng of DNA-free RNA was reverse-transcribed using the RevertAid Reverse Transcriptase (Thermo Fisher Scientific) according to the manufacturer's manual.

To calculate the *JAK2* R1063H/wild type and *JAK2* V617F/wild type allele ratio, respectively ddPCR was employed. One reaction of ddPCR was performed using 100 ng of genomic DNA, 1 µl of ddPCR™ Mutation Detection Assay mix for human *JAK2* R1063H/WT (20x assay mix, custom designed: dHsaMDS460320799; Biorad) or 1 µl of each probe PrimePCR™ ddPCR™ Mutation Assay for human *JAK2* V617F/WT (*JAK2* WT for p.V617: dHsaCP2000062 and *JAK2* p.F617: dHsaCP2000061; Biorad), 10 µl ddPCR™ Supermix for Probes (No dUTP; Biorad) and 1 µl of restriction enzyme *HindIII* (Thermo Scientific™) in total of 20 µl of reaction. Droplets were created using Droplet Generation Oil for Probes in QX200™Droplet Generator. PCR was performed in C1000 Touch™Thermal Cycler using conditions as follows, 95 °C for 10 min, 40 cycles of 30 s at 94 °C and 1 min at 55 °C, and a final step at 98 °C for 10 min. The ramp rate was always limited for 2 °C/sec. After the PCR reaction, droplet florescence was measured by QX200 Droplet Reader. Data were analyzed using QuantaSoft (Bio-Rad, V1.7.4). *P1ii*

Gene expression experiments were performed on LightCycler 480 system (Roche) with the following TaqMan probes: Hs00234567_m1 *JAK2* and reference genes 4333761F *RPLP0* and 4333767F *GUSB*. *P2*

Gene expression experiments were performed on LightCycler 480 system (Roche) with the following TaqMan probes: Hs00765553_m1 *CCND1,* Hs00153380_m1 *CCND2,* Hs00236949_m1 *CCND3*, Hs00254392_m1 *EGLN1,* Hs00363196_m1 *EGLN2,* Hs00222966_m *EGLN3,* Hs00900055_m1 *VEGFA,* Hs00892681_m1 *SLC2A1,* Hs00175976_m1 *HK1,* Hs00818121_m1 *FOXO3A* and reference genes 4333761F *RPLP0* and 4333767F *GUSB*. All experiments were investigated in triplicate. The data reported represent the mean of three independent experiments; T bars designate SD. For statistical analysis Student's paired t test with unequal variance was employed and P values <0.05 were considered statistically significant. *P3*

3.3 *Cis/trans* configuration of *JAK2* V617F and R1063H mutations

Patients' DNA-free RNA isolated by our cooperating lab, either from whole blood or from peripheral blood leukocytes, was reverse transcribed by High Capacity cDNA Reverse Transcription Kit (Thermo Fisher Scientific). The position of V617F mutation relative to R1063H mutation was determined by amplifying a region spanning exons 14 – 24 of *JAK2* gene. The semi-nested PCR using primers (1st round, F1 5' ACGGTCAACTGCATGAAAC
P1ii A 3', R1 5' AGGAGGGGCGTTGATTTACA 3'; 2nd round, R2 5' ATCTCATCTGGGCAT CCATC 3') was performed. The amplicon was gel-purified using Zymoclean™ Gel DNA Recovery Kit (Zymo Research) and cloned into pGEM-T easy vector (Promega). Single colonies positive for the recombinant plasmid were picked after overnight incubation, plasmid DNA was purified using the High Pure Plasmid Isolation Kit (Roche) and the PCR insert was sequenced at SEQme company, Czech Republic. At least 20 colonies per each amplicon (patient sample) were analyzed.

3.4 Plasmids, mutagenesis, CRISPR/Cas9 editing, virus production and infection

HA-tagged human *G-CSFR* cDNA was cloned in the retroviral pMX-IRES-GFP vector, as described previously.[230,231] The construct was co-transfected into retroviral producing cells HEK 293T together with the envelope encoding construct pCMV-VSV and Gag-Pol
P1ii construct. Retroviral particles were collected at 48 and 72 hours after transfection and concentrated using filtration system Vivaspin® 20 (Sartorius). HEK 293 cells were then infected two times sequentially with the concentrated viral media overnight. Cells were GFP-sorted 72 hours after the second infection and the expression of G-CSFR was confirmed by Western blot.

U2-OS carrying *JAK2* V617F mutation were created using clustered regularly interspaced short palindromic repeats (CRISPR)/Cas9 system. CRISPR construct pXPR_001 plasmid (Addgene plasmid #49535) was cloned according to the Lentiviral CRISPR ToolBox protocol
P2 GeCKO [Zhang lab, http://genome-engineering.org /gecko/] using a guide RNA sequence for targeting the *JAK2* gene 5' ACGAGAGTAAGTAAAACTAC 3'. CRISPR/Cas9 vector was co-transfected using Lipofectamine 2000 (Thermo FisherScientific; according to the

manufacturer's protocol) with a homologous template for HR repair corresponding to a sequence encoding for *JAK2* V617F created by amplifying a 1818 base-pair (bp) long fragment from U2-OS genomic DNA (gDNA, PCR using primers forward 5' ACGGTCAAC TGCATGAAACA 3' and reverse 5' CTAGACACTGGGTTGCCGTA 3') and cloning it into pGEM-T easy vector (Promega). Homologous template was wobbled (protospacer adjacent motif [PAM] sequence mutated to prevent CRISPR cleavage *in vitro* while preserving the amino-acid sequence) using forward 5' GCTCTGAGAAAGGCATTAGAAAGAATGTAG TTTTACTTACTCTCGTCT 3' and reverse 5' AGACGAGAGTAAGTAAAACTACATTC TTTCTAATGCCTTTCTCAGAGC 3' primers, and subsequently mutated to *JAK2* V617F by site directed mutagenesis using forward 5' TCTCGTCTCCACAGAAACATACTCCATA ATTTAAAACCAAATGCT 3' and reverse 5' AGCATTTGGTTTTAAATTATGGAGTAT GTTTCTGTGGAGACGAGA 3' primers. For higher efficiency of HR, HR template was linearized using restriction enzyme *ScaI* and gel-purified using Zymoclean™ Gel DNA Recovery Kit (Zymo Research). HEL cells carrying *JAK2* WT were produced similarly to U2-OS *JAK2* V617F cells, only instead of a homologous template carrying mutated *JAK2* a wobbled homologous template encoding for *JAK2* WT was used. HEL cells were transfected using Amaxa™ Nucleofector™ electroporation system (according to manufacturer's protocol, kit V, program X-005). Both cell lines co-transfected with a control plasmid pART, based on a reconstitution of a turbo red fluorescent protein (tRFP) open reading frame (ORF) through a single strand annealing repair mechanism[232] (forward primer 5' ACGAGAGTAA GTAAAACTACAGGCGAT 3' and reverse primer 5' CGCCTGTAGTTTTACTTACTCT CGT 3'). It also encodes for enhanced green fluorescent protein (eGFP) to monitor transfected cells. Two days after transfection, cells were single cell sorted based on their fluorescence and single cell colonies grown in 96-well plates. *P2*

Further analysis of single clones restriction enzyme cutting screen of a PCR product was performed (PCR ran from gDNA using forward 5' CTGAACTATTTATGGACAACAG TCAAAC 3' and reverse 5' GAATAGTCCTACAGTGTTTTCAGTTTCA 3' primers) by *BsaXI* enzyme. *BsaXI* cleaves *JAK2* WT, it, however, does not recognize the *JAK2* V617F site. Alternatively, PCR amplification-refractory mutation system (ARMS) was performed from gDNA of single cell clones as it can distinguish a single point mutation and amplify the *P2*

DNA strand accordingly (IN primer G 5' GCATTTGGTTTTAAATTATGGAGTATATG 3', IN primer T 5' GTTTTACTTACTCTCGTCTCCACAAAA 3', forward OUT primer 5' CTGAACTATTTATGGACAACAGTCAAAC 3', reverse OUT primer 5' GAATAGTCCT ACAGTGTTTTCAGTTTCA 3'). *JAK2* DNA region of interest in selected colonies was amplified using primers spanning the homologous template region (forward 5' GGCATGGA AGGCAAAATGAGA 3' and reverse 5' GGCTCAAGGGAATGTTGTGA 3') and sequenced by GATC Biotech Company.

KAP1 knock-out was performed using CRISPR/Cas9 method as above, two sgRNAs were designed that target exon 13 (KAP1 pXPR_001 #1 = KAP1 X1, sgRNA sequence 5' – GATG ACAGTGCCACCATTTG – 3') and exon 2 (KAP1 pXPR_001 #2 = KAP1 X2, sgRNA sequence 5' – GACGCACCTGGTTCGCATCC – 3') together with their corresponding control pART vectors. Lentiviruses were created by transfecting (polyethylenimine [PEI] transfection) HEK 293FT cells with 2nd generation lentiviral packaging plasmid psPAX2 (Addgene plasmid #12260), envelope expressing plasmin pCMV-VSV-G (Addgene plasmid #8454) and either KAP1 X1 or KAP1 X2. After 72 hours of lentiviral production lentiviral media was centrifuged at room temperature for 15 minutes at 3 000 xg. Viral supernatant was then used for transduction of HEL JAK2 HR cell clones by incubating them in 1:1 RPMI : viral media and centrifuging them in plates for 60 minutes at 1 200 xg, 30°C. In order to improve transduction efficiency 4 µg/ml of hexadimethrine bromide (Polybrene) was used. Viral media was exchanged for growth media (RPMI including additives described above) with selection (2 µg/ml puromycin) 24 hours after cell centrifugation. Cas9 protein was introduced into HEL JAK2 HR clones by lentiviral infection. Cas9 expressing lentiviruses were produced in HEK 293FT cells and HEL cells transduced as described above using lentiCas9-Blast plasmid (Addgene plasmid #52962). Cells were selected with 12 µg/ml blasticidin and the expression of Cas9 was verified by Western blotting. Cas9-expressing cells were used for transduction with sgRNA expressing lentivirus (lentiGuide-Puro [LG], Addgene plasmid #52963) using the same KAP1 targeting sgRNA sequences as listed above. Cells were subsequently electroporated (Amaxa™ Nucleofector™ system, according to manufacturer's protocol, kit V, program X-005) with their corresponding control plasmid pART 24 hours after LG transduction. In parallel HEL JAK2 HR clones without Cas9 were electroporated with KAP1 X1 or KAP1 X2 together with their corresponding control plasmid

pART. Cells in both setups were sorted 48 hours after electroporation as a mixed cell culture based on their fluorescent status. *P2*

Lentiviral LentiCas9-Blast (Addgene plasmid #52962) and LentiGuide-Puro (Addgene plasmid #52963) single guide RNA plasmids were processed according to Lentiviral CRISPR ToolBox protocol GeCKO. Briefly, HEK 293T packaging cell line was used for LentiCas9 amplification using packaging plasmids pVSVg (AddGene #8454) and psPAX2 (AddGene #12260). The viruses were collected 24h after transfection, precipitated with PEG-it reagent (System Biosciences) and Mino cells were infected in the presence of 4 μg/ml Polybrene (hexadimethrine bromide) prior to drug selection (blasticidin 18 μg/ml) to produce cell line stably expressing Cas9 (Mino LentiCas9). The LentiCRISPR single guide RNA plasmid was digested by *BsmBI* enzyme, purified from agarose gel (Roche, High Pure PCR Product Purification Kit) and ligated with phosphorylated and annealed oligo pairs for single guide RNA (target sequence for *FOXO3A* 5' GTGGGTACGCACCTTCCAGC 3', for *EGLN2/ PHD1* 5' TGATGCAGCGCCCATCGCCG 3'). Mino LentiCas9 cell line was infected as described above in the presence of 4 μg/ml Polybrene prior to drug selection (puromycin 1μg/ml). *P3*

3.5 Dual luciferase transcriptional assays

STATs dependent transcriptional activity was measured using firefly luciferase STATs reporter (pGl4.26/GRR4.cz) in HCT116, U2-OS and HEL cells. Reporter plasmid was constructed with STATs response elements[233], where single-stranded oligonucleotides were annealed, ligated and cloned into the pGl4.26 reporter back-bone. The ratios of the constructs in the transfection mixtures (i.e. plasmids producing JAK2, EPOR, STATs, the luciferase reporter and the Renilla control vector) were determined by titration experiments. The luciferase assay was performed according to the supplier's protocol using Dual-Glo Luciferase Assay System (Promega). *P1i + P2*

3.6 Western blot analysis and immunoprecipitation

HA-tagged receptor expressing HEK 293 cells cultured in DMEM + 10 % FBS and no additional cytokines, were transfected with pCMV-Puro-JAK2 variants using Lipofectamine 2000 (Thermo Fisher Scientific). 48 hours post transfection cells were lysed using lysis buffer (NaCl, Tris, Triton-X, CaCl2, MgCl2, EDTA) and a cocktail of proteinase inhibitors. For immunoprecipitation EZview™ Red ANTI-FLAG® M2 Affinity Gel (Sigma) was used according to the manufacturer's instructions. For maximal specificity elution using 3X FLAG® Peptide (Sigma) was performed. Proteins were resolved on SDS-polyacrylamide gels and electro-blotted onto PVDF membranes (Millipore). Receptors were detected using anti-HA rabbit monoclonal antibody (Cell Signalling, #3724) and JAK2 using anti-FLAG rabbit monoclonal antibody (Cell Signalling, #14793). Total cell lysates (TCL) were immunoblotted alongside the immunoprecipitated samples, anti-HA and anti-FLAG antibodies used for the detection are listed above, and a loading control anti-CtBP (Santa Cruz, sc-17759) was used. Quantitation of HA and Flag signals was performed using densitometric analysis by ImageJ software according to the software manual. Three biological replicates were performed.

P1ii

Cells were harvested to an ice cold RIPA buffer (Sigma-Aldrich) supplemented with a cocktail of protease inhibitors. Proteins were resolved on SDS-polyacrylamide gels and electro-blotted onto PVDF membranes (Millipore) or nitrocellulose membranes (Biorad). Membranes were incubated with following rabbit anti-human primary antibodies: JAK2 (#3230S, Cell Signaling, 1:1000), pJAK2 (#3776S, Cell Signaling, 1:1000), STAT5 (#9358S, Cell Signaling, 1:1000), pSTAT5 (#4322S, Cell Signaling, 1:1000), Cas9 (#14697, Cell Signaling, 1:1000), actin (SAB4301137, Sigma-Aldrich, 1:1000), cyclin D1 (#2922S, Cell Signaling, 1:1000), EGLN2/PHD1 (NB100-310, Novus Biologicals, 1:500), EGLN1/PHD2 (NB100-137, Novus Biologicals, 1:500), HSP90 (#4877, Cell Signaling, 1:2000), FOXO3A (#2497, Cell Signaling, 1:1000), KAP1 (home-made); and mouse anti-human primary antibody CtBP (sc-17759, Santa Cruz, 1:1000) at 4°C overnight, washed in PBS with 0.05% Tween 20, and incubated for 1h with goat anti-rabbit or goat anti-mouse horseradish peroxidase (HRP)-conjugated secondary antibody (ThermoFisher Scientific). HRP activity was detected with an ECL detection kit (Pierce, ThermoFisher Scientific). Quantitation of

P2 + P3

cyclin D1 signals was performed using densitometric analysis by ImageJ software according to the software manual. *P2 + P3*

3.7 Proliferation assay, cell cycle and apoptosis analysis

Cell number and viability were determined using CellometerAutoT4 (Nexcelom Bio-science) based on the trypan blue exclusion method or by CellTitre-Blue reagent (Promega) and Perkin-Elmer Envision analyzer. Cell cycle of cell cultures were synchronized by serum starvation as described elsewhere.[6] Briefly, cells were washed with PBS and serum-starved for 24 hours at 37°C. Starved cells were stimulated with 10% FBS for 16 hours at 37°C in the presence or absence of 250 μM DFO, 1 mM DMOG and 50 μM FG-4497. Cells were harvested and washed with ice-cold PBS, fixed with 70% ethanol, dyed with propidium iodide (PI) and the cell cycle was analyzed using a BD FACSCanto II flow cytometer (BD Biosciences) and FlowJo™ software. Apoptosis was evaluated by flow cytometry using an Annexin V-FITC Kit apoptosis detection kit (Miltenyi Biotec) as recommended by the manufacturer. *P3*

3.8 Statistical analysis

The corresponding statistical analyses are specified in the text.

3.9 Methods performed by cooperating investigators

Patients' sample collection, patients' DNA and RNA isolation
Whole exome sequencing
JAK2 molecular and BFU-E analysis *P1i*
Generation and characterization of Ba/F3-EPOR cell lines expressing *JAK2* variants
Western blot analysis

P1ii	Patients' sample collection, patients' DNA and RNA isolation Real-time PCR assay for *JAK2* R1063H mutation screening using TaqMan SNP Genotyping Assay Next-generation sequencing for targeted mutational screening Microarray analysis (array-comparative genomic hybridization/single-nucleotide polymorphism [aCGH/SNP])SNP array assay Vector construction *In vitro* Ruxolitinib sensitivity assay
P3	Cell treatment, proliferation assays, qRT-PCR and Western blotting analysis

4 Results and Discussion

Chapter *Results* is divided into sections according to the projects I participated in.

4.1 JAK2 germline mutations predisposing patients to Myeloproliferative Neoplasms

4.1.1 Coexistence of gain-of-function *JAK2* germline mutations with *JAK2* V617F in polycythemia vera

In 2014, a study performed by our cooperating lab in Utah, USA, analyzed the mutational landscape of 31 *JAK2* V617F-positive PV patients by whole exome sequencing.[1] Two novel germline mutations in *JAK2* gene were identified, *JAK2* T108A and *JAK2* L393V. These variants are located at the conserved *JAK2* residues as displayed in Figure 4, T108A in the FERM domain and L393V seven amino acids upstream of the SH2-like domain (see Figure 2, page 8). FERM domain is required for association with the receptor and the relief of the inhibitory conformation of kinase domain leads to JAK2 activation.[76,77] Unfortunately, at the time of the study *in silico* modeling of potential interactions of JAK2 germline variants could not be obtained since the structure of the JAK2 FERM domain was not yet available. However, our collaborating investigators in Belgium found out that these residues are exposed in the structure of the TYK2 FERM domain and do not appear to interact with other residues which lack the kinase and pseudokinase domains or with partners of other receptor subunits. Interestingly, the JAK2 variants contain precise residues of TYK2 at the 108 (Ala) and 393 (Val) positions, suggesting that, in themselves, they are compatible with functional JAK kinases. TYK2 functions in heteromeric receptor complexes, while JAK2 functions in homodimeric receptor complexes, and it is possible that these exposed residues play a role in limiting JAK2 self-activation. Protein prediction algorithms SIFT[234], AGVGD[235] and PolyPhen[236] considered both variants as *tolerated*, *benign* and *light*, respectively, but both variants were predicted to be *damaging* by MutationTaster[237] and *possibly damaging* by LoFtool. Nevertheless, the functional significance of these germline JAK2 variants and their putative predisposition to PV are not known.

Both mutations were verified to be heterozygous germline mutations by Sanger sequencing from the patients' T cells and nail tissue DNA. The allele burden of *JAK2* V617F mutation in the patients' granulocyte DNA was 41% in the first patient (*JAK2* T108A) and at 1% in the second (*JAK2* L393V). The analysis of individual BFU-Es from patient with *JAK2* L393V for EPO-independent growth revealed that all individually genotyped colonies had *JAK2* WT and L393V alleles in similar proportions, and only one colony (1/16) had an equal proportion of *JAK2* V617F and WT alleles (heterozygous). Material from patient with *JAK2* T108A mutation was not available, however, we analyzed the configuration of the germline mutation and *JAK2* V617F by amplifying the *JAK2* region of messenger RNA isolated from granulocytes and cloning into T-vector (pGEM-T easy, Promega) followed by sequencing of the colonies. In the first patient's sample the two mutations *JAK2* V617F and T108A were found to be in *cis*. We were unable to determine the configuration of the *JAK2* mutations in the second patient due to low frequency of the *JAK2* V617F mutation in patient's granulocytes.

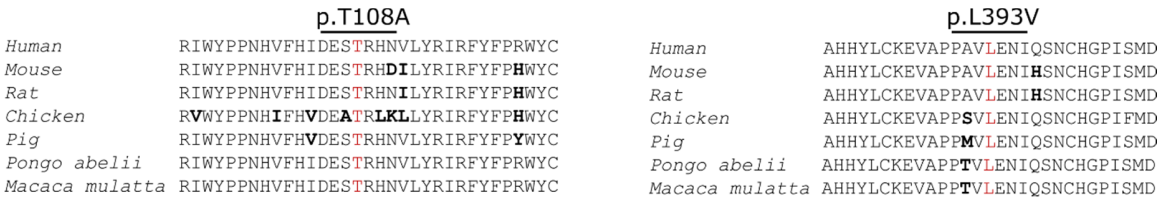

Figure 4. Alignments of amino acid sequences of JAK2 residues surrounding T108A and L393V. Amino acid sequences 93 – 125 and 379 – 407 (human JAK2 nomenclature) aligned from different species show highly conserved pattern. Conserved residues are colored in black, differences are in bold, and the residues at which the mutation occurs are in red.

The first PV patient (*JAK2* T108A) presented with thrombocytosis and mild leukocytosis, and also suffered from pulmonary embolism. Treatment with hydroxyurea stabilized his blood counts, however, subsequently he developed bone pain, thrombocytopenia and anemia that required transfusion. He later died with rapid blast transformation. The second patient (*JAK2* L393V) was ethnic Japanese who had suffered from thrombocytosis in the preceding 12 years, had a history of coronary thrombocytosis and developed erythrocytosis. He was also treated with hydroxyurea that normalized his blood counts. A year after the study he developed anemia and the HU treatment was stopped. At that time his bone marrow showed ~10% of blasts. He later developed progressive pancytopenia and after refusing supportive

therapy in the coming years he developed leukocytosis and peripheral blood blast count exceeding 75%. He refused further supportive therapy and died. In both patients one can observe a continuum of the MPN diseases resulting in PV phenotype that transforms to myelofibrosis characteristic with anemia and thrombocytopenia (patient 1 presented with anemia and thrombocytopenia, while in the second patient pancytopenia – a reduction in the number of erythrocytes, leukocytes and platelets – was observed), eventually transforming to the blast phase. Both patients were of higher age, patient 1 was 87 and patient 2 was 90 years old, and therefore in higher risk of clonal hematopoiesis and acquisition of somatic mutations. In fact, at the time of the study additional somatic mutations were detected, patient 1 carried mutations on genes *IDH2* and *ALK*, and patient 2 in *DNMT3*, *ALK* and *GATA-2*. These likely contributed to the disease development and more somatic mutations were possibly acquired in that process.

We generated stably transfected Ba/F3 cell lines expressing EPOR and *JAK2* variants (T108A, L393V, V617F and WT) in order to determine the functional consequences of *JAK2* germline mutations on the PV phenotype. As presented in Figure 5, cells expressing *JAK2* V617F were EPO independent, and their viability was significantly increased in comparison with *JAK2* WT expressing cells. Cells expressing *JAK2* WT did not grow in the absence of EPO and proliferated less at various EPO concentrations. The two studied *JAK2* mutants were dependent on EPO but were hypersensitive (Figure 5).

We further evaluated signal transduction of JAK2 mutant and WT kinases, as measured by STATs activation, using dual luciferase assays with STATs responsive elements reporter plasmid. STATs activation was markedly increased in the absence of EPO for the driver mutant JAK2 V617F. In both germline variant it was significantly increased when compared to JAK2 WT ($P < 0.05$; Figure 6A), although less so than JAK2 V617F. Using double mutants in the luciferase assay, only *cis* configuration of T108A/V617F increased the STATs activation above *JAK2* V617F signal ($P < 0.05$; Figure 6B). The L393V mutation does not seem to synergize in augmenting V617F signaling, which is consistent with only 1% V617F allele burden in the patients' granulocytes. We then stimulated cells with different EPO concentrations (0,1 and 1 U/mL, EPO added 24 h after transfection), and determined STATs activation. STATs activation by EPO was significantly increased only at low concentrations

of EPO ($P < 0.05$; Figure 6C) for both germline mutants, whereas no further increase of STATs activation was observed in already markedly hyperactive *JAK2* V617F transfected cells after addition of EPO.

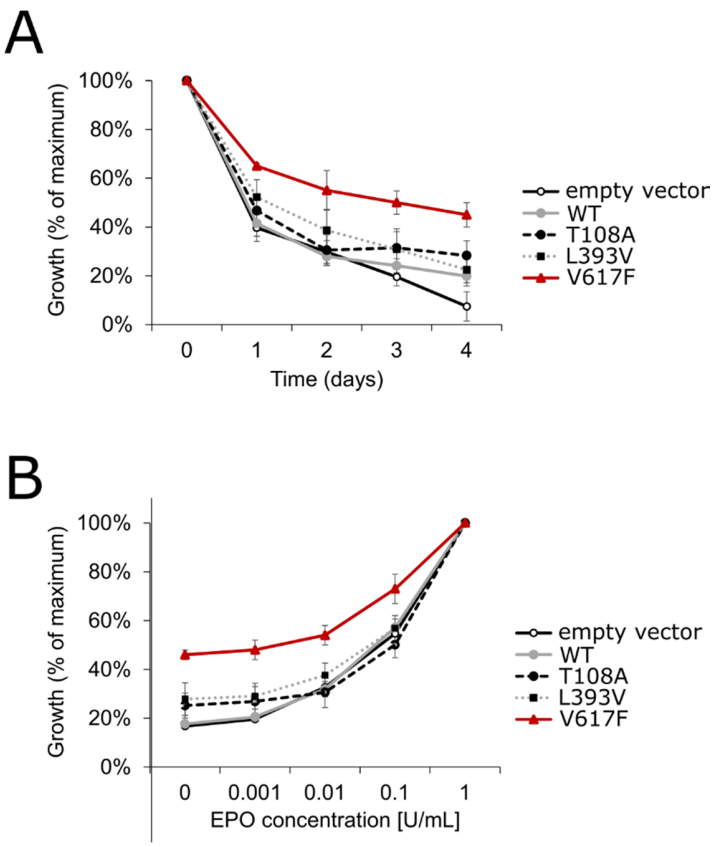

Figure 5. Functional modeling and characterization of two *JAK2* germline mutations T108A and L393V in Ba/F3 cell lines. Proliferation of cells was quantified by CellTitre-Blue reagent (Promega, Madison, WI) and Perkin-Elmer Envision analyzer. Results are shown as the mean (± SD) of three independent experiments performed in triplicate. (A) Proliferation of cells in the absence of EPO; data are expressed as a percentage of maximum value at starting point (Day 0). (B) Proliferation of cells in decreased concentration of EPO (0, 0.001, 0.01, 0.1 and 1 U/mL); data are expressed as a percentage of maximum value (EPO 1 U/mL).

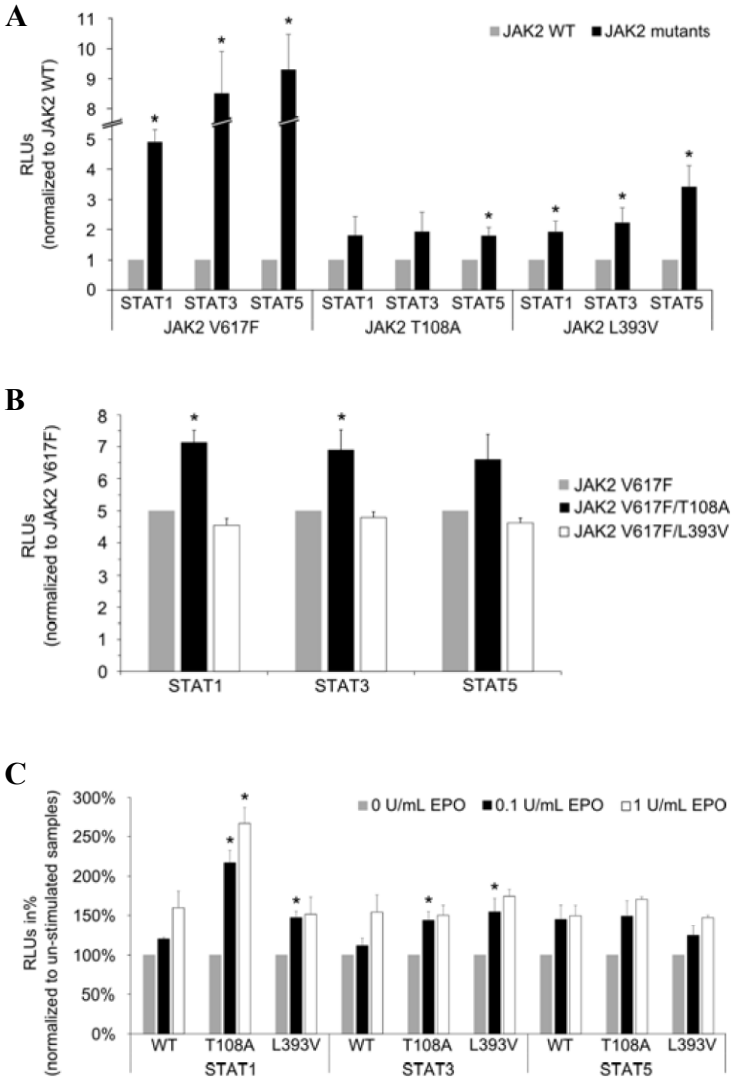

Figure 6. Functional modeling and characterization of two *JAK2* germline mutations T108A and L393V by dual luciferase assay. STATs dependent transcriptional activity induced by JAK2 variants was measured using firefly luciferase STATs reporter (as described in the chapter *Materials and Methods*) in HCT116 cells. Luminescence was measured 48 h after transfection and Renilla counts were used as internal control. Two-tailed t test: *P > 0.05. (A) JAK2 mutants are compared to JAK2 WT using STAT1, 3 and 5. Shown are averages ± SEM of 5 independent experiments performed in duplicate. (B) JAK2 double mutants were used compared to JAK2 V617F alone. Shown are averages ± SEM of 3 independent experiments performed in duplicate. (C) Luminescence was measured 24 hours after EPO stimulation (48 h after transfection). Shown are averages ± SEM of 3 independent experiments performed in duplicate.

We also investigated JAK/STATs signaling in stably transfected Ba/F3-EPOR cell lines by Western blotting. Cells were cytokine-starved for 6 hours and then stimulated with an increased concentration of EPO for 15 minutes. Similar levels of human JAK2 protein in all cell lines were verified by Western blot using anti-DDK antibody (Cell Signaling Technology, Danvers, MA). Constitutively active - phosphorylated STAT5 was exhibited in *JAK2* V617F expressing cells in the absence of EPO. We repeatedly observed stronger phosphorylation of JAK2 and STAT5 at low concentrations of EPO in both mutant variants (T108A, L393V) in comparison to *JAK2* WT cell line (Figure 7).

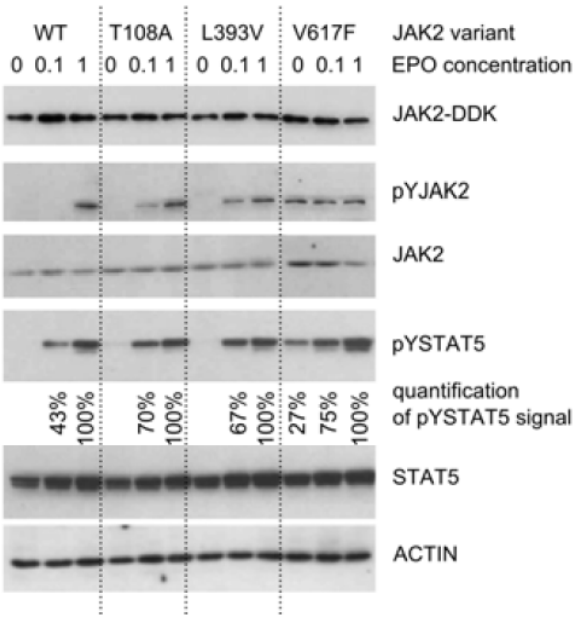

Figure 7. Functional modeling and characterization of two *JAK2* germline mutations T108A and L393V by Western blotting. The level of human JAK2 protein in stably transfected Ba/F3-EPOR cell-lines is equal, as indicated by western blot using anti-DDK antibody (Cell Signaling Technology, Danvers, MA). Ba/F3-EPOR cells expressing different JAK2 WT and mutant variants were cytokine-starved for 6 hours and then shortly stimulated. Western blots were performed with rabbit JAK2, pYJAK2 (Tyr 1007/1008), pYSTAT5 (Tyr 694), STAT5 (Cell Signaling Technology, Danvers, MA) antibodies and actin (Sigma-Aldrich, St. Louis, MO) was used as a loading control. JAK2 V617F samples for JAK2/pJAK2 were run on separate gel than the rest of the samples. Signal for pYSTAT5 was quantified using densitometric analysis by ImageJ software.

To summarize, we show that the germline mutations *JAK2* T108A and L393V are weakly activating mutations that lead to hypersensitivity to EPO that confers a proliferative advantage and that the cooperation of the *JAK2* mutations V617F and T108A lead to higher activation of JAK-STAT signaling. We further hypothesize that *JAK2* germline mutations may represent a mechanism which may precede acquisition of *JAK2* V617F lesion during the evolution of PV phenotype and may contribute to further genomic alterations in PV clone and perhaps even leukemic transformation. To our knowledge, this is the first description of an association of gain-of-function germline *JAK2* mutations coexisting with *JAK2* V617F in subjects with PV phenotypes. Interestingly, these patients had documented normal blood count years before diagnosis, however, after developing the PV phenotype, both eventually progressed to AML or to MDS transforming within months to AML. Whether these germline mutations increase the probability of acquiring PV is suggestive. Moreover, the L393V mutation was found with increased frequency among diffuse large B-cell tumors[238], and T108A has been reported in an adenocarcinoma cell line[239], further supporting their potential to predispose to malignancy.

4.1.2 Co-occurring *JAK2* V617F and R1063H mutations increase JAK2 signaling and neutrophilia in MPN patients

Recently, two germline *JAK2* mutations, E846D and R1063H, were described in a case of hereditary erythrocytosis[2], while the same *JAK2* R1063H variant was initially reported in 3 out of 93 PV patients that were *JAK2* V617F-positive.[3] The frequency cited in the normal population for R1063H in the Exome Aggregation Consortium database[240] is much lower (0.004377), being described as a very rare polymorphism. In cooperation with the team of Dr. Constantinescu, Dr. Divoky and Dr. Mambet from Romania, we assessed the presence of *JAK2* V617F and *JAK2* R1063 mutations in a cohort of 390 MPN patients from Romania and Belgium, to characterize phenotypically the double mutation carriers and gain insight into the functional consequences of coexisting mutations on JAK2 signaling.

Samples from 390 MPN patients positive for *JAK2* V617F from Romania (314) and Belgium (76) were collected for the study. *JAK2* R1063H mutation screening was performed using a custom TaqMan SNP Genotyping Assay. 14 MPN patients out of 390 *JAK2* V617F-positive MPN patients were found to carry concurrently *JAK2* V617F and R1063H mutations, their clinical features and hematological data recorded at disease onset being summarized in Table 1. ET was the most frequent diagnosis in double *JAK2* V617F and R1063H mutation carriers (9/14). After taking into account the bone marrow histological findings and the new WHO 2016 criteria for PV diagnosis[241], 2 patients were reconsidered as having PV.

When analyzing hematological parameters in MPN patients at the time of diagnosis a significantly higher WBC count (P=0.023) and, correspondingly, a significantly higher neutrophil count (P=0.025) were observed in double mutation carriers compared to patients harboring only *JAK2* V617F. Although a tendency towards higher hemoglobin levels and platelet counts was observed in carriers of both mutations, the differences were not statistically significant (Figure 8A). When patients with ET diagnosis were analyzed separately, we found that carriers of both mutations displayed a significantly higher neutrophil count (P=0.031) and hemoglobin level (P=0.046) than V617F-positive ET patients (Figure 8B). Furthermore, in 5 patients there was at least one thrombotic event during the course of the disease, including 2 cases of portal vein thrombosis, stroke, recurrent arterial

and venous thromboses and additionally, 1 PV patient manifested multiple superficial thrombophlebitis. Interestingly, in a recent genomic study of patients with venous thromboembolism, *JAK2* R1063H was identified in one case, being considered a probable disease-causing variant.[242] One additional patient originally included into the cohort was after revision found to be *JAK2* V617F-negative, but R1063H-positive and carried *CALR* somatic mutation (CALRdel52).

Table 1. Clinical data of *JAK2* V617F-positive MPN patients (n = 390) subdivided according to *JAK2* R1063H mutation status. (data analyzed by a cooperating investigator) Data for V617F only (n = 376) and V617F/R1063H double mutation carriers (n = 14) were recorded at diagnosis. Abbreviations: PV, Polycythemia Vera; ET, Essential Thrombocythemia; PMF, Primary Myelofibrosis; MPN-U, MPN Unclassifiable; WBC, White Blood Cell

Variables	Patients JAK2 V617F/R1063H positive (n=14)	Patients JAK2 V617F positive (n=376)	*P* value
Sex ratio (male/female)	5/9	157/219	
Age, years, median (range)	60 (34-80)	61(16-92)	
MPN subtype (PV/ET/PMF/MPN-U)	5/7/2/0	115/205/34/22	
Hemoglobin g/dL, median (range)	15.8 (10.6 - 19.5)	14.7 (7.3 - 24.0)	0.43
WBC count × 10^9/L, median (range)	13.3 (9.9 - 41.6)	10.2 (4.6 - 31.6)	**0.023**
Neutrophil count × 10^9/L, median (range)	9.0 (6.9 - 34.2)	7.4 (2.6 – 26.8)	**0.025**
Platelet count × 10^9/L, median (range)	730 (363 - 1000)	670 (74 - 2025)	0.87
JAK2 V617F allele burden %, median (range)	21.3 (7.1 - 83.5)	32.0 (5.5 - 89.9)	0.78

.

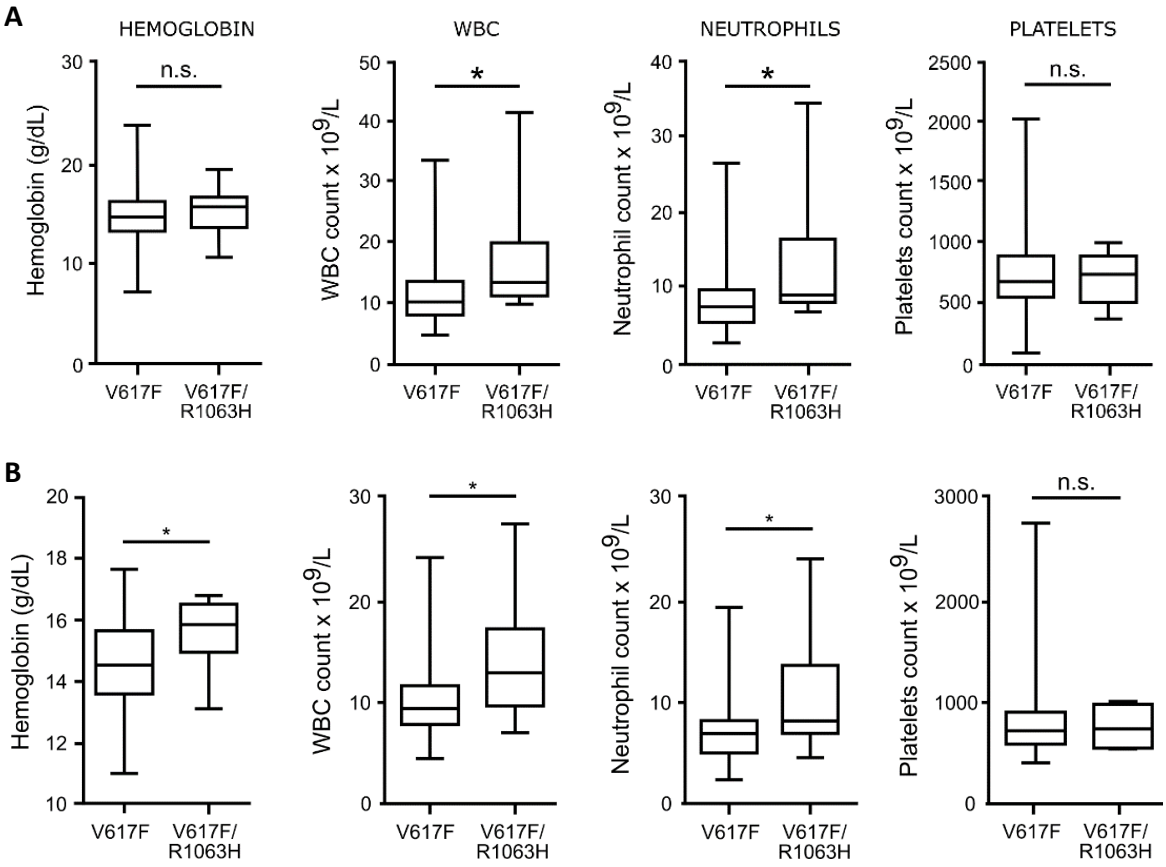

Figure 8. Hematological data of *JAK2* V617F MPN patients (n = 390) and ET patients (n = 212) subdivided according to the *JAK2* R1063H mutation status. (data analyzed by a cooperating investigator) (A) Hematological data for MPN patients V617F only (n = 376) and V617F/R1063H double mutation carriers (n = 14). (B) Data recorded for ET patients *JAK2* V617F only (n = 205) and V617F/R1063H double mutation carriers (n = 7). Data were recorded at diagnosis. The boxes represent 25% to 75% interquartile range, horizontal lines within the boxes indicate medians, and vertical bars show the range of values (minimum to maxium). Mann-Whitney U test was used to assess the statistical significance. P values <0.05 were considered statistically significant.

In order to evaluate whether the presence of *JAK2* R1063H mutation is associated with increased molecular complexity and mutational load, we searched for the presence of additional mutations in genes known to be involved in myeloid malignancies using targeted next-generation sequencing (NGS) panel. We compared the frequency of additional somatic mutations in the analyzed patient group of double-mutated patients with 53 randomly selected patients from the *JAK2* V617F cohort without the R1063H variant (Table 2 and 3). Additional mutations were identified in 8 out of 14 screened double-mutated patients and a total of 11

variants in 7 genes were detected. Five of these mutations are indexed in the dbSNP database, and 4 of these specific variants are listed in the COSMIC catalogue. One additional mutation in *DNMT3A* was published recently.[243] Two other mutations (frameshift in *TET2* and premature stop codon in *DNMT3A*) do not have SNP/COSMIC IDs, but are documented on VarSome genomic variant database. The *GATA2* (A164T) allele (Patient 12) was recently detected in higher than expected frequency in MDS, suggesting a possible predisposing function in myeloid malignancies.[244] Two patients harbor unique undescribed variants, Patient 1 in *BCOR* and Patient 9 in *TET2*. The *BCOR* variants were identified in two patients (both are missense mutations); their variant frequency being of 54% for Patient 1 and 99.5% for Patient 11. They could be germline variants; both were estimated to be 'damaging' or 'probably damaging' by 2 algorithms (Sift, PolyPhen). Additional mutations in 12 out of 53 screened *JAK2* V617F patients (after the exclusion of *GATA2* (A164T) variant, which was recently associated with increased risk of developing myeloid malignancy[244]) were identified, and a total of 17 variants in 8 genes were detected. Two of these mutations are indexed in the dbSNP database, and 7 of these specific variants are listed in the COSMIC catalogue. Seven patients harbor unique undescribed variants. Although a trend toward a higher mutational load was observed in the double mutated V617F/R1063H group, compared to V617F group, the difference did not reach statistical significance (P=0.092). The mutational landscape and the number of additional somatic mutations seemed to be comparable to previous studies of *JAK2* V617F-positive MPNs.[245] All mutations were identified in DNA collected at the time of diagnosis; acquisition of additional mutations during disease evolution was not studied. The analysis of NGS was performed in cooperation with Dr. Belickova and Mgr. Vesela from the Institute of Hematology and Blood Transfusion, Prague, Czech Republic.

Next, we aimed to characterize the configuration of JAK2 mutations in the double-positive MPN patients. *Cis/trans* configurations of *JAK2* V617F and R1063H mutations were established by sequencing single colonies of sub-cloned *JAK2* cDNA obtained from peripheral blood leukocytes in 10 out of 14 double-mutated patients. *Cis* configuration of the mutations was detected in 6 cases and *trans* configuration in 4 cases (Table 4).

Table 2. Detailed information about mutations identified by TruSight Myeloid Sequencing Panel for the MPN patients exhibiting *JAK2* V617F and *JAK2* R1063H mutations. (data analyzed by a cooperating investigator) ** Denotes likely inherited *GATA2* (A164T) variant, recently associated with increased risk of developing myeloid malignancy.[244] Abbreviations: D, deleterious; PD, probably damaging; T, tolerated; B, benign; NA, not available. DbSNP ID: ID in The Single Nucleotide Polymorphism database. (1) This variant does not have SNP/COSMIC ID, but has been repeatedly viewed on VarSome.

Patient	Diagnosis	Additional mutations										
		Gene	CDS mutation	Protein change	Chr	Type	Var Freq [%]	Var Type	Sift	PolyPhen	dbSNP ID	References
1	PV	*BCOR*	c.1231C>T	p.R411W	X	snv	54.0	missense	D	PD	NA	
2	ET	*TET2*	c.3556_3557insA	p.G1187fs	4	insertion	3.1	frameshift	NA	NA	NA	(1) www.varsome.com/variant
3	ET	*not detected*										
4	ET	*DNMT3A*	c.1095C>G	p.Y365*	2	snv	3.7	stop	NA	NA	NA	(1) www.varsome.com/variant
		TET2	c.2599T>C	p.Y867H	4	snv	51.2	missense	D	PD	rs144386291	COSM327337
5	PV	*not detected*										
6	ET	*not detected*										
7	ET	*not detected*										
8	PMF	*not detected*										
9	PMF	*TET2*	c.4820C>A	p.S1607*	4	snv	2.3	stop	NA	NA	NA	
10	PV	*DNMT3A*	c.2104G>T	p.D702Y	2	snv	9.1	missense	D	PD	NA	PMC4797027
		CBLB	c.1399G>A	p.V467I	3	snv	61.8	missense	T	B	rs371993076	COSM1035961
		ZRSR2	c.1314_1315insAGCCGG	p.R448_R449insSR	X	insertion	39.4	in-frame	NA	NA	rs779595035	COSM5762985
11	ET	*BCOR*	c.4943C>T	p.P1648L	X	snv	99.5	missense	D	PD	rs763651353	
12	PV	*GATA2***	c.490G>A	p.A164T	3	snv	57.5	missense			rs2335052	
13	PV	*not detected*										
14	ET	*EZH2*	c.1582T>A	p.C528S	7	snv	7.0	missense			NA	

As we only had an access to granulocyte DNA, in order to detect the genotype of the R1063H variant we emloyed the absolute quantification method digital droplet PCR (ddPCR). In 8 patients the R1063H variant was heterozygous, likely inherited, as shown previously[2] (the percentage of the mutant allele being around 50%). Strikingly, in 3 patients with a high *JAK2* V617F allelic burden a nearly homozygous status for R1063H was identified (a fractional abundance >80%). As shown in Figure 9, the presence of minor fraction of the wild-type allele excluded germline homozygosity, suggesting that one R1063H allele was inherited and the second one was acquired by uniparental disomy (UPD). In 3 other patients who exhibited trans configuration of *JAK2* mutations (Table 4, Figure 9), low R1063H allele burden was found (allele percentage between 20.7% - 31.5%), raising the hypotheses that R1063H was either acquired in the course of the disease, or it was partially lost due to UPD of the V617F-non-R1063H clone which, when amplified, decreased R1063H allelic burden. Because non-myeloid tissue DNA was not available for the study, we used a combined array-comparative genomic hybridization/single-nucleotide polymorphism (aCGH/SNP) assay to detect unbalanced chromosomal changes and copy number neutral loss of heterozygosity in DNA samples with low R1063H allele burden. We detected UPD on chromosome 9p in 2 out of 3 samples, suggesting that both hypotheses could be valid (experiment performed by a cooperating investigator; data not shown). However, without germline DNA, the origin of R1063H mutation cannot be unequivocally established.

Table 3. Detailed information about mutations identified by TruSight Myeloid Sequencing Panel for the *JAK2* V617F-positive/R1063H-negative patients in our cohort. (data analyzed by a cooperating investigator) Additional mutations were identified in 12 out of 53 screened patients (after the exclusion of *GATA2* (A164T) SNP). # Denotes variants that are listed in the COSMIC catalogue; ** Denotes likely inherited *GATA2* (A164T) variant (11 times in heterozygous and 2 times in homozygous configuration), the variant comprises 14% of allele frequency, which is consistent with the expected frequency (European non-Finnish 15% allelic frequency - http://gnomad.broadinstitute.org/variant/3-128204951-C-T; European 18% allelic frequency - https://www.ncbi.nlm.nih.gov/projects/SNP/snp_ref.cgi?

rs=2335052). Abbreviations: PV, Polycythemia Vera; ET, Essential Thrombocythemia; PMF, Primary Myelofibrosis; NA, not available; dbSNP ID: ID in The Single Nucleotide Polymorphism database.

Patient	Diagnosis	JAK2 V617F allele burden [%]	Gene	Protein change	Type	Var Freq [%]	dbSNP ID	
1	ET	4.0	not detected					
2	PMF	38.9	not detected					
3	PV	51.8	*GATA2***	p.A164T	snv	58.7	rs2335052#	COSM445531
4	ET	5.9	not detected					
5	PV	10.2	*ETV6*	p.R14*	snv	5.5	NA	
			*GATA2***	p.A164T	snv	56.7	rs2335052#	COSM445531
6	PMF	38.6	*GATA2***	p.A164T	snv	50.0	rs2335052#	COSM445531
7	PV	32.3	not detected					
8	PMF	19.5	*GATA2***	p.A164T	snv	99.1	rs2335052#	COSM445531
9	PV	83.1	not detected					
10	ET	10.6	*GATA2***	p.A164T	snv	48.9	rs2335052#	COSM445531
11	ET	5.4	*JAK2*	p.N542_E543del	deletion	10.0	NA#	COSM1757322
12	PV	54.7	not detected					
13	ET	34	not detected					
14	PV	46.6	*GATA2***	p.A164T	snv	56.3	rs2335052#	COSM445531
15	ET	18.6	*GATA2***	p.A164T	snv	47.5	rs2335052#	COSM445531
16	ET	8.4	not detected					
17	ET	14.9	not detected					
18	ET	38.9	not detected					
19	ET	19.8	*GATA2***	p.A164T	snv	49.0	rs2335052#	COSM445531
20	ET	18.1	not detected					
21	PMF	26.3	not detected					
22	ET	29.2	not detected					
23	PV	49.4	not detected					
24	PV	70.1	not detected					
25	ET	14.7	*GATA2***	p.A164T	snv	50.6	rs2335052#	COSM445531
26	PV	46.8	not detected					
27	PV	65.3	not detected					
28	ET	11.6	*ASXL1*	p.P805fs	deletion	6.8	NA	
29	ET	26.6	*KDM6A*	p.Q1377*	snv	4.6	NA#	COSM255009
30	PMF	41.2	*ZRSR2*	p.E362*	snv	89.1	NA#	COSM211059
			TET2	p.N377fs	deletion	10.4	NA	
31	PMF	91.6	not detected					
32	ET	18.6	not detected					
33	PMF	4.4	*KRAS*	p.R68S	snv	15.5	NA#	COSM183929
			SRSF2	p.H63P	snv	5.5	NA	
34	ET	12.3	not detected					
35	PV	22.1	not detected					
36	ET	13.5	*GATA2***	p.A164T	snv	56.8	rs2335052#	COSM445531
37	ET	28.0	not detected					
38	ET	32.8	*DNMT3A*	p.A884fs	deletion	35.3	NA	
39	PMF	19.9	*ASXL1*	p.P647fs	insertion	12.0	NA	
40	ET	13.8	not detected					
41	PMF	27.8	not detected					
42	PV	41.6	*TET2*	p.Q1030*	snv	45.8	rs780043982#	COSM4766113
43	ET	16.0	*GATA2***	p.A164T	snv	97.5	rs2335052#	COSM445531
44	early PV	23.3	*GATA2***	p.A164T	snv	48.4	rs2335052#	COSM445531
45	PV	80.3	*TET2*	p.D1384G	snv	18.2	NA#	COSM6023668
			DNMT3A	p.V897D	snv	17.8	NA#	COSM87000
46	PV	30.8	not detected					
47	ET	11.1	not detected					
48	ET	21.4	*GATA2***	p.A164T	snv	53.8	rs2335052#	COSM445531
49	PV	45.4	*TET2*	p.P1536fs	insertion	32.5	NA	
			TET2	p.L1065fs	deletion	12.8	NA	
			ASXL1	p.Q757*	snv	5.3	rs779078826#	COSM132979
50	PV	16.4	not detected					
51	ET	54.0	not detected					
52	PV	59.6	not detected					
53	ET	28.1	*TET2*	p.L1515*	snv	34.7	NA#	COSM5945064

We employed cellular models and dual luciferase assay to assess the functional consequences of coexisting *JAK2* V617F and *JAK2* R1063H mutations. We examined whether the *cis* or *trans* configuration of the 2 mutations might exert an additive effect on constitutive signaling over the *JAK2* V617F only expression. The analysis of STAT5 transcriptional activity induced by JAK2 WT, JAK2 V617F, JAK2 R1063H, and JAK2 V617F/R1063H (*cis*) mutants in γ-2A cells revealed a statistically significant higher constitutive activity of the double mutant compared to that of JAK2 V617F, in both homozygous and heterozygous configurations and with all 3 cytokine receptors, although JAK2 R1063H alone exhibits a similar level of basal activity as JAK2 WT (Figure 10). In the *trans* configuration of JAK2 V617F and JAK2 R1063H we did not observe a significant difference compared to JAK2 V617F and JAK2 WT. However, the transient nature of the experiment may have masked a weak effect. These results are supported by Western blot analysis, which assessed activated phosphorylated forms of JAK2, STAT5 and ERK1/2 demonstrating a higher level of constitutive activation of JAK2 and consequently STAT5 and ERK1/2 generated by the double V617F/R1063H mutant versus JAK2 V617F (Figure 10D). Leroy et al.[246] previously identified a specific circuit for activation of the JAK2 kinase domain by the V617F in the pseudokinase domain. Substitution of glutamic acid residue with a basic residue at position 596 of JAK2 (E596R) blocked JAK2 V617F constitutive activity, without affecting the cytokine-inducible signaling of wild-type or mutant JAK2. Both JAK2 V617F and JAK2 V617F/R1063H mutants decreased the constitutive STAT5 transcriptional activity of mutant JAK2 to the same extent when the E596R mutation was introduced. Thus, the R1063H variant amplifies signaling via the same circuit as V617F (Figure 10).

Table 4. Diagnosis, *JAK2* V617F allele burden, *JAK2* R1063H fractional abundance, *JAK2* V617F/R1063H mutations configuration and additional mutations identified by targeted NGS. (i) *JAK2* V617F allele frequency obtained from NGS study and compared with allele burden determined via qPCR and ddPCR assay. (ii) *JAK2* R1063H fractional abundance was determined using ddPCR in whole blood samples collected at the time of diagnosis. The *JAK2* R1063H mutation was considered as genuine germline only when the fractional abundance of the *JAK2* R1063H variant was 50 (±1.0) %. *JAK2* R1063H in three samples with percentage frequency of the mutant DNA between 20.7% - 31.5% (Samples no. 1, 5 and 14) could be considered as either acquired somatic mutation or an inherited variant that was partially lost due to UPD of the V617F-non-R1063H clone. (iii) *cis*/*trans JAK2* V617F/R1063H mutations configuration was determined through sequencing of subcloned RT-PCR products spanning exons 14 – 24 of the *JAK2* gene. (iv) TruSight Myeloid Sequencing Panel (Illumina, San Diego, CA, USA) was used for targeted mutational screening of *JAK2* R1063H-positive patients. # denotes variants that are listed in the COSMIC catalogue; § denotes the mutations that not have SNP/COSMIC IDs, but are documented on VarSome genomic variant database. All mutations were identified in DNA collected at the time of diagnosis. Abbreviations: PV, Polycythemia Vera; ET, Essential Thrombocythemia; PMF, Primary Myelofibrosis; NA, not available; ND, not done. DbSNP ID: ID in The Single Nucleotide Polymorphism database.

Patient	Diagnosis	*JAK2* V617F allele burden [%] (NGS/qPCR/ddPCR)	*JAK2* R1063H fractional abundance [%] (ddPCR)	*JAK2* VF/RH configuration	Additional mutations				
					Gene	Protein change	Type	Var Freq [%]	dbSNP ID
1	PV	66.6/56.4/64.2	9p UPD (20.7)	*trans*	***BCOR***	p.R411W	snv	54.0	NA
2	ET	9.6/8.8/11.1	heterozygous (50.8)	ND	***TET2***	p.G1187fs	insertion	3.1	NA§
3	ET	12.6/10.3/15.3	heterozygous (49.7)	ND	***not detected***				
4	ET	83.5/83.5/83.6	nearly homozygous (92.0)	*cis*	***DNMT3A***	p.Y365*	snv	3.7	NA§
					TET2	p.Y867H	snv	51.2	rs144386291#
5	PV	53.1/50.0/52.8	no 9p UPD (31.5)	*trans*	***not detected***				
6	ET	23.3/18.9/21.2	heterozygous (50.6)	ND	***not detected***				
7	ET	19.2/17.4/19.4	heterozygous (49.1)	*trans*	***not detected***				
8	PMF	26.8/23.7/25.4	heterozygous (50.5)	*cis*	***not detected***				
9	PMF	17.1/18.0/17.8	heterozygous (49.5)	*cis*	***TET2***	p.S1607*	snv	2.3	NA
10	PV	8.1/7.1/7.69	heterozygous (50.2)	*cis*	***DNMT3A***	p.D702Y	snv	9.1	NA20
					CBLB	p.V467I	snv	61.8	rs371993076#
					ZRSR2	p.R448_R449insSR	insertion	39.4	rs779595035#
11	ET	18.2/ND/16.4	heterozygous (49.7)	ND	***BCOR***	p.P1648L	snv	99.5	rs763651353
12	PV	73.2/72.7/73.2	nearly homozygous (84.5)	*cis*	***GATA2****	p.A164T	snv	57.5	rs2335052
13	PV	76.2/81.2/79.9	nearly homozygous (89.1)	*cis*	***not detected***				
14	ET	46.0/31.8/47.7	9p UPD (27.6)	*trans*	***EZH2***	p.C528S	snv	7.0	NA

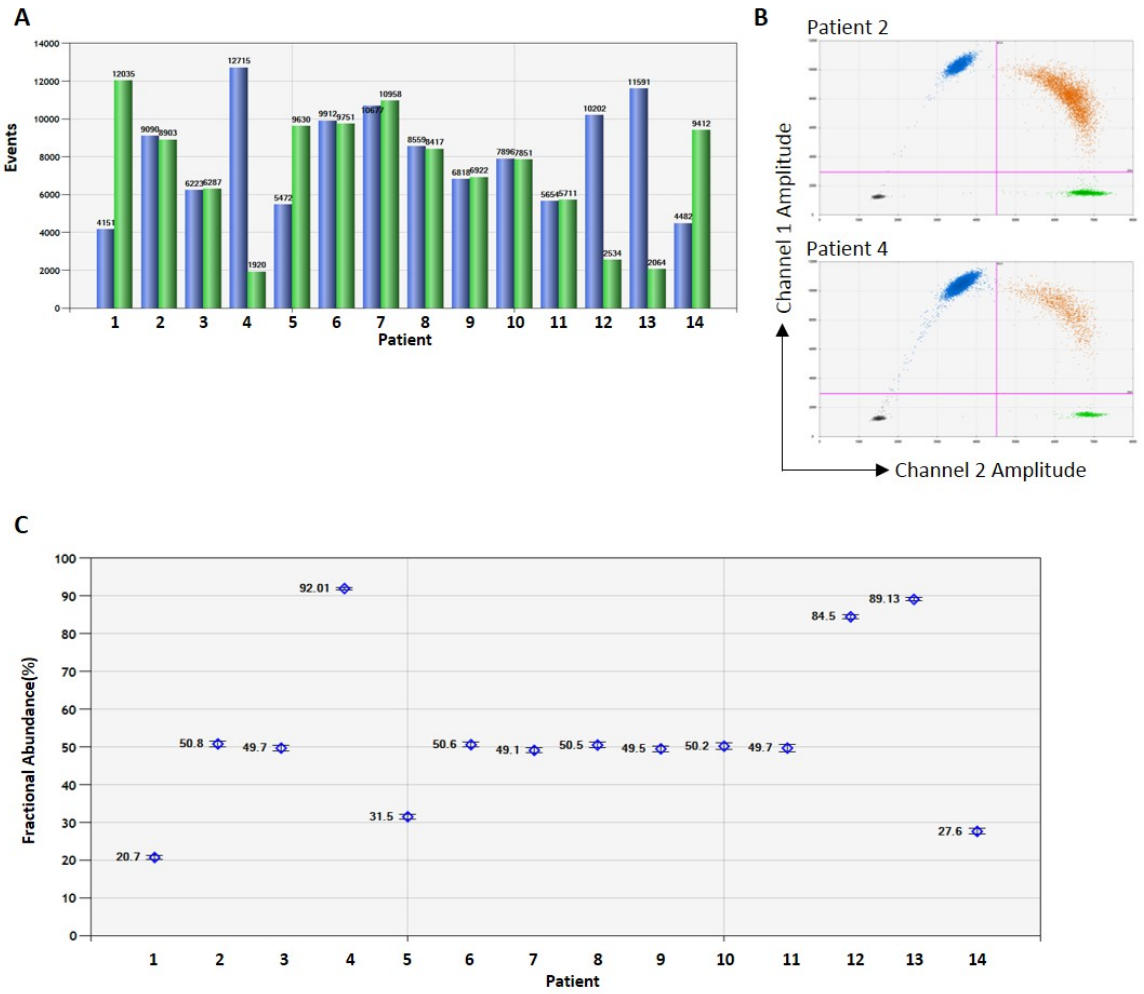

Figure 9. Quantification of *JAK2* R1063H allele in MPN patient samples using digital droplet PCR. Single-well measurements of hybridization probes FAM/HEX specific for *JAK2* R1063H and *JAK2* WT were analyzed by QuantaSoft software and the count collection areas were held constant for each sampling. (A) Comparison of number of events (amount of FAM- and HEX-positive droplets) of all analyzed patients. FAM fluorescence specific for the mutant allele is shown in blue while the HEX fluorescence specific for WT allele is shown in green. (B) 2-D fluorescence amplitude plot generated by QuantaSoft software shows single-well measurement of a sample from one patient. The black cluster on the plot represents the negative droplets, the blue FAM cluster represents the droplets that are positive for the mutant DNA only, the green HEX cluster is specific for wild-type DNA only, and the orange cluster represents the droplets that are positive for both mutant and wild-type DNA. Patient 2 is presented as an example of a heterozygous sample compared to nearly homozygous sample obtained from Patient 4. (C) Fractional abundance plot shows the percentage frequency of the mutant DNA in a wild-type DNA background. As presented in the boxplot, patients 1, 5 and 14 have low *JAK2* R1063H mutation allelic burden (20.7%,

31.5% and 27.6% of template copies detected carried the mutation, respectively) and were examined for the presence of 9p UPD. Patients 4, 12 and 13 are nearly homozygous since 92.01%, 84.50% and 89.13% template copies carry the *JAK2* R1063H mutation, respectively. We hypothesize that one allele was inherited while the second one was acquired by UPD. This is also supported by the fact that allelic burden of *JAK2* V617F mutation in these patients is 83.5%, 73.2% and 76.2%, respectively. All the rest of the patients analyzed are heterozygous. All error bars generated by QuantaSoft software represent the 95% confidence interval.

In a previous study[246], a specific circuit was identified for activation of the JAK2 kinase domain by the V617F mutation in the pseudokinase domain. We asked whether the R1063H variant in *cis* amplifies signaling via the same circuit or creates distinct conformational effects. In the same study it was demonstrated that substitution of glutamic acid residue with a basic residue at position 596 of JAK2 (E596K and E596R) abolished the JAK2 V617F constitutive activity without affecting the cytokine-dependent signaling via mutant or wild-type JAK2.[246] We sought to test the effect of the E596R mutation on the activity of the JAK2 V617F/R1063H double mutant. As described above, we introduced the E596R mutation into pMEGIX coding for human JAK2 V617F, R1063H, and V617F/R1063H constructs and STAT5 transcriptional activity of the new mutants was assessed in γ-2A cells by dual luciferase assay, in the presence of TPOR. Introducing the E596R mutation decreased to the same extent the constitutive transcriptional activity of both JAK2 V617F and JAK2 V617F/R1063H mutants (Figure 10E), suggesting that the R1063H variant amplifies signaling via the same circuit as V617F.

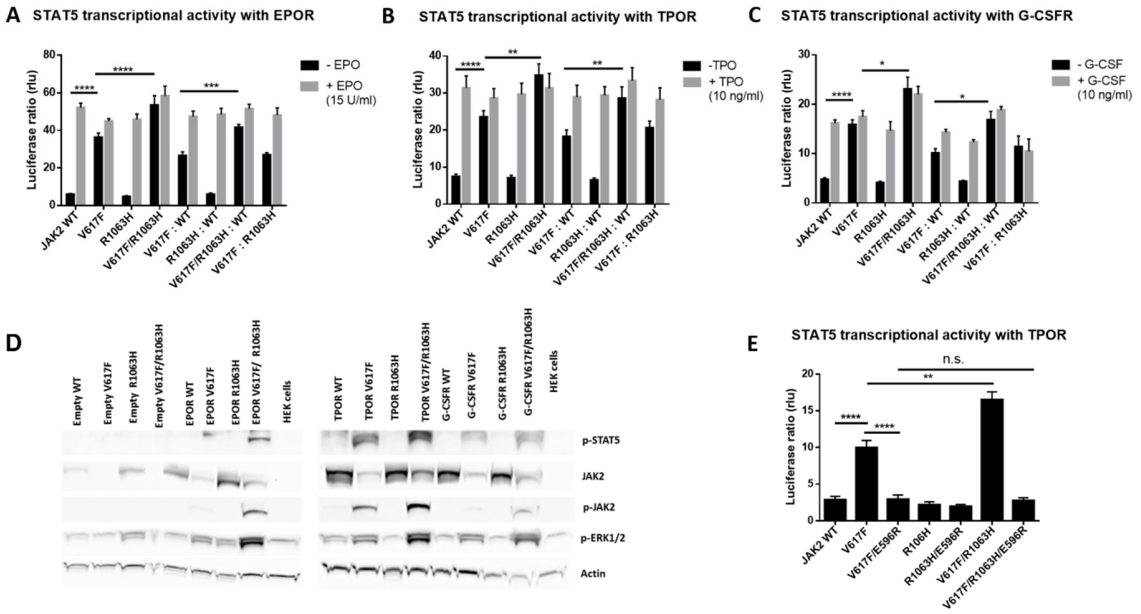

Figure 10. STAT5 transcriptional activity and the status of activation of downstream signaling by human JAK2 V617F and R1063H in the presence of dimeric myeloid cytokine receptors. (experiment performed by a cooperating investigator) (A-C) Constitutive and cytokine-dependent STAT5 transcriptional activity assessed by dual-luciferase assay in γ2A cells transfected with JAK2 WT, JAK2 V617F, JAK2 R1063H, and JAK2 V617F/R1063H double mutant in the presence of EPOR (A), TPOR (B) and G-CSFR (C). Homozygous as well as heterozygous states of JAK2 mutants are mimicked. Shown are averages of nine replicates from three independent experiments ± standard error of the mean (SEM). Statistical analysis was assessed by one-way ANOVA followed by the post-hoc Tukey's test. *P <0.05, **P<0.01, ***P <0.001, ****P<0.0001. rlu: relative light unit. (D) Western blot analysis of the constitutive JAK2, STAT5 and ERK 1/2 phosphorylation levels (indicative of activated status) induced by human JAK2 mutants co-expressed with empty vector/cytokine receptors in HEK 293T cells. β-actin antibody was used as a loading control. Higher levels of p–JAK2 (p-Tyr1007/1008), p-STAT5 (p-Tyr694) and p-ERK ½ (p-Thr 202/p-Tyr 204) are observed in cells expressing JAK2 V617F/R1063H double mutant in comparison to JAK2 V617F. Image shown is representative of three independent experiments. (E) The effect of E596R mutation on the constitutive STAT5 activation induced by JAK2 V617F and JAK2 V617F/R1063H evaluated by dual luciferase assay in γ2A cells in the presence of TPOR. Both mutated proteins exhibit a similar decline in constitutive activity. The graphs display the averages of nine replicates from three independent experiments ± standard error of the mean (SEM). One-way ANOVA followed by the post-hoc Tukey's test was used for statistical analysis. ****P<0.0001. n.s.: not significant, rlu: relative light unit.

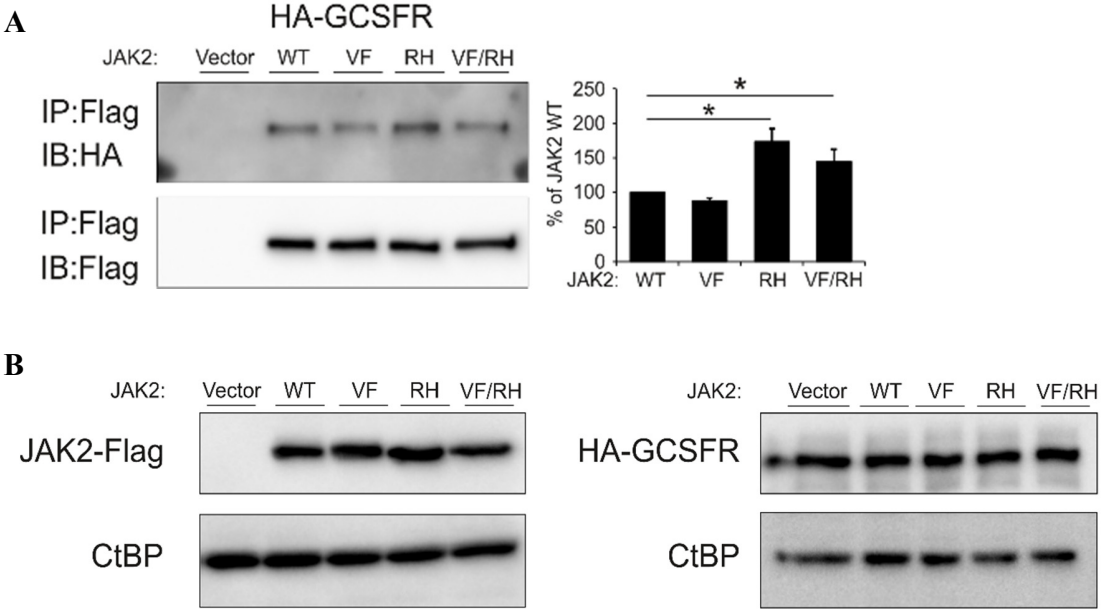

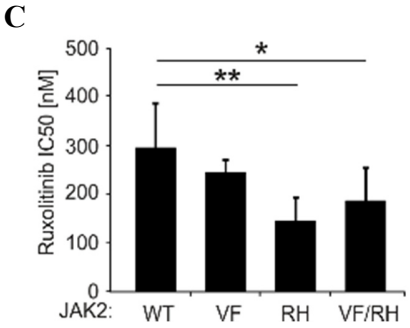

Figure 11. The binding affinities of JAK2 mutants to G-CSFR (A-B) and *in vitro* drug sensitivity assay (C). (A) JAK2 mutants bind to cytokine receptor G-CSFR with different affinities. Flag-tagged JAK2 mutants were transiently expressed in HEK 293 cells in which HA-tagged G-CSFR was stably expressed. Interaction was examined by co-immunoprecipitation with anti-Flag affinity gel. Immunoblot band intensity was quantified by ImageJ software and normalized to a loading control, and wild-type JAK2 intensity was set to 100%. The data represent the mean of three independent experiments; T bars designate standard error of the mean (SEM). For statistical analysis Student's paired t test with equal variance was employed and P values <0.05 were considered statistically significant. WT: wild type, VF: V617F, RH: R1063H, VF/RH: V617F/R1063H, IP: immunoprecipitation. IB: immunoblot. (B) Levels of HA-tagged G-CSFR and FLAG-tagged JAK2 in lysates are comparable when different JAK2 mutants are expressed in HEK 293 cells. TCL were immunoblotted alongside the immunoprecipitated samples. As a loading control CtBP protein was detected. WT: wild type, VF: V617F, RH: R1063H, VF/RH: V617F/R1063H. (C) (experiment performed by a cooperating investigator) *In vitro* drug sensitivity assay. Stably transfected Ba/F3/EPOR cells expressing JAK2 WT, JAK2 V617F, JAK2 R1063H, and JAK2 V617F/R1063H were cultivated for 72 hours with decreasing concentration of JAK2 inhibitor Ruxolitinib (concentrations: 1; 0.5; 0.25; 0.1; 0.05; 0.01; 0.001; 0 μM). The IC50 value was defined as drug concentration needed to inhibit 50% of cell growth (using GraphPad Prism 6.01 software). The data show mean of 7 independent

experiments performed in triplicates (see also supplemental Material and Methods for details). T bars designate standard deviation (SD). When the Ruxolitinib sensitivity of mutant cells is compared to wild-type cells, the sensitivity of V617F-positive cells is not statistically significant, while R1063H-positive and V617F/R1063H double mutant cells are significantly more sensitive to Ruxolitinib than wild-type cells. Statistical significance was assessed using one-way ANOVA followed by post-hoc Tukey's test and $P<0.05$ was considered as statistically significant. Experiments with AZ-960 revealed comparable results (not shown). WT: wild type, VF: V617F, RH: R1063H, VF/RH: V617F/R1063H.

Although in patients we observed a significant increase in neutrophilia, all 3 receptors, not only G-CSFR, supported the higher activation of signaling by JAK2 V617F/R1063H. This is possibly an outcome of our overexpressing system. To further investigate the observed neutrophilia in JAK2-double mutant patients, irrespective of *cis* or *trans* configuration, we assessed the binding affinities of JAK2 mutants to G-CSFR, which regulates neutrophilic granulocyte formation. Using co-immunoprecipitation, a significant biochemical association was detected between JAK2 R1063H and JAK2 V617F/R1063H and G-CSFR, when compared to JAK2 V617F or JAK2 (Figure 11A). This might have a significant impact on signaling at low receptor levels *in vivo.* The interpretation of JAK2 variants' binding to G-CSFR is not so straightforward, as the association of JAK V617F mutant with the receptor is lower than the one of JAK2 WT, even though it leads to stronger receptor activation. Also, it is possible that R1063H variant might exert an effect on G-CSFR stimulated pathways other than JAK2/STAT5. Linking neutrophilia to the increased association of JAK2 V617F/R1063H to G-CSFR is in agreement with a recent study where differential coupling of JAK2 mutants to different receptors impacted the *in vivo* phenotypes induced by the different mutants.[101] In ET double-mutant carriers, the higher level of hemoglobin that accompanied the higher neutrophil count supports the hypothesis that co-occurrence of *JAK2* V617F and R1063H mutations would lead to an ET phenotype with PV-like features, due to a cumulative effect on *JAK2* signaling.[247] Furthermore, we show that JAK2 V617F/R1063H-expressing cells are more sensitive to Ruxolitinib when compared to single V617F-mutants, which may have therapeutic implications (Figure 11B).

We demonstrated that *JAK2* R1063H variant when present on the same allele with the *JAK2* V617F mutation increases the constitutive activity of *JAK2* V617F, which is the most prevalent MPN driver mutation. The frequency of R1063H in our *JAK2* V617F-positive MPN

cohort (14/390) is consistent with the initial report (3/93 PV patients), which is much higher than the frequency cited in the normal population for R1063H in the Exome Aggregation Consortium database.[240] More studies on control populations of different regions, on large patient populations, and on families with MPNs, would be necessary for determining whether *JAK2* R1063H predisposes to acquisition of the *JAK2* V617F mutation, and also to assess its role in MPN progression. One of the patients (patient 5) included in the cohort possibly acquired the JAK2 R1063H mutations, which would represent a new mechanism by which JAK2 oncogene can acquire increased oncogenic activity, in addition to known V617F homozygosity, as a consequence of acquired UPD of chromosome 9p13 or amplification of JAK2 in certain lymphomas.[248] Interestingly, the cooperation of R1063H and V617F mutations leads to neutrophilia, but in previous report the cooperation of R1063H and E846D mutations lead to erythrocytosis without an increase in neutrophil levels.[2] The precise mechanism of action of the JAK2 R1063H in cooperation with other *JAK2* mutations remains to be elucidated.

4.2 Protective molecular mechanisms preventing the progression of Myeloproliferative Neoplasms

In order to functionally characterize the role of KAP1 in cells harboring *JAK2* V617F mutation, we created cell line U2-OS (human bone osteosarcoma epithelial cells) harboring *JAK2* V617F mutation by homologous repair mediated with CRISPR/Cas9 system. The homologous template was created as described in the chapter *Methods and Materials*, and its mutagenesis was verified by sequencing (Figure 12A). U2-OS cell line is often used in DNA repair studies as it is easy to manipulate with and has a well characterized DNA damage repair pathway, including wild-type p53 protein. For this reason we decided to study DDR mechanisms induced by the *JAK2* V617F mutation in this particular cell line.

After cell sorting, 171 single cell colonies were screened using restriction enzyme cutting of a PCR product by *BsaXI* enzyme (Figure 12B). 18 were screened as homozygous for *JAK2* V617F allele and 18 screened as heterozygous *JAK2* WT/V617F. In 5 of the proposed homozygous and 5 heterozygous clones *JAK2* DNA region of interest was sequenced by GATC Biotech Company to confirm the presence of V617F mutation. Two homozygous clones were confirmed to be homozygous (matching the reference sequence 100%), clone 162 and 171 (Figure12C). All the proposed heterozygotes had one allele repaired according to the HR template (*JAK2* V617F) while the second one contained aberrations such as insertions and deletions, and were therefore excluded from further studies.

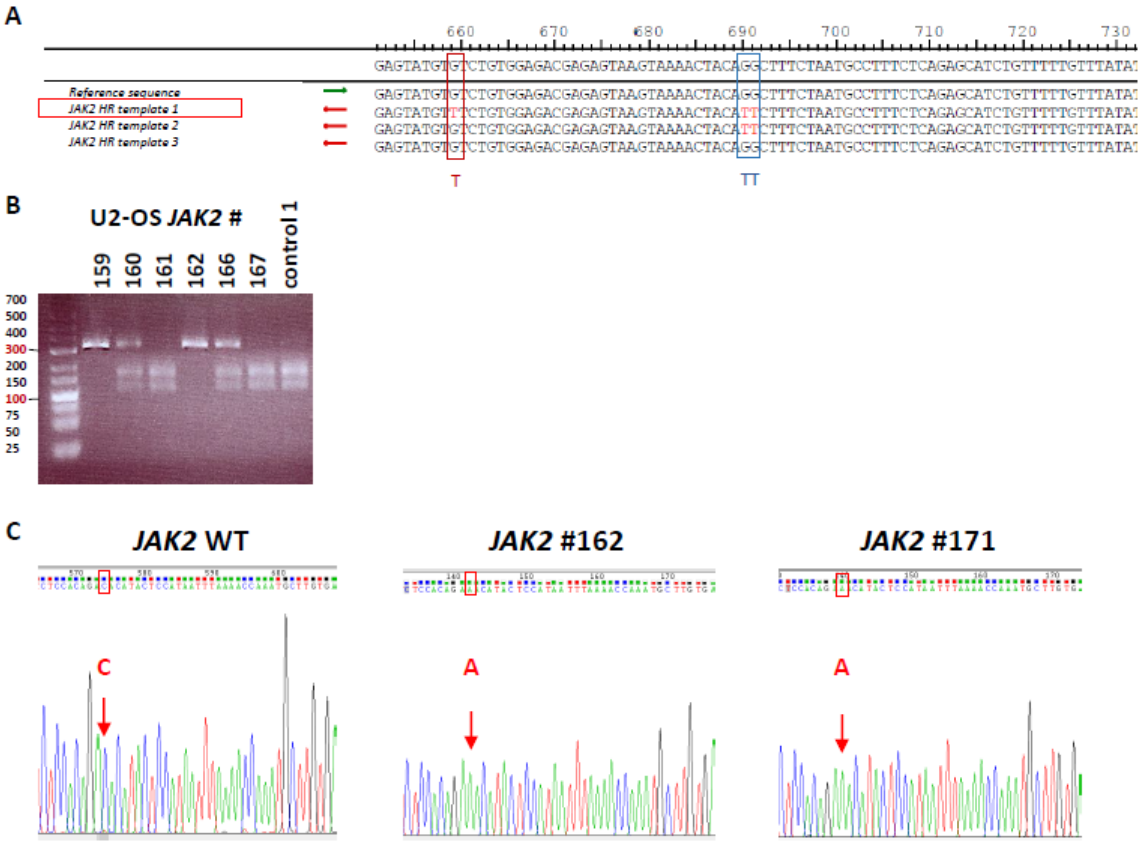

Figure 12. Generation of U2-OS JAK2 V617F clones. (A) Sequencing of the homologous template revealed a mutation in the part of *JAK2* gene c.1849G>T (V617F) highlighted in red and wobbling of the PAM sequence GG>TT highlighted in blue. Homologous template 1 was used for homologous recombination in U2-OS cells and homologous template 2 was used for homologous recombination in HEL cells. (B) An example of electrophoresis gel shows restriction enzyme cutting screen of U2-OS clones. Cell clones were single cell sorted, expanded and their genomic DNA extracted, serving as a template for PCR. PCR product was subsequently digested using *BsaXI* enzyme which recognizes *JAK2* WT and cuts it into two fragment of 145 bp and 158 bp. PCR fragment containing *JAK2* V617F mutation is not recognized and stays intact, 303 bp long. (C) Sequencing analysis of *JAK2* mutations in cell clones U2-OS JAK2 HR 162 and 171, confirming they carry homozygous *JAK2* V617F mutation.

We evaluated the functional consequences of the *JAK2* mutation V617F on STAT transcriptional activation by employing a dual luciferase assay measured with STATs responsive elements reporter. As presented in Figure 13, the basal level of JAK-STAT signaling activity is unchanged in U2-OS JAK2 clones 162 and 171 compared to control cells.

As the amount of STAT5 protein is very low in U2-OS cells (Figure 13C), it was provided externally by co-transfecting STAT5-expressing plasmid together with the reporter and pRL control. No difference in the luciferase production was, however, observed when comparing the studied clones and control cells. Consequently, we decided to test, whether these cells would respond to EPO stimulation given that we provide them with EPOR. As seen in Figure 13B, stimulation with EPO does not activate STATs signal in these cells. Immunoblotting further demonstrates that the levels of JAK2 and STAT5 proteins are below detectable level. *JAK2* expression is on average about 32 – 64 times (5 - 6 cycles) lower in U2-OS cells than in control human erythroleukemia (HEL) cells as shown by qRT-PCR. We therefore concluded that U2-OS cell line is not a suitable cell line for studying JAK2 signaling and its effect on DDR.

Consequently, we studied the effect of *JAK2* V617F mutation on DDR in a cell line with activated JAK-STAT signaling - HEL cell line. HEL cells are homozygous for *JAK2* V617F mutation and we decided to study DDR mechanisms and the role of KAP1 protein in PV progression in this cell line despite the fact that they carry a mutated *TP53* gene encoding for p53.

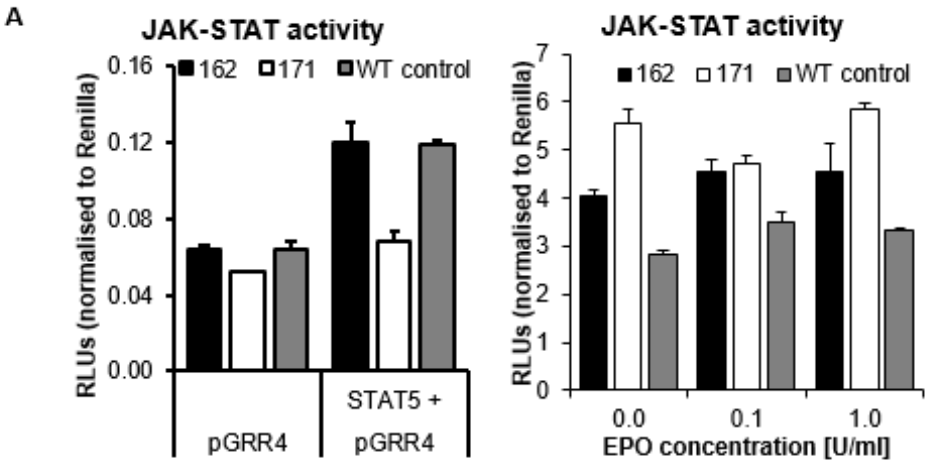

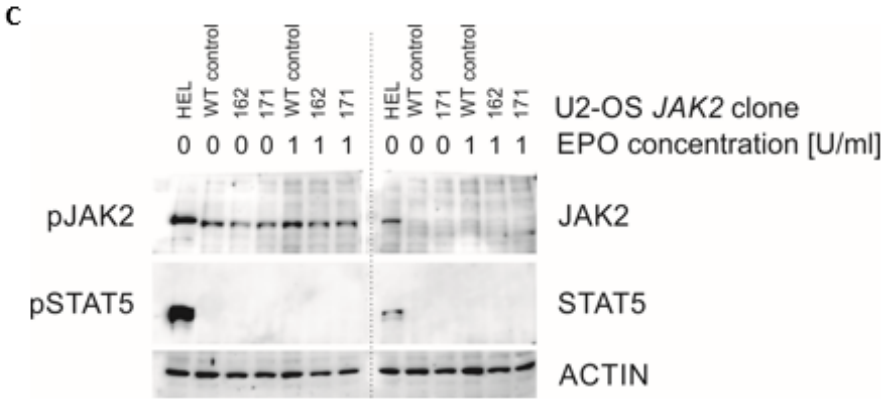

D

	WT control	162	171	HEL
GUSB	24.82	25.54	25.89	25.72
RPLP0	20.78	20.58	20.98	20.53
JAK2	32.54	32.54	32.92	26.87

Figure 13. Functional analysis of U2-OS JAK2 V617F clones. (A) Luciferase assay was performed by transfecting cells with pGRR4-Luc reporter both alone or together with STAT5 expressing vector (plus transfection control pRL) and measuring luciferase signal from cell lysates 48 hours after transfection. U2-OS JAK2 V617F clones do not exhibit elevated JAK-STAT signaling even when STAT5 is provided to them externally compared to control cells. JAK-STAT signaling is unaffected in U2-OS JAK2 clone 171 with the expression of STAT5 unlike in U2-OS JAK2 clone 162 and control cells. Bars represent mean from transfection triplicate ± standard deviation. (B) Luciferase assay (same as in A, STAT5 and EPOR expressing plasmids co-transfected with reporter plasmid and a transfection control pRL) was performed in U2-OS cell clones that were stimulated with two concentrations of EPO 24 hours after transfection. Luciferase signal was measured 24 hours after stimulation from cell lysates. JAK-STAT signaling is elevated in U2-OS JAK2 clone 171 compared to control

cells, however, none of the signals increase after EPO stimulation. Bars represent mean from transfection triplicate ± standard deviation. (C) Western blot from cell lysates of U2-OS JAK2 clones and control cells stimulated with EPO. Cells were transfected with EPOR expressing plasmid and stimulated with two concentrations of EPO 24 hours later. 24 hours after the stimulation cells were lysed using RIPA buffer and used for immunoblotting. Phosphorylated JAK2 protein is detected in U2-OS cells even though the total JAK2 protein is not visible,. However, the molecular weight of pJAK2 visible on the blot is lower than that of pJAK2 from the positive control HEL cells. This might be an indicator that the pJAK2 band from U2-OS cells is non-specific and pJAK2 of the correct size is not detectable. STAT5 was not detected in U2-OS cells. (D) qRT PCR data show low *JAK2* expression in U2-OS cells which is about 32 – 64 times (5 - 6 cycles) lower than in a positive control HEL cells. House-keeping genes *GUSB* and *RPLP0* were used as a control.

To characterize the differences in cell signaling initiated by *JAK2* V617F mutation, *JAK2* gene was 'repaired' by homologous recombination using CRISPR/Cas9 system. HEL cells were problematic to transfect and despite using a system with highest efficiency of transfection (as measured in a pilot experiment) - Amaxa® system electroporation, the survival rate after electroporation was shown to be only about 34% (determined by DNA stain Hoechst 33258 during cell sorting), while the transfection efficiency was about 16% of living cells (as measured during cell sorting by the GFP signal expressed from the control plasmid pART, after gating the living Hoechst 33258-negative cells). Due to poor cell survival the procedure was repeated several times in order to obtain clones positive for *JAK2* WT. However, the generation of HEL *JAK2* WT homozygotes was unsuccessful. I propose that this was due to the importance of *JAK2* V617F oncogene for the survival of HEL cells. The dependency on oncogene for cell survival has been reported previously[249,250] and is also termed 'oncogene addiction'. Although HEL cells are most probably not entirely dependent on the *JAK2* V617F mutation for their survival, as one of the clones did survive *JAK2* loss-of-function (LOF) and was further proliferating (Figure 14), their fitness and ability to form colonies from a single cell is affected. They seem not to survive the physical stress of electroporation and subsequent cell sorting efficiently. After adjusting the cell treatment conditions to sorting in warm media (thus not changing the temperature during the procedure of cell sorting) and using conditioned media for collecting cells the cell survival was increased from 1% (percentage of number of colonies grown per number of cells sorted) to approximately 5% of sorted cells. Furthermore, using HR activators RS-1 (7.5μM), Brefeldin

A (0.1μM) and NHEJ inhibitor SCR7 (1μM) did not enhance HR and thus further improve the fitness of cells.

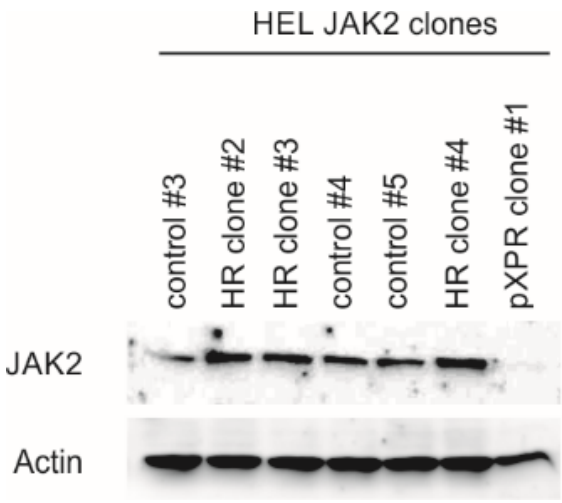

Figure 14. Western blot analysis of JAK2 protein level in cell lysates of HEL JAK2 HR clones and control cells. Cell lysates of HEL JAK2 HR clones from 2 runs of cell sorting with their respective controls are analyzed by Western blotting. Clone HEL JAK2 pXPR #1 is a clone created by electroporating HEL cells with CRISPR/Cas9 plasmid targeting *JAK2* (*JAK2*_pXPR001) and without the homologous template, thus leading to aberrations in the *JAK2* gene repaired by NHEJ creating *JAK2* LOF. As a result, JAK2 protein is not detected in the HEL JAK2 pXPR clone #1.

PCR amplification-refractory mutation system (ARMS) was performed from gDNA of single cell clones as it can distinguish a single point mutation and amplify the DNA strand accordingly. Based on PCR ARMs cell clone number 1 was selected (JAK2 WT/-; corresponding Control 1 clone). As seen in Figure 15B, PCR ARMs produces three bands, one large band (303 bp) amplifying the region targeted by sgRNA, and the two smaller bands each amplifying either WT or V617F mutant allele. When the large *JAK2* HR region is amplified (blue region in Figure 15A), products of two sizes are visible on electrophoresis gel, suggesting a large deletion in the area of *JAK2* HR region (region amplified for homologous template). In order to determine whether one of the alleles was truly 'repaired' by homologous recombination and the WT band is not only an artefact of homologous template being incorporated into another genomic locus primers spanning the region of *JAK2* HR template were used for a PCR together with primers specific for either WT or V617F allele (Figure 15). As displayed in Figure 15B, there is a product specific for *JAK2* V617F formed when compared to a negative control (U2-OS gDNA). The whole region was sequenced using primers spanning the template sequence revealing three alleles, one WT allele, one allele containing a deletion of 442 bp and a third V617F allele containing a single bp deletion in the intron area, 11 bps downstream of exon 14, which might lead to splicing abnormalities. To rule out the possibility of contamination of the clone with a different HEL

clone, thus detecting three alleles, we sub-cloned the HEL JAK2 WT/- cells by seeding and expanding single cells. More than 20 subclones were screened for their mutational status all resulting in the same three alleles detected. We thus concluded that HEL JAK2 WT/- cell clone does indeed carry three *JAK2* alleles, which might be a result of chromosomal aberration rather than contamination of the cell clone. The second selected clone HEL JAK2 VF/- (corresponding Control 4 clone) contains two alleles based on the sequencing data, one original V617F allele while the second one contains 3 bp deletion in the intron area (9 bps downstream of exon 14, one of the three base pairs missing is actually the same one as the one missing in V617F allele of the HEL JAK2 WT/- clone). As the allele with a deletion of 442 bp is not functional in HEL JAK2 WT/- cells and the aberration in the second allele is very similar to the one in HEL JAK2 VF/- clone, the major difference in the other two alleles is in *JAK2* WT and V617F coding sequence. Based on such hypothesis these cell clones were selected for further analysis and will be all together addressed as HEL JAK2 HR clones. The corresponding control clones HEL JAK2 Control 1 and 4 were simultaneously electroporated with a non-targeting CRISPR, *JAK2* WT homologous template and *JAK2* pART followed by single-cell sorting.

To assess the functional consequences of JAK2 mutations in HEL JAK2 HR clones on JAK/STAT signaling we employed a dual luciferase assay using STATs responsive elements reporter plasmid. The activity of JAK-STAT signal is shown to be significantly decreased in HEL JAK2 WT/- clone compared to the activity of a control, while the activity of JAK-STAT signaling in HEL JAK2 VF/- is decreased non-significantly (Figure 16). HEL JAK2 WT/- clone exhibits statistically significant decrease of *JAK2* expression to about 50% of the control clone, the expression of *JAK2* in HEL JAK2 VF/- is shown to be about 80% of the corresponding control clone. These data are supported by immunoblotting which shows much lower levels of phosphorylated JAK2 protein in both HEL JAK2 WT/- and HEL JAK2 VF/- clones. Less JAK2 protein in total is produced in HEL JAK2 WT/- clone compared to a control. As a result, decreased levels of phosphorylated STAT5 are detected in both clones while the total amount of STAT5 remains the same (Figure 16). The presented data suggest that HEL JAK2 WT/- cells do indeed have downregulated JAK-STAT signaling as less JAK2 protein is being produced and wild-type JAK2 does not phosphorylate STAT5 to the same extend as JAK2 V617F in control cells.

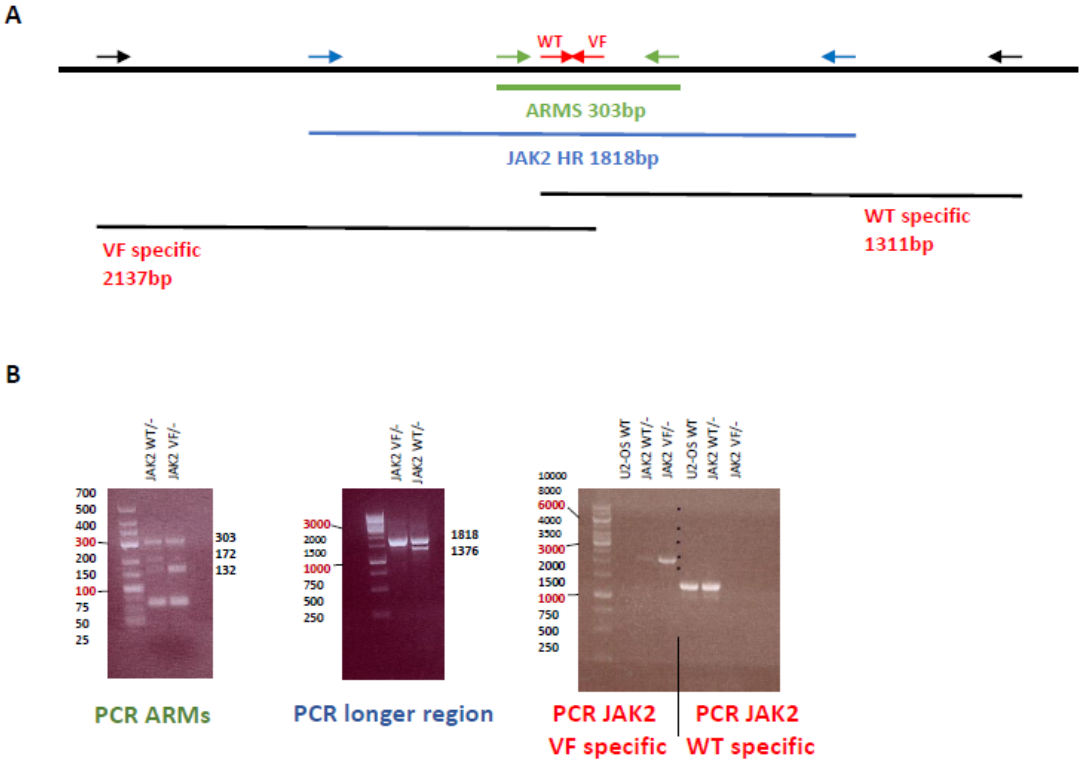

Figure 15. Detection of *JAK2* aberrations in HEL JAK2 HR clones using PCR. (A) A part of *JAK2* gene is visualized, primer annealing positions and PCR product lengths are indicated. WT and VF primers are primers specific for *JAK2* WT or *JAK2* V617F sequence; JAK2 HR primers were used for homologous template amplification. (B) Electrophoresis gels visualizing PCR products of *JAK2* gene in HEL JAK2 HR clones. PCR ARMs shows bands specific for both *JAK2* WT and *JAK2* V617F allele in HEL JAK2 WT/- clone, while only *JAK2* V617F allele is detected in JAK2 VF/- cell clone. PCR of a longer JAK2 HR region clearly shows a larger deletion of 442 bp in *JAK2* gene of HEL JAK2 WT/- clone. PCR specific for *JAK2* WT and *JAK2* V617F spanning the region amplified for homologous template demonstrates that *JAK2* WT allele in HEL JAK2 WT/- clone is detected due to recombination of the parental *JAK2* V617F allele.

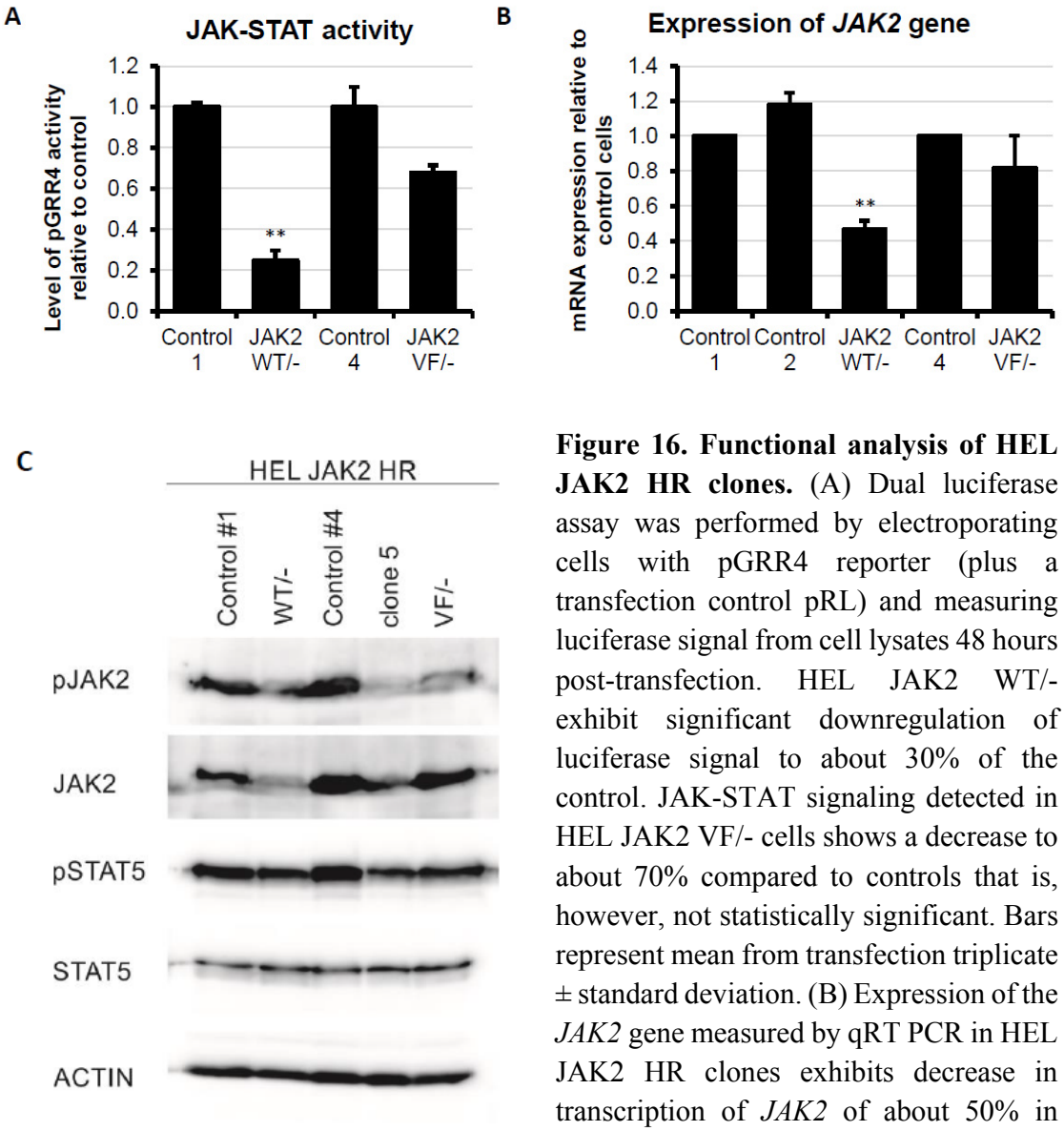

Figure 16. Functional analysis of HEL JAK2 HR clones. (A) Dual luciferase assay was performed by electroporating cells with pGRR4 reporter (plus a transfection control pRL) and measuring luciferase signal from cell lysates 48 hours post-transfection. HEL JAK2 WT/- exhibit significant downregulation of luciferase signal to about 30% of the control. JAK-STAT signaling detected in HEL JAK2 VF/- cells shows a decrease to about 70% compared to controls that is, however, not statistically significant. Bars represent mean from transfection triplicate ± standard deviation. (B) Expression of the *JAK2* gene measured by qRT PCR in HEL JAK2 HR clones exhibits decrease in transcription of *JAK2* of about 50% in HEL JAK2 WT/- compared to control cells. The transcription of *JAK2* gene is not significantly affected in HEL JAK2 VF/- cells, although there is a tendency to lower *JAK2* expression. Data are normalizes to house-keeping genes *GUSB* and/or *RPLP0* ± standard deviation. (C) Western blot from cell lysates of HEL JAK2 HR clones and control cells. Clone 5 was not suitable for our study and will therefore not be discussed. Lower amount of phosphorylated and total JAK2 protein is detected in both HEL JAK2 WT/- and VF/- cell clones compared to control cells. Correspondingly, decreased levels of phosphorylated STAT5 were detected in these cells while the amount of total STAT5 remains unchanged. **P<0.01, Student's unpaired t test with unequal variance.

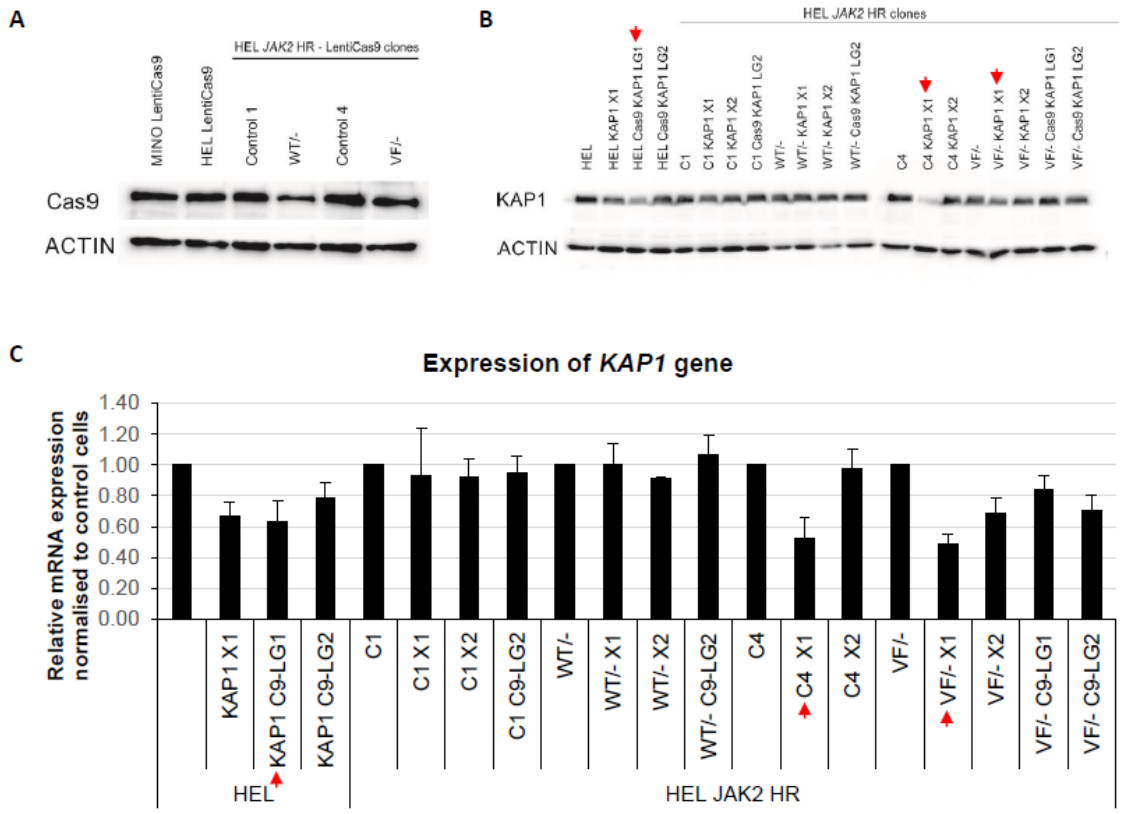

Figure 17. HEL JAK2 HR KAP1 KO cell clones. (A) Western blotting confirming the production of recombinant Cas9 protein in HEL JAK2 HR Cas9 clones and parental HEL cells. MINO Cas9 cells serve as a positive control for the presence of Cas9. (B) Western blot analysis of HEL JAK2 HR KAP1 KO cells. Three cell clones that produce lower amounts of KAP1 protein in HEL JAK2 HR KAP1 KO clones are detected and depicted by red arrows. (C) The expression of *KAP1* gene in HEL JAK2 HR KAP1 KO clones after cell sorting measured by qRT PCR. A visible decrease in the expression of *KAP1* in clones matching immunoblotting data is apparent (depicted by red arrows), these are HEL Cas9 KAP1 LG1 (HEL KAP1 KO), HEL JAK2 HR Control 4 KAP1 X1 (HEL C4 KAP1 KO) and HEL JAK2 VF/- KAP1 X1 (HEL VF/- KAP1 KO) cells. Data are normalized to *GUSB* and *RPLP0* reference genes.

In order to study the impact of *JAK2* V617F mutation on KAP1 protein function in DDR, KAP1 was knocked-out in HEL JAK2 HR clones JAK2 WT/- and JAK2 VF/-. Using CRISPR/Cas9 method followed by antibiotic selection, none of the puromycin-selected clones displayed any reduction in KAP1 production visualized by immunoblotting. The selected HEL JAK2 HR clones were control cell clones Control 1 and Control 4. Integration

of pXPR001 backbone was verified by PCR from gDNA, however, it was the second time pXPR001 carrying puromycin resistance cassette was introduced to these cells, first time being when electroporated with control pXPR001 lacking targeting sgRNA. It is therefore possible that these clones have pXPR001 backbone integrated into their genome making them resistant to puromycin. Consequently, a different approach was chosen to create KAP1 KO cells. In order to increase the efficiency of lentiviral transduction, we firstly introduced Cas9 into HEL JAK2 HR clones with subsequent transduction of lentivirus expressing *KAP1*-targeting sgRNA (LentiGuide – LG). Instead of selecting cells with puromycin, they were electroporated with their corresponding pART control plasmid 24 hours after LG transduction. In parallel, HEL JAK2 HR clones without Cas9 were co-electroporated with KAP1 X1 or KAP1 X2 in combination with the corresponding control plasmid pART. Cells in both set-ups were sorted 48 hours after electroporation as a mixed cell culture based on their fluorescent status. All these cell cultures were expanded and used for further analysis.

KAP1 knock-out efficiency was analyzed by immunoblotting and qRT PCR. As seen in Figure 17, a visible reduction of KAP1 protein was detected in cell clones HEL Cas9 KAP1 LG1 (HEL KAP1 KO), HEL JAK2 HR Control 4 KAP1 X1 (HEL C4 KAP1 KO) and HEL JAK2 VF/- KAP1 X1 (HEL VF/- KAP1 KO). None of the other cell clones show significant reduction of *KAP1* expression. KAP1 X1 seems to be most efficient in knocking-out *KAP1* and will therefore be used to knock it out in the remaining cell clones in future. The cell survival under stress conditions will then be tested to further analyze the role of KAP1 in cells with *JAK2* V617F mutation. Their capability to differentiate will also be tested by incubating them with hemin.

4.3 The role of *EGLN2*/Proline hydroxylase 1 in regulation of cyclin D1 in mantle cell lymphoma

In the present study we looked at the effect of iron chelators in mantle cell lymphoma cell lines, exploring the downregulation effect of cyclin D1. We first confirmed that deferoxamine (DFO)-induced iron chelation can inhibit cell growth and promote apoptosis in mantle cell-derived cell lines. Human MCL cell lines Jeko-1, Mino and HBL-2 were grown with media only or with DFO (250 μM). At 24 and 48 hours of incubation with an iron chelator, MCL cell lines had decreased viability and increased apoptosis (Figure 18A). We also examined the iron depletion effect on the cell lines which do not have constitutively active cyclin D1, SUDHL-6 originating from diffuse large B-cell lymphoma and DG-75 isolated from Burkitt's lymphoma. As expected, the cell growth in non-MCL cell lines was decreased but not fully inhibited (statistically significant difference in the growth rate of MCL vs. non-MCL cell lines at 48 hour time point, Figure 18B) and apoptosis level comparable to MCL cell lines (Figure 18B). The growth limiting and cytotoxic effects were prevented by co-incubation with an iron source FAC (ammonium ferric citrate), confirming that these effects are due to iron depletion (Figure 18A).

All MCL cell lines had detectable levels of cyclin D1 at baseline (Figure 18C). In mantle cell lines, cyclin D1 protein was no longer apparent by Western blot after 24 hours of incubation with the chelator and post-incubation with FAC restored cyclin D1 protein level (Figure 18C). Cell cycle analysis revealed that MCL cell lines do not abrogate the cell cycle in the G1 phase under serum-starved conditions, suggesting that overexpression of cyclin D1 promotes cell proliferation (Figure 18D). Moreover, the overexpression of cyclin D1 makes MCL cells more susceptible to the treatment with DFO (percentage of G1 cells of MCL cell lines is significantly higher than in non-MCL cell lines, Figure 18D).

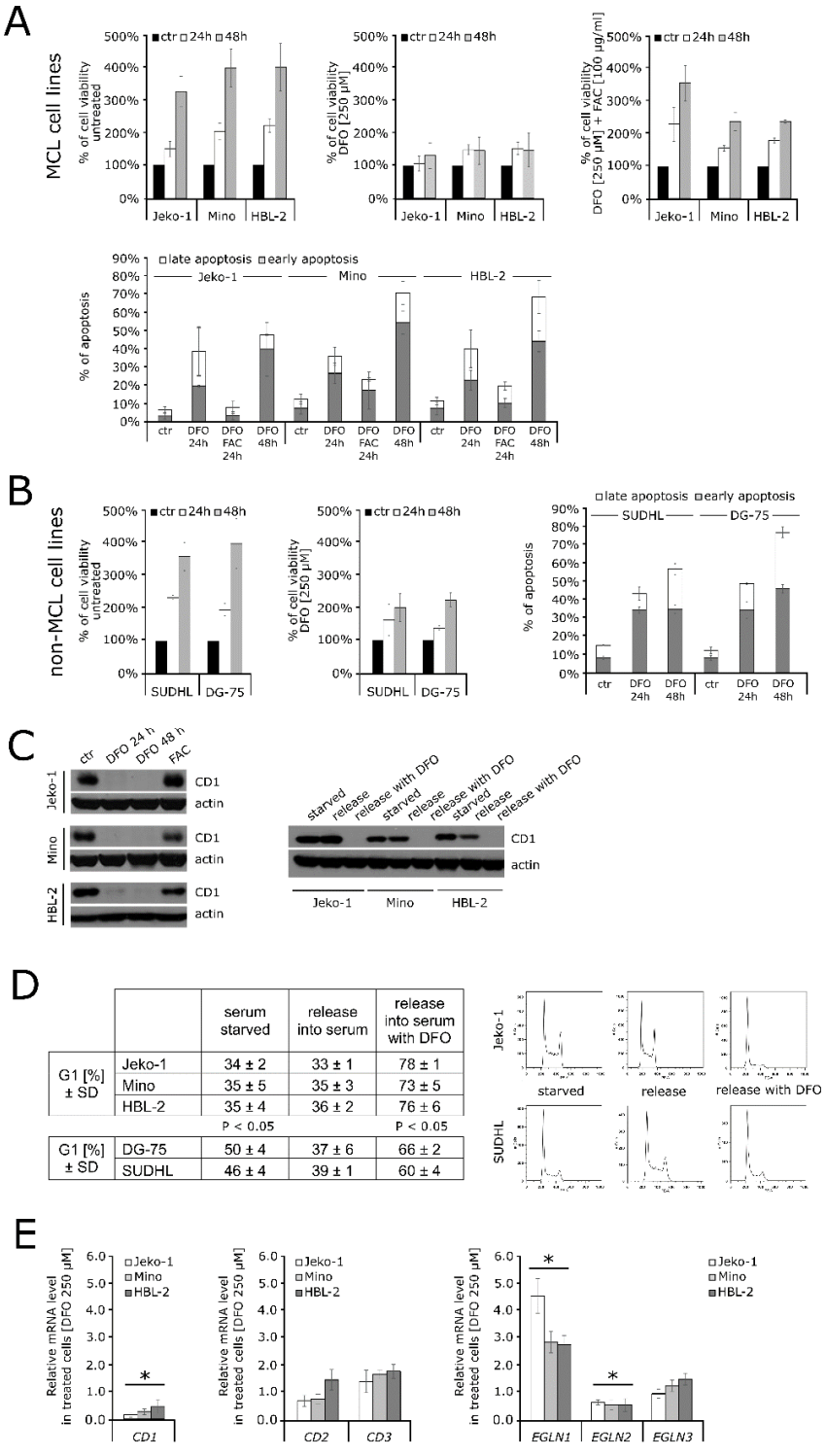

Figure 18. The effect of iron depletion on human mantle cell lymphoma cell lines (Jeko-1, Mino and HBL-2) and two lymphoma cell lines (SUDHL-6 and DG-75) which do not harbor t(11;14)(q13;32) translocation. All data are represented as the mean of three

independent experiments; T bars designate standard deviations; *P < .05. (A) (Upper panel) Proliferation rates during DFO (250 μM) treatment in MCL cell lines. Cellular Fe depletion inhibited the growth of all MCL cell lines but co-incubation of DFO treated cells with Fe source FAC (100 μg/ml) abolished the effect. Cell number and viability were determined using CellometerAutoT4 based on the trypan blue exclusion method. The results are demonstrated as percentage of cell growth in comparison to the untreated cells at time 0. (Lower panel) Percentage of total apoptotic cells (divided into early and late fractions) during DFO treatment. All cell lines exhibited increase in the percentage of apoptotic cells already after 24 hours after Fe depletion but co-incubation of DFO treated cells with Fe source FAC (100 μg/ml) abolished the effect. For detection of apoptotic cells, cell-surface staining was performed with FITC-labeled anti–Annexin V antibody and PI co-staining. (B) (Left panels) Proliferation rates during DFO treatment (250 μM) in non-MCL cell lines. Iron chelator DFO impaired the growth of non-MCL cell lines but did not inhibit it. Cell number and viability were determined using CellometerAutoT4 based on the trypan blue exclusion method. The results are demonstrated as percentage of cell growth in comparison to number of cells at time 0. (Right panel) Percentage of total apoptotic cells (divided into early and late fractions) during DFO treatment. Both lines exhibited increase in the percentage of apoptotic cells after 24-hour treatment. For detection of apoptotic cells, cell-surface staining was performed with FITC-labeled anti–Annexin V antibody and PI co-staining. (C) (Left panel) Treatment with DFO (250 μM) depleted cyclin D1 protein level. The level of cyclin D1 was not detectable in MCL cell line treated with DFO already after 24 hours. Re-incubation of DFO-treated cells with FAC (100 μg/ml) for 24 hours restores cyclin D1 protein levels. (Right panel) Cyclin D1 protein level in MCL cell lines after serum-starvation (24 h) and after the release into the medium with 10% FBS or 10% FBS with DFO (250 μM). (D) Cellular Fe depletion induces a G1/S arrest in MCL cell lines. MCL cell lines do not stop cell cycle under serum-starved condition (comparing to non-MCL cell lines SUDHL-6 and DG-75) suggesting their dependence on overexpressed cyclin D1 sensitizing them to treatment with DFO (250 μM). Cell were synchronized by serum-starvation for 24 hours and then released to medium containing 10% FBS or 10% FBS with DFO. Data are demonstrated as percentage of cells in G1 phase. Representative cell cycle histograms analysis by FlowJo™ software. (E) Expression analysis of selected genes in DFO-treated (250 μM) MCL cell lines after 24 hours were determined by quantitative PCR. (Left panel) Treatment with DFO significantly decreases mRNA expression of *cyclin D1*. (Middle panel) The mRNA expression of *cyclin D1* homologs, *cyclin D2 (CD2)* and *cyclin D3 (CD3)*, is not significantly affected by DFO treatment. (Right panels) Expression of *EGLN1* gene is significantly increased, the expression of *EGLN2* is significantly decreased and the expression of *EGLN3* is not affected by DFO treatment. In all experiments, data are normalized to *GUSB* and *RPLP0* reference genes.

We further investigated the molecular mechanism underlying decreased cyclin D1 levels in MCL cell lines after DFO treatment. Contradictory to the initial report suggesting that iron

chelation caused posttranslational proteasomal degradation of cyclin D1[6], Fe depletion caused downregulation of *cyclin D1* mRNA expression (Figure 18E). We also investigated the possible compensatory effect described by Klier et al.[251], where a specific shRNA-mediated knockdown of *cyclin D1* mRNA has minimal effects on cell survival because of upregulation of *cyclin D2* mRNA and protein expression. After treatment with DFO, we did not detect upregulation of *cyclin D2* and *cyclin D3* mRNA (Figure 18E). We further tested whether the DFO effect may be due to inhibition of one of the iron-dependent hypoxia-inducible factor prolyl hydroxylases. Expression analysis in MCL cell lines treated with DFO revealed downregulation of PHD1 encoded by the *EGLN2* gene and upregulation of *EGLN1/*PHD2 (Figure 18E).

PHD1 has previously[4] been linked to cyclin D1 regulation by means of hydroxylating FOXO3A, leading us to decipher whether iron chelation downregulates cyclin D1 in mantle cell lymphoma by downregulating PHD1. We treated MCL cell lines Jeko-1, MINO and HBL-2 with inhibitor of prolyl hydroxylases DMOG (dimethyloxaloylglycine, a synthetic analogue of 2-ketoglutarate) and show that the inhibitor reduces cell growth after 24, 48, 72 and 96 hours (Figure 19). Treatment with DMOG abolishes the protein levels of cyclin D1 in all three MCL lines tested. These results are consistent with the mRNA expression data showing that PHD inhibition by DMOG downregulates the expression of *cyclin D1*, but not *cyclin D2* and *cyclin D3*. Similarly to DFO, DMOG mimics hypoxia and thus upregulates the HIF target genes *EGLN1/*PHD2*, EGLN3/*PHD3*, VEGFA* and *SLC2A*. *EGLN2*/PHD1 mRNA expression remains unchanged as DMOG does not directly affect the expression of PHD hydroxylases (Figure 19). Since DMOG is predicted to inhibit broad spectrum of hydroxylases it is possible that these hydroxylases have additional substrates with ability to regulate aberrantly expressed cyclin D1 in MCL cells.

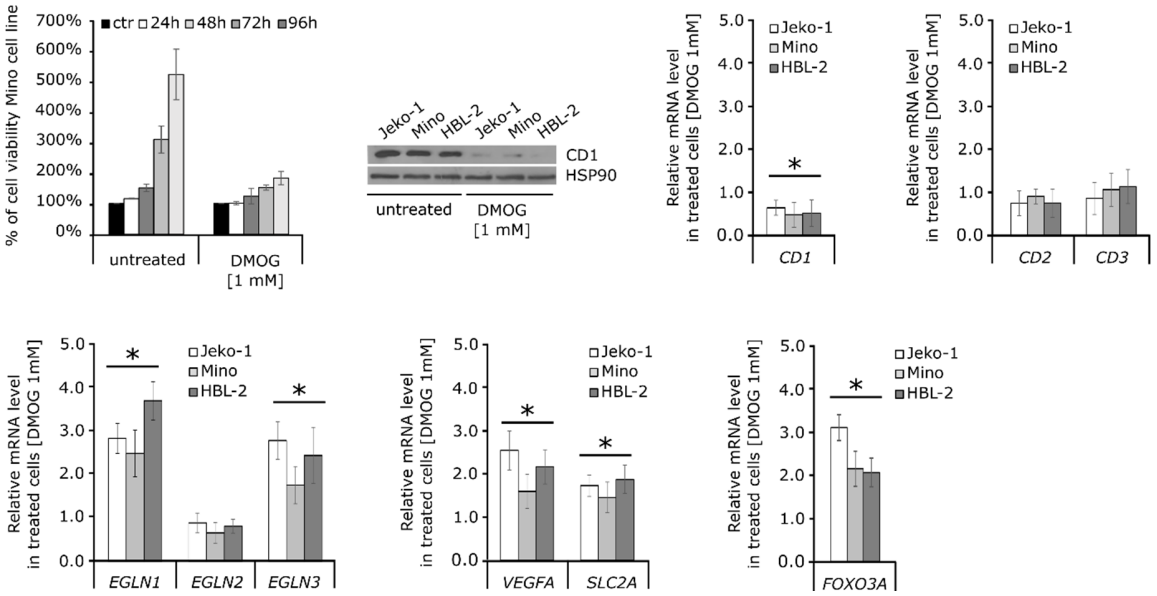

Figure 19. The effect of PHD inhibitor DMOG (1 mM) on human mantle cell lymphoma cell lines (Jeko-1, Mino and HBL-2). All data are represented as the mean of three independent experiments; T bars designate standard deviations. (Upper left panel) Proliferation rates during DMOG treatment. Inhibition of PHDs has significant effect on growth of Mino cell line compared to a non-treated control. Cell number and viability were determined using CellTiter-Blue® Cell Viability Assay (Promega). The results are demonstrated as percentage of cell growth in comparison to the untreated cells at time 0. (Upper middle, right panels) The level of cyclin D1 was markedly reduced in MCL cell line after incubation with DMOG for 24 hours. The expression of cyclin D1 was reduced in MCL cell lines after incubation with DMOG for 24 hours on protein and also mRNA level. The mRNA expression of *cyclin D1* homologs, *cyclin D2 (CD2)* and *cyclin D3 (CD3)*, is not significantly affected by DMOG treatment. (Lower panel) Expression analysis of *EGLN* genes, selected HIF target genes (*VEGF* and, *SLC2A*) and *FOXO3A* were determined by quantitative PCR after incubation with DMOG for 24 hours of interest in DMOG-treated cells. *$P < .05$

In order to rule out the impact of drugs' unspecificity and to further explore the mechanism of regulation of cyclin D1 we created PHD1 and FOXO3A loss-of-function (LOF) Mino cell lines. Strikingly, PHD1 LOF does not lead to the downregulation of *cyclin D1* expression in MCL cell line Mino (Figure 20A). In order to validate our loss-of-function CRISPR/Cas9 system we created *EGLN2*/PHD1 loss-of-function in HEK 293 cells and as expected, we observed downregulation of *cyclin D1* on mRNA level (Figure 21) suggesting that transcriptional regulation of *cyclin D1* in MCL cell lines is not controlled by *EGLN2*/PHD1.

FOXO3A LOF, too, does not show any effect on the cyclin D1 mRNA and protein level in MCL cell lines. PHD1 was previously reported to be reactive to estrogen and to regulate cyclin D1 in breast cancer.[4,209] We show that in MCL cell lines cyclin D1 might escape this regulation.

We further examined the effect of iron chelation on cyclin D1 regulation in these settings. As expected, level of cyclin D1 was reduced on protein and also mRNA level after DFO treatment and restored when Fe source FAC was present in medium, in both loss-of-function cell lines (Figure 20). Loss-of-function of FOXO3A in MCL line Mino did not prevent *cyclin D1* downregulation after DFO treatment (Figure 20). Interestingly, *FOXO3A* upregulation was detected in MCL cell lines after DFO treatment (Figure 20C). These data suggest that iron depletion in MCL cell lines leads to up-regulation of *FOXO3A*, but FOXO3A is not required for cyclin D1 repression. Cyclin D1 downregulation upon iron depletion is not mediated by PHD hydroxylases, but is a result of another, as yet unknown mechanism. We hypothesize, that in MCL cells production of cyclin D1, due to t(11;14) translocation, escapes the *ENGL2*/PHD1-FOXO3A regulation.

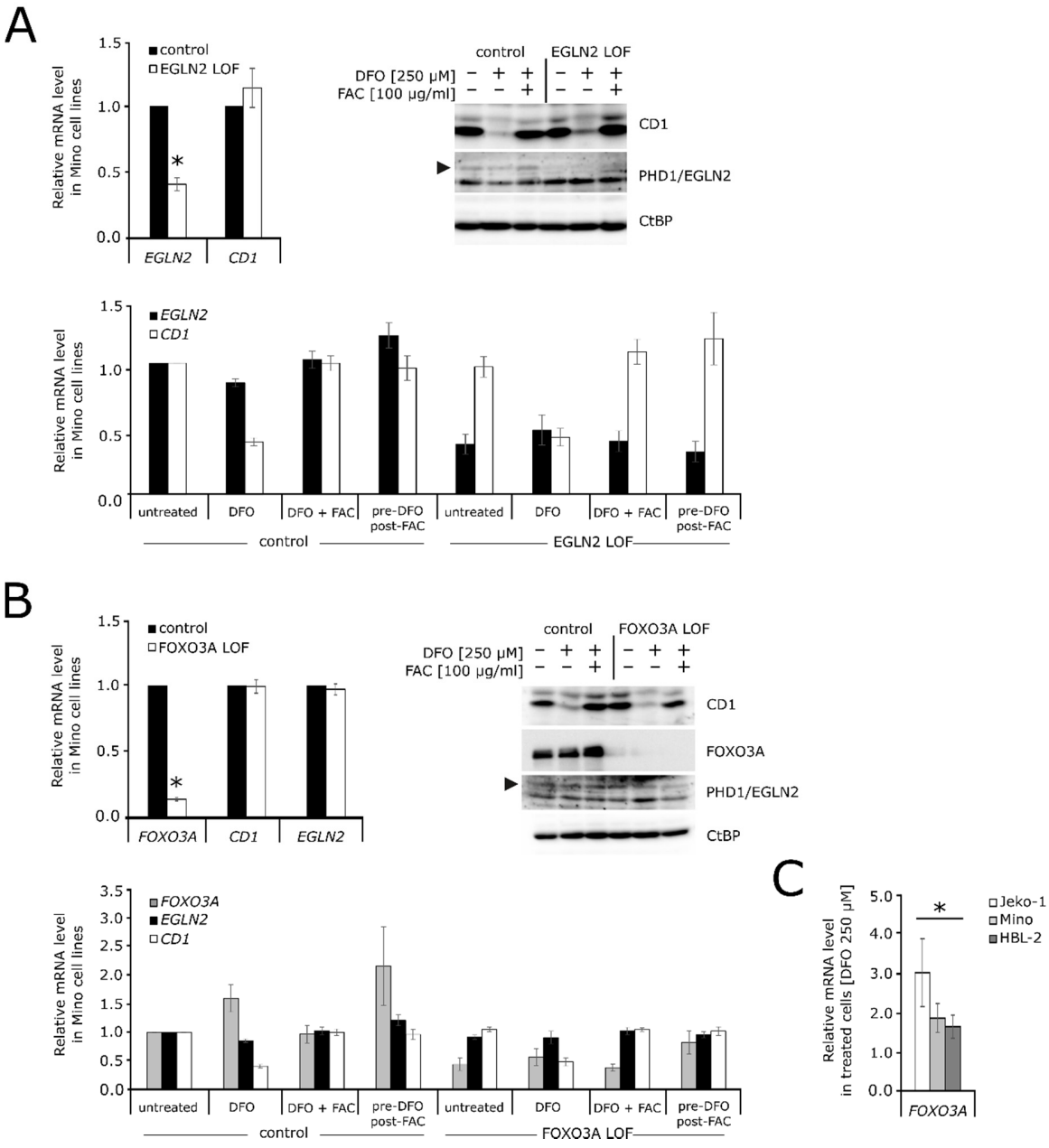

Figure 20. Regulation of cyclin D1 in MCL cell lines is not controlled by *EGLN2*/PHD1 and its hydroxylation target FOXO3A. All data are represented as the mean of three independent experiments; T bars designate standard errors. **P* < .05. Expression analyses are normalized to *GUSB* and/or *RPLP0* reference gene. (A) Loss-of-function of *EGLN2*/PHD1 does not affect cellular level of cyclin D1. (Upper left panel) The decreased expression of *EGLN2* after CRISPR-Cas9 mediated loss-of-function in Mino cell line was determined by quantitative PCR. The expression of *cyclin D1* in these cells did not change. (Upper right panel) Mino cell line and *EGLN2*/PHD1 LOF Mino cell line were treated with DFO (250

μM) only or in combination with FAC (100 μg/ml) for 24 hours and protein levels of cyclin D1, PHD1 and CtBP (loading control) were determined by Western blot. (Lower panel) The expression analysis of Mino cell line and *EGLN2*/PHD1 LOF Mino cell line after DFO (250 μM) and FAC (100 μg/ml) treatment for 24 hours. (B) Loss-of-function of FOXO3A does not affect cellular level of *EGLN2*/PHD1 and cyclin D1. (Upper left panel) The decreased expression of *FOXO3A* after CRISPR-Cas9 mediated loss-of-function in Mino cell line was determined by quantitative PCR. The expression of *cyclin D1* and *EGLN2* in these cells did not change. (Upper right panel) Mino cell line and FOXO3A LOF Mino cell line were treated with DFO (250 μM) only or in combination with FAC (100 μg/ml) for 24 hours and protein levels of FOXO3A, cyclin D1, PHD1 and CtBP (loading control) were determined by Western blot. (Lower panel) The expression analysis of Mino cell line and FOXO3A LOF Mino cell line after DFO (250 μM) and FAC (100 μg/ml) treatment for 24 hours. (C) FOXO3A upregulation after DFO (250 μM) treatment. Treatment with iron chelator for 24 hours increased expression of *FOXO3A* gene in MCL cell lines Jeko-1, Mino and HBL-2.

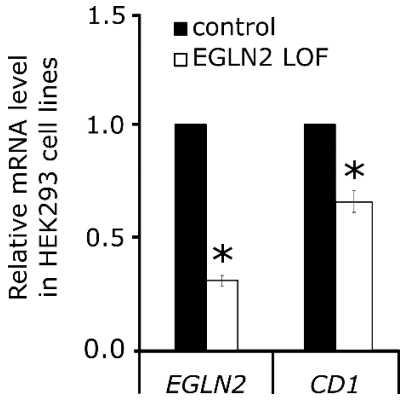

Figure 21. Expression profiling of PHD1 loss-of-function HEK 293 cells. In PHD1 LOF HEK 293 cells the expression of *cyclin D1* and *EGLN2*/PHD1 is downregulated. T bars designate standard errors. **P* < .05. Expression analysis is normalized to *GUSB* and/or *RPLP0* reference gene.

As iron depletion gives rise to hypoxic conditions, we wanted to rule out the possibility that *EGLN2*/PHD1 is downregulated as a result of hypoxia. We cultured MCL cell lines for 24 hours in hypoxia chamber with 1% O_2 atmosphere and performed expression analysis. The level of *cyclin D1* was not significantly altered (Figure 22i), but we found downregulation of *EGLN2/*PHD1 and accumulation of *FOXO3A* mRNA (Figure 22ii+iii). Induction of hypoxia was confirmed by expression of HIF target genes *EGLN1/*PHD2*, EGLN3/*PHD3*, VEGFA* and *SLC2A* (Figure 22iv). These data demonstrated that observed downregulation of *EGLN2* and accumulation of *FOXO3A* mRNA after DFO treatment is rather a consequence of induced hypoxia than the direct effect of Fe depletion.

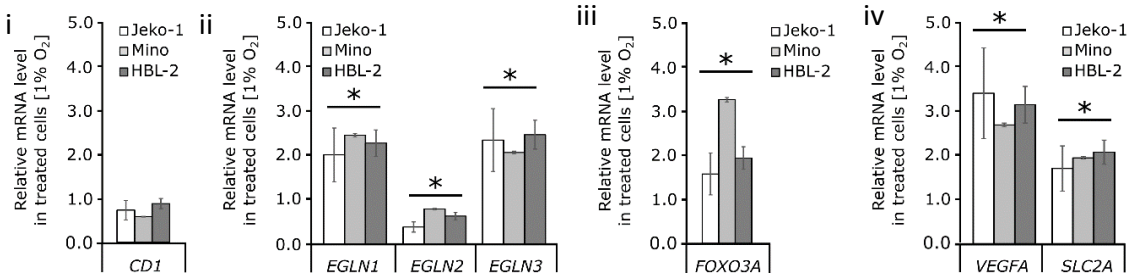

Figure 22. Hypoxia treatment of MCL cell lines. T bars designate standard errors. *$P < .05$. Expression analyses are normalized to *GUSB* and/or *RPLP0* reference gene. Hypoxia (1% O_2) decreases the expression level of *EGLN2* and increases the expression level of FOXO3A. Expression levels of *cyclin D1*, *EGLNs*, selected HIF target genes (*VEGFA* and *SLC2A*) and *FOXO3A* were determined by quantitative PCR after incubation in hypoxia chamber with 1% O_2 for 24 hours.

We further explored the possibility that ubiquitin-independent degradation might play a role in the downregulation of cyclin D1 in iron deplete cells, as suggested by Nurtjaha-Tjendraputra et al.[6] NQO1 has previously been described to protect proteins from 20S proteosomal degradation by physically interacting with them in an NADPH-dependent manner.[252] We tested whether the inhibition of NQO1 has an effect on cyclin D1 stability in mantle cell lymphoma cell lines by treating cells with dicoumarol (DIC), a small molecule drug that competes specifically with NADH for binding to NQO1.[253,254] Similarly to DFO, DIC decreases the protein levels of cyclin D1 in MCL cell lines (Figure 23A). This degradation is proteasome mediated, as co-incubation of cells with proteosomal inhibitor MG132 prevents the DIC-mediated degradation of cyclin D1 (Figure 23B). Expression analysis demonstrates that NQO1 inhibition by DIC leads to decreased *CCND1* expression, while the expression of PHD hydroxylases and HIF target genes remain unchanged (Figure 23C). It remains unclear whether the cyclin D1 repression is an outcome of NQO1 having a specific protective role in cyclin D1 degradation or a result of unspecific inhibition of its oxidoreductase activity.

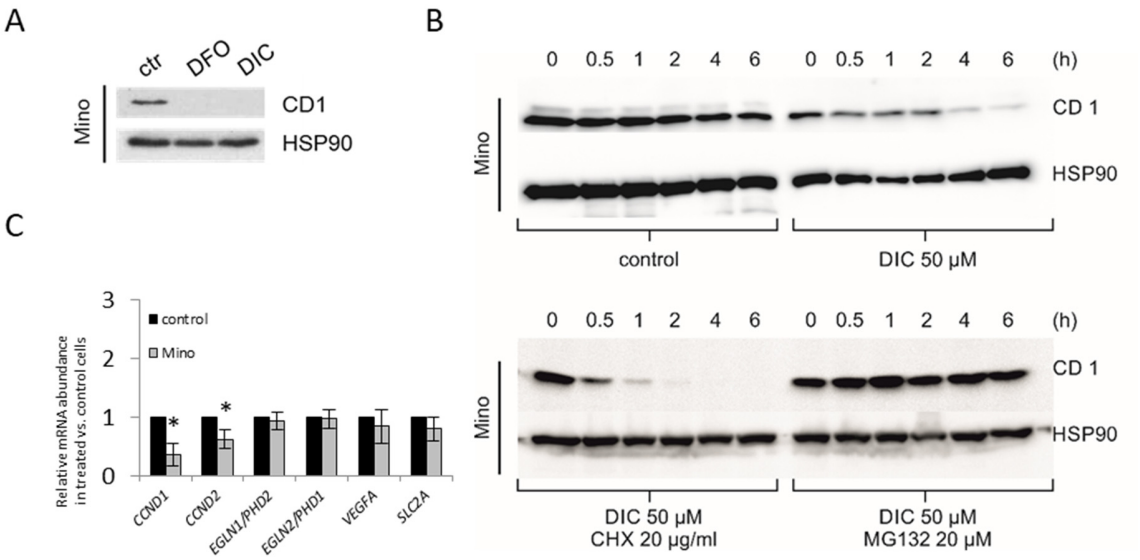

Figure 23. The effect of NQO1 inhibitor DIC (50 µM) on MCL cell line Mino. (A) Treatment with DIC decreases cyclin D1 protein level. The level of cyclin D1 was not detectable in Mino cell line after incubation with DFO and DIC for 24 hours. (B) Inhibition of cyclin D1 upon DIC treatment is proteasome-driven. Cells were treated with DIC only, or DIC in combination with CHX (20 µg/ml), or MG-132 (20 µM) and the protein lysate was prepared at time points 0 – 6 hours. (C) Expression analysis of genes of interest in DIC-treated cells. Treatment with DIC significantly decreases the mRNA expression of *cyclin D1* and *cyclin D2*, and does not affect the mRNA expression of HIF-response genes *EGLN1/PHD2*, *VEGFA* and *SLC2A*. It neither affects the expression level of *EGLN2/PHD1*. Data are normalized to *GUSB* and/or *RPLP0* reference genes. Data are represented as the mean of three independent experiments; T bars designate standard deviations. **P* < .05

5 Conclusion

Firstly, our research on genetic variants of *JAK2* gene gave rise to two publications. We characterized three *JAK2* germline variants and their impact on JAK-STAT signaling. We show that *JAK2* T108A and *JAK2* L393V are weakly activating mutations and lead to hypersensitivity to low amounts of EPO, which could predispose cells carrying these mutations to proliferate at higher rate in physiological conditions. It is suggestive that these two variants could precede the acquisition of *JAK2* V617F mutation and contribute to further genomic alterations in PV clone and perhaps even leukemic transformation. We further characterized the double mutant *JAK2* V617F/R1063H in MPN patients. The two mutations cooperate to further increase JAK-STAT signaling. MPN patients with these two mutations present with neutrophilia, which could be linked to biochemical association of the JAK2 R1063H mutant to G-CSFR.

Secondly, in order to characterize the role of KAP1 in DDR of *JAK2* V617F-positive cells we created HEL cell line carrying *JAK2* WT allele and consequently we knocked-out *KAP1* gene in these cells. KAP1 will be studied in this setting, its role in cell proliferation upon induced DNA damage, differentiation and its impact on genomic instability will be studied. Upon DNA damage KAP1 becomes phosphorylated, it would be therefore of interest to see if *JAK2* V617F-positive cells phosphorylate KAP1 to a higher extend compared to *JAK2* WT cells. Due to technical difficulties only one heterozygous cell clone carrying *JAK2* WT allele and one heterozygous cell clone carrying *JAK2* V617F were created. The impact of KAP1 downregulation could therefore be investigated in a different system, such as in CD34+ patient progenitors harboring *JAK2* V617F mutation and their counterparts harboring wild-type *JAK2*. KAP1 could be then downregulated either by KAP1 targeting siRNA or CRISPR/Cas system in order to study its role in DDR in these cells.

Thirdly, we show that in MCL cell lines iron chelation is effective in inhibiting proliferation, inducing apoptosis and cell cycle arrest by means of regulating cyclin D1 levels. We also show that the overexpression of cyclin D1 in these cells makes them more susceptible to chelation treatment. It has been previously[4] reported that an inability of PHD1 to hydroxylate FOXO3A promotes its accumulation in cells, which in turn suppresses *cyclin D1* expression

by a yet unknown mechanism. All members of the PHD protein family contribute to regulation of cellular O_2 sensing, but only *EGLN2*/PHD1 and *EGLN3*/PHD3 were demonstrated to have HIF-independent functions, such as in DNA-damage control[195,255] and NF-κB activity.[204,205] We explored the mechanism of cyclin D1 downregulation upon iron chelation in mantle cell lymphoma and found out that the expression of *EGLN2*/PHD1 is downregulated and *FOXO3A* upregulated as a consequence of hypoxic conditions brought on by iron chelation. We further demonstrate that cyclin D1 is not downregulated in hypoxia. Additionally, its downregulation in iron deplete cells is not prevented by FOXO3A loss-of-function. We therefore suggest that cyclin D1 escapes the PHD1 – FOXO3A regulation circuit in mantle cell lymphoma and cyclin D1 downregulation upon iron depletion is regulated by a different yet unknown mechanism. Future studies will be needed to determine whether iron chelation would be relevant in mantle cell lymphoma treatment.

In the last years the ubiquitin independent proteasomal degradation by 20S proteasomes has been shown to play a considerable part in mammalian degradation as it was demonstrated to cleave more than 20% of all cellular proteins. Ubiquitin-independent protein degradation could in some cases provide optimal regulation and thus lead to protein homeostasis. NQO1, apart from its enzymatic activity, can bind proteins to prevent their ubiquitin-independent degradation.[216–218] We employed NQO1 inhibitor dicoumarol to determine whether its unavailability could lead to destabilization of cyclin D1 protein in MCL cell lines. DIC-treated cells exhibited downregulation of cyclin D1 mRNA and protein levels. Interestingly, iron depletion was shown to regulate cyclin D1 repressor p21 where it induces ubiquitin-independent degradation of the protein.[221,222] The precise mechanism has not been identified yet, although it has been proposed that it might be mediated via NQO1 or antizyme.[221,222] It remains unclear whether the observed cyclin D1 repression is an outcome of NQO1 having a specific protective role in protein degradation or a result of unspecific inhibition of its oxidoreductase activity. The project has now been concluded and is being revised for a submission. The manuscript of the paper is included in the chapter *Supplements and Appendices*.

III. Supplements and Appendices

6 Abbreviations

AID	autoimmune diseases
AKT	protein kinase B
AML	acute myeloid leukemia
ASXL1	additional sex combs like 1
ATM	ataxia telangiectasia mutated
ATP	adenosine triphosphate
BCL-X_L	B-cell lymphoma-extra large
bFGF	basic fibroblast growth factor
BFU-E	burst forming unit-erythroid
CALR	calreticulin
CBP	p300/CREB-binding protein
CD1	cyclin D1
CFU-E	colony forming unit-erythroid
CLP	common lymphoid progenitor
CMP	common myeloid progenitor
CRP	C-reactive protein
DDR	DNA damage response
DFO	deferoxamine
DIC	dicoumarol
DMOG	dimethyloxaloylglycine
DNMT3A	DNA (cytosine-5)-methyltransferase 3A
DSB	DNA double stranded break
EPO	erythropoietin
EPOR	erythropoietin receptor
ET	essential thrombocytosis

EZH2	enhancer of zeste homolog 2
FAC	ammonium ferric citrate
FERM	N-terminal Band 4.1, ezrin, radixin, moesin
FOXO3A	forkhead box O 3A
GATA-1	GATA-binding factor 1
G-CSF	granulocyte-colony stimulating factor
G-CSFR	granulocyte-colony stimulating factor receptor
GRB2	growth factor receptor-bound protein 2
HIF	hypoxia-inducible factor
HK1	hexokinase-1
Hph	Hif-1 prolyl hydroxylase
HR	homologous recombination
HRE	hypoxia response enhancer
HSC	hematopoietic stem cell
HU	hydroxyurea
IFI	interferon-inducible
IFN-γ	interferon-γ
IL-3, 6	interleukin-3, 6
INSL4 and INSL6	insulin like 4 and insulin like 6
ITH	intratumor heterogeneity
JAK2	Janus kinase 2
KI	knock-in
KLF-1	Krüppel-like factor 1
KO	knock-out
KRAB-ZFPs	Krüppel-associated box domain - containing zinc finger proteins
MAPK	mitogen-activated protein kinase
MCL	mantle cell lymphoma
MDM2	mouse double minute 2 homolog
MDS	myelodysplastic syndrome

MEP	megakaryocyte–erythroid progenitor cell
MPL/TPOR	thrombopoietin receptor
MPNs	myeloproliferative neoplasm
NF-E2	nuclear factor - erythroid-derived 2
NHE-1	sodium-hydrogen exchanger isoform 1
NHEJ	non-homologous end joining
p53	tumor protein 53
PDGF	platelet-derived growth factor
peg	pegylated
PI3K	p85a regulatory subunit of PI 3-kinase
PKB	protein kinase B
PMF	primary myelofibrosis
PV	polycythaemia vera
Rb	retinoblastoma
RECQL5	RecQ Like Helicase 5
ROS	reactive oxygen species
rux	ruxolitinib
SCF	stem cell factor
SH2	Src homology 2
SLC2A	solute carrier family 2A
SHP-1, SHP-2	Src homology region 2 domain-containing phosphatase-1 and -2
SOCS	suppressor of cytokine signaling
SRSF2	arginine/serine-rich splicing factor 2
STAT1/3/5	signal transducer and activator of transcription 1/3/5
TET2	TET methylcytosine dioxygenase 2
TGF-β	transforming growth factor β
TME	tumor microenvironment
TNFα	tumor necrosis factor alpha

TPO	thrombopoietin
UPD	uniparental disomy
VEGFA	vascular endothelial growth factor A
WT	wild-type
γH2AX	histone variant H2AX at serine 139

7 Bibliography

1. Wang L, Swierczek SI, Drummond J, et al. Whole-exome sequencing of polycythemia vera revealed novel driver genes and somatic mutation shared by T cells and granulocytes. *Leukemia*. 2014;28(4):935–938.
2. Kapralova K, Horvathova M, Pecquet C, et al. Cooperation of germ line JAK2 mutations E846D and R1063H in hereditary erythrocytosis with megakaryocytic atypia. *Blood*. 2016;128(10):1418–23.
3. Levine RL, Wadleigh M, Cools J, et al. Activating mutation in the tyrosine kinase JAK2 in polycythemia vera, essential thrombocythemia, and myeloid metaplasia with myelofibrosis. *Cancer Cell*. 2005;7(4):387–397.
4. Zhang Q, Gu J, Li L, et al. Control of Cyclin D1 and Breast Tumorigenesis by the EglN2 Prolyl Hydroxylase. *Cancer Cell*. 2009;16(5):413–424.
5. Vazana-Barad L, Granot G, Mor-Tzuntz R, et al. Mechanism of the antitumoral activity of deferasirox, an iron chelation agent, on mantle cell lymphoma. *Leuk. Lymphoma*. 2013;54(4):851–9.
6. Nurtjahja-Tjendraputra E, Fu D, Phang JM, Richardson DR. Iron chelation regulates cyclin D1 expression via the proteasome: a link to iron deficiency-mediated growth suppression. *Blood*. 2007;109(9):4045–54.
7. Heppner GH. Tumor heterogeneity. *Cancer Res.* 1984;44(6):2259–65.
8. Swanton C. Intratumor Heterogeneity: Evolution through Space and Time. *Cancer Res.* 2012;72(19):4875–4882.
9. Nowell PC. The clonal evolution of tumor cell populations. *Science*. 1976;194(4260):23–8.
10. Greaves M, Maley CC. Clonal evolution in cancer. *Nature*. 2012;481(7381):306–313.
11. Johnson BE, Mazor T, Hong C, et al. Mutational analysis reveals the origin and therapy-driven evolution of recurrent glioma. *Science*. 2014;343(6167):189–193.
12. Cahill DP, Kinzler KW, Vogelstein B, Lengauer C. Genetic instability and darwinian selection in tumours. *Trends Biochem. Sci.* 1999;24(12):M57–M60.
13. Spencer SL, Gerety RA, Pienta KJ, Forrest S. Modeling Somatic Evolution in Tumorigenesis. *PLoS Comput. Biol.* 2006;2(8):e108.
14. Bonnet D, Dick JE. Human acute myeloid leukemia is organized as a hierarchy that originates from a primitive hematopoietic cell. *Nat. Med.* 1997;3(7):730–7.
15. Kreso A, Dick JE. Evolution of the cancer stem cell model. *Cell Stem Cell*. 2014;14(3):275–91.

16. Stieglitz E, Loh ML. Genetic predispositions to childhood leukemia. *Ther. Adv. Hematol.* 2013;4(4):270–90.

17. Godley LA. Inherited Predisposition to Acute Myeloid Leukemia. *Semin. Hematol.* 2014;51(4):306–321.

18. Dameshek W. Some speculations on the myeloproliferative syndromes. *Blood*. 1951;6(4):372–5.

19. Vainchenker W, Kralovics R. Genetic basis and molecular pathophysiology of classical myeloproliferative neoplasms. *Blood*. 2017;129(6):667–679.

20. Tefferi A, Vardiman JW. Classification and diagnosis of myeloproliferative neoplasms: the 2008 World Health Organization criteria and point-of-care diagnostic algorithms. *Leukemia*. 2008;22(1):14–22.

21. Tefferi A, Elliott M. Thrombosis in myeloproliferative disorders: prevalence, prognostic factors, and the role of leukocytes and JAK2V617F. *Semin. Thromb. Hemost.* 2007;33(4):313–20.

22. Tefferi A, Gangat N, Wolanskyj AP, et al. 20+ yr without leukemic or fibrotic transformation in essential thrombocythemia or polycythemia vera: predictors at diagnosis. *Eur. J. Haematol.* 2008;80(5):386–90.

23. Berk PD, Goldberg JD, Donovan PB, et al. Therapeutic recommendations in polycythemia vera based on Polycythemia Vera Study Group protocols. *Semin. Hematol.* 1986;23(2):132–43.

24. Landolfi R, Marchioli R, Kutti J, et al. Efficacy and safety of low-dose aspirin in polycythemia vera. *N. Engl. J. Med.* 2004;350(2):114–24.

25. Hoffman R, Rondelli D. Biology and treatment of primary myelofibrosis. *Hematology Am. Soc. Hematol. Educ. Program*. 2007;346–54.

26. Zauli G, Visani G, Catani L, et al. Reduced responsiveness of bone marrow megakaryocyte progenitors to platelet-derived transforming growth factor beta 1, produced in normal amount, in patients with essential thrombocythaemia. *Br. J. Haematol.* 1993;83(1):14–20.

27. Le Bousse-Kerdilès MC, Martyré MC. Involvement of the fibrogenic cytokines, TGF-beta and bFGF, in the pathogenesis of idiopathic myelofibrosis. *Pathol. Biol. (Paris).* 2001;49(2):153–7.

28. Martyré MC, Le Bousse-Kerdiles MC, Romquin N, et al. Elevated levels of basic fibroblast growth factor in megakaryocytes and platelets from patients with idiopathic myelofibrosis. *Br. J. Haematol.* 1997;97(2):441–8.

29. Castro-Malaspina H, Rabellino EM, Yen A, Nachman RL, Moore MA. Human megakaryocyte stimulation of proliferation of bone marrow fibroblasts. *Blood*. 1981;57(4):781–7.

30. Dragoni S, Reforgiato M, Zuccolo E, et al. Dysregulation of VEGF-induced proangiogenic Ca2+ oscillations in primary myelofibrosis-derived endothelial colony-forming cells. *Exp. Hematol.* 2015;43(12):1019–1030.e3.

31. Hasselbalch HC, Bjørn ME. MPNs as Inflammatory Diseases: The Evidence, Consequences, and Perspectives. *Mediators Inflamm.* 2015;2015:102476.

32. Skov V, Thomassen M, Riley CH, et al. Gene expression profiling with principal component analysis depicts the biological continuum from essential thrombocythemia over polycythemia vera to myelofibrosis. *Exp. Hematol.* 2012;40(9):771–780.e19.

33. Gregory CJ, Eaves AC. Human marrow cells capable of erythropoietic differentiation in vitro: definition of three erythroid colony responses. *Blood*. 1977;49(6):855–64.

34. Allen TD, Dexter TM. Ultrastructural aspects of erythropoietic differentiation in long-term bone marrow culture. *Differentiation.* 1982;21(2):86–94.

35. Chasis JA, Mohandas N. Erythroblastic islands: niches for erythropoiesis. *Blood*. 2008;112(3):470–478.

36. Gregory CJ, Eaves AC. Three stages of erythropoietic progenitor cell differentiation distinguished by a number of physical and biologic properties. *Blood*. 1978;51(3):527–37.

37. Iscove NN. The role of erythropoietin in regulation of population size and cell cycling of early and late erythroid precursors in mouse bone marrow. *Cell Tissue Kinet.* 1977;10(4):323–34.

38. Iscove NN, Sieber F, Winterhalter KH. Erythroid colony formation in cultures of mouse and human bone marrow: Analysis of the requirement for erythropoietin by gel filtration and affinity chromatography on agarose-concanavalin A. *J. Cell. Physiol.* 1974;83(2):309–320.

39. Lodish H, Flygare J, Chou S. From stem cell to erythroblast: regulation of red cell production at multiple levels by multiple hormones. *IUBMB Life*. 2010;62(7):492–6.

40. Doulatov S, Notta F, Laurenti E, Dick JE. Hematopoiesis: A Human Perspective. *Cell Stem Cell*. 2012;10(2):120–136.

41. Bazan JF. Structural design and molecular evolution of a cytokine receptor superfamily. *Proc. Natl. Acad. Sci. U. S. A.* 1990;87(18):6934–8.

42. Wu H, Liu X, Jaenisch R, Lodish HF. Generation of committed erythroid BFU-E and CFU-E progenitors does not require erythropoietin or the erythropoietin receptor. *Cell*. 1995;83(1):59–67.

43. Richmond TD, Chohan M, Barber DL. Turning cells red: signal transduction mediated by erythropoietin. *Trends Cell Biol.* 2005;15(3):146–155.

44. Tefferi A, Gilliland DG. JAK2 in Myeloproliferative Disorders Is Not Just Another Kinase. *Cell Cycle*. 2005;4(8):4053–4056.

45. Weiss MJ, Orkin SH. Transcription factor GATA-1 permits survival and maturation of erythroid precursors by preventing apoptosis. *Proc. Natl. Acad. Sci. U. S. A.* 1995;92(21):9623–7.

46. Welch JJ, Watts JA, Vakoc CR, et al. Global regulation of erythroid gene expression by transcription factor GATA-1. *Blood*. 2004;104(10):3136–3147.

47. Tallack MR, Whitington T, Shan Yuen W, et al. A global role for KLF1 in erythropoiesis revealed by ChIP-seq in primary erythroid cells. *Genome Res.* 2010;20(8):1052–1063.

48. Tallack MR, Magor GW, Dartigues B, et al. Novel roles for KLF1 in erythropoiesis revealed by mRNA-seq. *Genome Res.* 2012;22(12):2385–2398.

49. Vandekerckhove J, Courtois J, Coulon S, Ribeil JA, Hermine O. Regulation of erythropoiesis. *ESH Handb. Disord. Iron Metab.* 2009;

50. Skoda RC, Duek A, Grisouard J. Pathogenesis of myeloproliferative neoplasms. *Exp. Hematol.* 2015;43(8):599–608.

51. Rumi E, Cazzola M. Diagnosis, risk stratification, and response evaluation in classical myeloproliferative neoplasms. *Blood*. 2017;129(6):680–692.

52. Harutyunyan AS, Kralovics R. Role of germline genetic factors in MPN pathogenesis. *Hematol. Oncol. Clin. North Am.* 2012;26(5):1037–51.

53. James C, Ugo V, Le Couédic J-P, et al. A unique clonal JAK2 mutation leading to constitutive signalling causes polycythaemia vera. *Nature*. 2005;434(7037):1144–8.

54. Ding J, Komatsu H, Wakita A, et al. Familial essential thrombocythemia associated with a dominant-positive activating mutation of the c-MPL gene, which encodes for the receptor for thrombopoietin. *Blood*. 2004;103(11):4198–200.

55. Beer PA, Campbell PJ, Scott LM, et al. MPL mutations in myeloproliferative disorders: analysis of the PT-1 cohort. *Blood*. 2008;112(1):141–149.

56. Pikman Y, Lee BH, Mercher T, et al. MPLW515L Is a Novel Somatic Activating Mutation in Myelofibrosis with Myeloid Metaplasia. *PLoS Med.* 2006;3(7):e270.

57. Pardanani A, Lasho T, McClure R, et al. Discordant distribution of JAK2V617F mutation in siblings with familial myeloproliferative disorders. *Blood*. 2006;107(11):4572–3.

58. Staerk J, Defour J-P, Pecquet C, et al. Orientation-specific signalling by thrombopoietin receptor dimers. *EMBO J.* 2011;30(21):4398–413.

59. Constantinescu SN, Keren T, Socolovsky M, et al. Ligand-independent oligomerization of cell-surface erythropoietin receptor is mediated by the

transmembrane domain. *Proc. Natl. Acad. Sci. U. S. A.* 2001;98(8):4379–84.

60. Pietra D, Rumi E, Ferretti V V, et al. Differential clinical effects of different mutation subtypes in CALR-mutant myeloproliferative neoplasms. *Leukemia*. 2016;30(2):431–8.

61. Klampfl T, Gisslinger H, Harutyunyan AS, et al. Somatic mutations of calreticulin in myeloproliferative neoplasms. *N. Engl. J. Med.* 2013;369(25):2379–90.

62. Nangalia J, Massie CE, Baxter EJ, et al. Somatic CALR mutations in myeloproliferative neoplasms with nonmutated JAK2. *N. Engl. J. Med.* 2013;369(25):2391–405.

63. Plo I, Zhang Y, Le Couédic J-P, et al. An activating mutation in the CSF3R gene induces a hereditary chronic neutrophilia. *J. Exp. Med.* 2009;206(8):1701–7.

64. Pardanani A, Lasho TL, Laborde RR, et al. CSF3R T618I is a highly prevalent and specific mutation in chronic neutrophilic leukemia. *Leukemia*. 2013;27(9):1870–1873.

65. Tefferi A. Myeloproliferative neoplasms: A decade of discoveries and treatment advances. *Am. J. Hematol.* 2016;91(1):50–8.

66. Kralovics R, Teo S-S, Li S, et al. Acquisition of the V617F mutation of JAK2 is a late genetic event in a subset of patients with myeloproliferative disorders. *Blood*. 2006;108(4):1377–80.

67. Hermouet S, Bigot-Corbel E, Gardie B. Pathogenesis of Myeloproliferative Neoplasms: Role and Mechanisms of Chronic Inflammation. *Mediators Inflamm.* 2015;2015:145293.

68. Maxson JE, Gotlib J, Pollyea DA, et al. Oncogenic *CSF3R* Mutations in Chronic Neutrophilic Leukemia and Atypical CML. *N. Engl. J. Med.* 2013;368(19):1781–1790.

69. Olcaydu D, Harutyunyan A, Jäger R, et al. A common JAK2 haplotype confers susceptibility to myeloproliferative neoplasms. *Nat. Genet.* 2009;41(4):450–454.

70. Jones A V, Chase A, Silver RT, et al. JAK2 haplotype is a major risk factor for the development of myeloproliferative neoplasms. *Nat. Genet.* 2009;41(4):446–449.

71. Kilpivaara O, Mukherjee S, Schram AM, et al. A germline JAK2 SNP is associated with predisposition to the development of JAK2V617F-positive myeloproliferative neoplasms. *Nat. Genet.* 2009;41(4):455–459.

72. Wilks AF, Harpur AG, Kurban RR, et al. Two novel protein-tyrosine kinases, each with a second phosphotransferase-related catalytic domain, define a new class of protein kinase. *Mol. Cell. Biol.* 1991;11(4):2057–65.

73. Harpur AG, Andres AC, Ziemiecki A, Aston RR, Wilks AF. JAK2, a third member of the JAK family of protein tyrosine kinases. *Oncogene*. 1992;7(7):1347–53.

74. Witthuhn BA, Quelle FW, Silvennoinen O, et al. JAK2 associates with the erythropoietin receptor and is tyrosine phosphorylated and activated following stimulation with erythropoietin. *Cell*. 1993;74(2):227–36.

75. Argetsinger LS, Campbell GS, Yang X, et al. Identification of JAK2 as a growth hormone receptor-associated tyrosine kinase. *Cell*. 1993;74(2):237–44.

76. Zhao L, Ma Y, Seemann J, Huang LJ. A regulating role of the JAK2 FERM domain in hyperactivation of JAK2(V617F). *Biochem. J.* 2010;426(1):91–8.

77. Funakoshi-Tago M, Pelletier S, Moritake H, Parganas E, Ihle JN. Jak2 FERM Domain Interaction with the Erythropoietin Receptor Regulates Jak2 Kinase Activity. *Mol. Cell. Biol.* 2008;28(5):1792–1801.

78. Ungureanu D, Wu J, Pekkala T, et al. The pseudokinase domain of JAK2 is a dual-specificity protein kinase that negatively regulates cytokine signaling. *Nat. Struct. Mol. Biol.* 2011;18(9):971–6.

79. Silvennoinen O, Hubbard SR. Molecular insights into regulation of JAK2 in myeloproliferative neoplasms. *Blood*. 2015;125(22):3388–92.

80. Kralovics R, Passamonti F, Buser AS, et al. A gain-of-function mutation of JAK2 in myeloproliferative disorders. *N. Engl. J. Med.* 2005;352(17):1779–90.

81. Baxter EJ, Scott LM, Campbell PJ, et al. Acquired mutation of the tyrosine kinase JAK2 in human myeloproliferative disorders. *Lancet (London, England)*. 2005;365(9464):1054–61.

82. Hammarén HM, Ungureanu D, Grisouard J, et al. ATP binding to the pseudokinase domain of JAK2 is critical for pathogenic activation. *Proc. Natl. Acad. Sci. U. S. A.* 2015;112(15):4642–7.

83. Dusa A, Mouton C, Pecquet C, Herman M, Constantinescu SN. JAK2 V617F constitutive activation requires JH2 residue F595: a pseudokinase domain target for specific inhibitors. *PLoS One*. 2010;5(6):e11157.

84. Hookham MB, Elliott J, Suessmuth Y, et al. The myeloproliferative disorder-associated JAK2 V617F mutant escapes negative regulation by suppressor of cytokine signaling 3. *Blood*. 2007;109(11):4924–9.

85. Scott LM. The JAK2 exon 12 mutations: a comprehensive review. *Am. J. Hematol.* 2011;86(8):668–76.

86. Grinfeld J, Nangalia J, Green AR. Molecular determinants of pathogenesis and clinical phenotype in myeloproliferative neoplasms. *Haematologica*. 2017;102(1):7–17.

87. Mead AJ, Rugless MJ, Jacobsen SEW, Schuh A. Germline JAK2 mutation in a family with hereditary thrombocytosis. *N. Engl. J. Med.* 2012;366(10):967–9.

88. Etheridge SL, Cosgrove ME, Sangkhae V, et al. A novel activating, germline JAK2 mutation, JAK2R564Q, causes familial essential thrombocytosis. *Blood*. 2014;123(7):1059–68.

89. Marty C, Saint-Martin C, Pecquet C, et al. Germ-line JAK2 mutations in the kinase domain are responsible for hereditary thrombocytosis and are resistant to JAK2 and HSP90 inhibitors. *Blood*. 2014;123(9):1372–83.

90. Lanikova L, Babosova O, Swierczek S, et al. Coexistence of gain-of-function JAK2 germ line mutations with JAK2V617F in polycythemia vera. *Blood*. 2016;128(18):.

91. Dawson MA, Bannister AJ, Göttgens B, et al. JAK2 phosphorylates histone H3Y41 and excludes HP1α from chromatin. *Nature*. 2009;461(7265):819–822.

92. Plo I, Nakatake M, Malivert L, et al. JAK2 stimulates homologous recombination and genetic instability: potential implication in the heterogeneity of myeloproliferative disorders. *Blood*. 2008;112(4):1402–12.

93. Walz C, Crowley BJ, Hudon HE, et al. Activated Jak2 with the V617F point mutation promotes G1/S phase transition. *J. Biol. Chem.* 2006;281(26):18177–83.

94. Scott LM, Tong W, Levine RL, et al. JAK2 exon 12 mutations in polycythemia vera and idiopathic erythrocytosis. *N. Engl. J. Med.* 2007;356(5):459–68.

95. Kralovics R, Guan Y, Prchal JT. Acquired uniparental disomy of chromosome 9p is a frequent stem cell defect in polycythemia vera. *Exp. Hematol.* 2002;30(3):229–36.

96. Scott LM, Scott MA, Campbell PJ, Green AR. Progenitors homozygous for the V617F mutation occur in most patients with polycythemia vera, but not essential thrombocythemia. *Blood*. 2006;108(7):2435–7.

97. Li J, Kent DG, Godfrey AL, et al. JAK2V617F homozygosity drives a phenotypic switch in myeloproliferative neoplasms, but is insufficient to sustain disease. *Blood*. 2014;123(20):3139–51.

98. Tiedt R, Hao-Shen H, Sobas MA, et al. Ratio of mutant JAK2-V617F to wild-type Jak2 determines the MPD phenotypes in transgenic mice. *Blood*. 2008;111(8):3931–40.

99. Vannucchi AM, Antonioli E, Guglielmelli P, et al. Clinical profile of homozygous JAK2 617V>F mutation in patients with polycythemia vera or essential thrombocythemia. *Blood*. 2007;110(3):840–846.

100. Godfrey AL, Chen E, Pagano F, et al. JAK2V617F homozygosity arises commonly and recurrently in PV and ET, but PV is characterized by expansion of a dominant homozygous subclone. *Blood*. 2012;120(13):2704–7.

101. Yao H, Ma Y, Hong Z, et al. Activating JAK2 mutants reveal cytokine receptor coupling differences that impact outcomes in myeloproliferative neoplasm. *Leukemia*. 2017;31(10):2122–2131.

102. Chen E, Beer PA, Godfrey AL, et al. Distinct clinical phenotypes associated with JAK2V617F reflect differential STAT1 signaling. *Cancer Cell*. 2010;18(5):524–35.

103. Ortmann CA, Kent DG, Nangalia J, et al. Effect of Mutation Order on Myeloproliferative Neoplasms. *N. Engl. J. Med.* 2015;372(7):601–612.

104. Lundberg P, Takizawa H, Kubovcakova L, et al. Myeloproliferative neoplasms can be initiated from a single hematopoietic stem cell expressing *JAK2* -V617F. *J. Exp. Med.* 2014;211(11):2213–2230.

105. Anand S, Stedham F, Beer P, et al. Effects of the JAK2 mutation on the hematopoietic stem and progenitor compartment in human myeloproliferative neoplasms. *Blood*. 2011;118(1):177–81.

106. James C, Mazurier F, Dupont S, et al. The hematopoietic stem cell compartment of JAK2V617F-positive myeloproliferative disorders is a reflection of disease heterogeneity. *Blood*. 2008;112(6):2429–38.

107. Larsen TS, Christensen JH, Hasselbalch HC, Pallisgaard N. The JAK2 V617F mutation involves B- and T-lymphocyte lineages in a subgroup of patients with Philadelphia-chromosome negative chronic myeloproliferative disorders. *Br. J. Haematol.* 2007;136(5):745–51.

108. Mullally A, Lane SW, Ball B, et al. Physiological Jak2V617F expression causes a lethal myeloproliferative neoplasm with differential effects on hematopoietic stem and progenitor cells. *Cancer Cell*. 2010;17(6):584–96.

109. Kent DG, Li J, Tanna H, et al. Self-Renewal of Single Mouse Hematopoietic Stem Cells Is Reduced by JAK2V617F Without Compromising Progenitor Cell Expansion. *PLoS Biol.* 2013;11(6):e1001576.

110. McKerrell T, Park N, Moreno T, et al. Leukemia-associated somatic mutations drive distinct patterns of age-related clonal hemopoiesis. *Cell Rep.* 2015;10(8):1239–45.

111. Genovese G, Kähler AK, Handsaker RE, et al. Clonal hematopoiesis and blood-cancer risk inferred from blood DNA sequence. *N. Engl. J. Med.* 2014;371(26):2477–87.

112. Sun J, Ramos A, Chapman B, et al. Clonal dynamics of native haematopoiesis. *Nature*. 2014;514(7522):322–7.

113. Hanahan D, Weinberg RA. Hallmarks of Cancer: The Next Generation. *Cell*. 2011;144(5):646–674.

114. Kristinsson SY, Landgren O, Samuelsson J, Björkholm M, Goldin LR. Autoimmunity and the risk of myeloproliferative neoplasms. *Haematologica*. 2010;95(7):1216–20.

115. Craver BM, El Alaoui K, Scherber RM, Fleischman AG. The Critical Role of Inflammation in the Pathogenesis and Progression of Myeloid Malignancies. *Cancers (Basel).* 2018;10(4):.

116. Tefferi A, Vaidya R, Caramazza D, et al. Circulating interleukin (IL)-8, IL-2R, IL-12, and IL-15 levels are independently prognostic in primary myelofibrosis: a comprehensive cytokine profiling study. *J. Clin. Oncol.* 2011;29(10):1356–63.

117. Anderson LA, Pfeiffer RM, Landgren O, et al. Risks of myeloid malignancies in patients with autoimmune conditions. *Br. J. Cancer*. 2009;100(5):822–828.

118. Barrett JC, Hansoul S, Nicolae DL, et al. Genome-wide association defines more than 30 distinct susceptibility loci for Crohn's disease. *Nat. Genet.* 2008;40(8):955–62.

119. Ferguson LR, Han DY, Fraser AG, et al. Genetic factors in chronic inflammation: single nucleotide polymorphisms in the STAT-JAK pathway, susceptibility to DNA damage and Crohn's disease in a New Zealand population. *Mutat. Res.* 2010;690(1–2):108–15.

120. Hermouet S, Vilaine M. The JAK2 46/1 haplotype: a marker of inappropriate myelomonocytic response to cytokine stimulation, leading to increased risk of inflammation, myeloid neoplasm, and impaired defense against infection? *Haematologica*. 2011;96(11):1575–9.

121. Myers JS. Proinflammatory Cytokines and Sickness Behavior: Implications for Depression and Cancer-Related Symptoms. *Oncol. Nurs. Forum*. 2008;35(5):802–807.

122. Mullally A, Bruedigam C, Poveromo L, et al. Depletion of Jak2V617F myeloproliferative neoplasm-propagating stem cells by interferon- in a murine model of polycythemia vera. *Blood*. 2013;121(18):3692–3702.

123. Coombs CC, Zehir A, Devlin SM, et al. Therapy-Related Clonal Hematopoiesis in Patients with Non-hematologic Cancers Is Common and Associated with Adverse Clinical Outcomes. *Cell Stem Cell*. 2017;21(3):374–382.e4.

124. Jaiswal S, Natarajan P, Silver AJ, et al. Clonal Hematopoiesis and Risk of Atherosclerotic Cardiovascular Disease. *N. Engl. J. Med.* 2017;377(2):111–121.

125. Barbui T, Finazzi G, Falanga A. Myeloproliferative neoplasms and thrombosis. *Blood*. 2013;122(13):2176–2184.

126. Vannucchi AM, Antonioli E, Guglielmelli P, Pardanani A, Tefferi A. Clinical correlates of JAK2V617F presence or allele burden in myeloproliferative neoplasms: a critical reappraisal. *Leukemia*. 2008;22(7):1299–1307.

127. Landolfi R, Di Gennaro L. Pathophysiology of thrombosis in myeloproliferative neoplasms. *Haematologica*. 2011;96(2):183–186.

128. Vannucchi A, Guglielmelli P. JAK2 Mutation-Related Disease and Thrombosis. *Semin. Thromb. Hemost.* 2013;39(05):496–506.

129. Quintas-Cardama A, Vaddi K, Liu P, et al. Preclinical characterization of the selective

JAK1/2 inhibitor INCB018424: therapeutic implications for the treatment of myeloproliferative neoplasms. *Blood*. 2010;115(15):3109–3117.

130. Barbui T, Carobbio A, Finazzi G, et al. Inflammation and thrombosis in essential thrombocythemia and polycythemia vera: different role of C-reactive protein and pentraxin 3. *Haematologica*. 2011;96(2):315–318.

131. Frederiksen H, Farkas DK, Christiansen CF, Hasselbalch HC, Sorensen HT. Chronic myeloproliferative neoplasms and subsequent cancer risk: a Danish population-based cohort study. *Blood*. 2011;118(25):6515–6520.

132. Hasselbalch H. Idiopathic myelofibrosis: A clinical study of 80 patients. *Am. J. Hematol.* 1990;34(4):291–300.

133. Pettersson H, Knutsen H, Holmberg E, Andréasson B. Increased incidence of another cancer in myeloproliferative neoplasms patients at the time of diagnosis. *Eur. J. Haematol.* 2015;94(2):152–156.

134. Hasselbalch HC. Perspectives on the increased risk of second cancer in patients with essential thrombocythemia, polycythemia vera and myelofibrosis. *Eur. J. Haematol.* 2015;94(2):96–98.

135. Enblom A, Lindskog E, Hasselbalch H, et al. High rate of abnormal blood values and vascular complications before diagnosis of myeloproliferative neoplasms. *Eur. J. Intern. Med.* 2015;26(5):344–347.

136. Skov V, Larsen TS, Thomassen M, et al. Whole-blood transcriptional profiling of interferon-inducible genes identifies highly upregulated IFI27 in primary myelofibrosis. *Eur. J. Haematol.* 2011;87(1):54–60.

137. Skov V, Larsen TS, Thomassen M, et al. Molecular profiling of peripheral blood cells from patients with polycythemia vera and related neoplasms: Identification of deregulated genes of significance for inflammation and immune surveillance. *Leuk. Res.* 2012;36(11):1387–1392.

138. Skov V, Thomassen M, Riley CH, et al. Gene expression profiling with principal component analysis depicts the biological continuum from essential thrombocythemia over polycythemia vera to myelofibrosis. *Exp. Hematol.* 2012;40(9):771–780.e19.

139. Skov V, Riley CH, Thomassen M, et al. Whole blood transcriptional profiling reveals significant down-regulation of human leukocyte antigen class I and II genes in essential thrombocythemia, polycythemia vera and myelofibrosis. *Leuk. Lymphoma*. 2013;54(10):2269–2273.

140. Fleischman AG. Inflammation as a Driver of Clonal Evolution in Myeloproliferative Neoplasm. *Mediators Inflamm.* 2015;2015:1–6.

141. Misteli T, Soutoglou E. The emerging role of nuclear architecture in DNA repair and

genome maintenance. *Nat. Rev. Mol. Cell Biol.* 2009;10(4):243–54.

142. Holthausen JT, Wyman C, Kanaar R. Regulation of DNA strand exchange in homologous recombination. *DNA Repair (Amst).* 2010;9(12):1264–72.

143. Takacova S, Slany R, Bartkova J, et al. DNA damage response and inflammatory signaling limit the MLL-ENL-induced leukemogenesis in vivo. *Cancer Cell*. 2012;21(4):517–31.

144. Halazonetis TD, Gorgoulis VG, Bartek J. An oncogene-induced DNA damage model for cancer development. *Science*. 2008;319(5868):1352–5.

145. Chen E, Ahn JS, Massie CE, et al. JAK2V617F promotes replication fork stalling with disease-restricted impairment of the intra-S checkpoint response. *Proc. Natl. Acad. Sci. U. S. A.* 2014;111(42):15190–5.

146. Marty C, Lacout C, Droin N, et al. A role for reactive oxygen species in JAK2 V617F myeloproliferative neoplasm progression. *Leukemia*. 2013;27(11):2187–95.

147. Li J, Spensberger D, Ahn JS, et al. JAK2 V617F impairs hematopoietic stem cell function in a conditional knock-in mouse model of JAK2 V617F-positive essential thrombocythemia. *Blood*. 2010;116(9):1528–38.

148. Zhao R, Follows GA, Beer PA, et al. Inhibition of the Bcl-x_L Deamidation Pathway in Myeloproliferative Disorders. *N. Engl. J. Med.* 2008;359(26):2778–2789.

149. Ahn JS, Li J, Chen E, et al. JAK2V617F mediates resistance to DNA damage-induced apoptosis by modulating FOXO3A localization and Bcl-xL deamidation. *Oncogene*. 2016;35(17):2235–46.

150. Nakatake M, Monte-Mor B, Debili N, et al. JAK2(V617F) negatively regulates p53 stabilization by enhancing MDM2 via La expression in myeloproliferative neoplasms. *Oncogene*. 2012;31(10):1323–33.

151. Klampfl T, Harutyunyan A, Berg T, et al. Genome integrity of myeloproliferative neoplasms in chronic phase and during disease progression. *Blood*. 2011;118(1):167–76.

152. Tefferi A, Guglielmelli P, Larson DR, et al. Long-term survival and blast transformation in molecularly annotated essential thrombocythemia, polycythemia vera, and myelofibrosis. *Blood*. 2014;124(16):2507–13; quiz 2615.

153. Chen E, Ahn JS, Sykes DB, et al. RECQL5 Suppresses Oncogenic JAK2-Induced Replication Stress and Genomic Instability. *Cell Rep.* 2015;13(11):2345–52.

154. Lemaître C, Soutoglou E. Double strand break (DSB) repair in heterochromatin and heterochromatin proteins in DSB repair. *DNA Repair (Amst).* 2014;19:163–8.

155. Barde I, Rauwel B, Marin-Florez RM, et al. A KRAB/KAP1-miRNA cascade regulates

erythropoiesis through stage-specific control of mitophagy. *Science*. 2013;340(6130):350–3.

156. Kim SS, Chen YM, O'Leary E, et al. A novel member of the RING finger family, KRIP-1, associates with the KRAB-A transcriptional repressor domain of zinc finger proteins. *Proc. Natl. Acad. Sci. U. S. A.* 1996;93(26):15299–304.

157. Friedman JR, Fredericks WJ, Jensen DE, et al. KAP-1, a novel corepressor for the highly conserved KRAB repression domain. *Genes Dev.* 1996;10(16):2067–78.

158. Iyengar S, Farnham PJ. KAP1 Protein: An Enigmatic Master Regulator of the Genome. *J. Biol. Chem.* 2011;286(30):26267–26276.

159. Cheng C-T, Kuo C-Y, Ann DK. KAPtain in charge of multiple missions: Emerging roles of KAP1. *World J. Biol. Chem.* 2014;5(3):308–20.

160. White DE, Negorev D, Peng H, et al. KAP1, a Novel Substrate for PIKK Family Members, Colocalizes with Numerous Damage Response Factors at DNA Lesions. *Cancer Res.* 2006;66(24):11594–11599.

161. Ziv Y, Bielopolski D, Galanty Y, et al. Chromatin relaxation in response to DNA double-strand breaks is modulated by a novel ATM- and KAP-1 dependent pathway. *Nat. Cell Biol.* 2006;8(8):870–876.

162. Goodarzi AA, Noon AT, Deckbar D, et al. ATM Signaling Facilitates Repair of DNA Double-Strand Breaks Associated with Heterochromatin. *Mol. Cell*. 2008;31(2):167–177.

163. Goodarzi AA, Kurka T, Jeggo PA. KAP-1 phosphorylation regulates CHD3 nucleosome remodeling during the DNA double-strand break response. *Nat. Struct. Mol. Biol.* 2011;18(7):831–839.

164. Garvin AJ, Densham RM, Blair-Reid SA, et al. The deSUMOylase SENP7 promotes chromatin relaxation for homologous recombination DNA repair. *EMBO Rep.* 2013;14(11):975–983.

165. Hu C, Zhang S, Gao X, et al. Roles of Kruppel-associated Box (KRAB)-associated Co-repressor KAP1 Ser-473 Phosphorylation in DNA Damage Response. *J. Biol. Chem.* 2012;287(23):18937–18952.

166. Bolderson E, Savage KI, Mahen R, et al. Krüppel-associated Box (KRAB)-associated Co-repressor (KAP-1) Ser-473 Phosphorylation Regulates Heterochromatin Protein 1β (HP1-β) Mobilization and DNA Repair in Heterochromatin. *J. Biol. Chem.* 2012;287(33):28122–28131.

167. White D, Rafalska-Metcalf IU, Ivanov A V., et al. The ATM Substrate KAP1 Controls DNA Repair in Heterochromatin: Regulation by HP1 Proteins and Serine 473/824 Phosphorylation. *Mol. Cancer Res.* 2012;10(3):401–414.

168. Spivak JL. Polycythemia Vera. *Curr. Treat. Options Oncol.* 2018;19(2):12.

169. Tashi T, Swierczek S, Kim SJ, et al. Pegylated interferon Alfa-2a and hydroxyurea in polycythemia vera and essential thrombocythemia: differential cellular and molecular responses. *Leukemia*. 2018;32(8):1830–1833.

170. Bjørn ME, Hasselbalch HC. Minimal residual disease or cure in MPNs? Rationales and perspectives on combination therapy with interferon-alpha2 and ruxolitinib. *Expert Rev. Hematol.* 2017;10(5):393–404.

171. Robbins E, Pederson T. Iron: its intracellular localization and possible role in cell division. *Proc. Natl. Acad. Sci. U. S. A.* 1970;66(4):1244–51.

172. Hoffbrand A V, Ganeshaguru K, Hooton JW, Tattersall MH. Effect of iron deficiency and desferrioxamine on DNA synthesis in human cells. *Br. J. Haematol.* 1976;33(4):517–26.

173. Yu Y, Kovacevic Z, Richardson DR. Tuning Cell Cycle Regulation with an Iron Key. *Cell Cycle*. 2007;6(16):1982–1994.

174. Joharapurkar AA, Pandya VB, Patel VJ, Desai RC, Jain MR. Prolyl Hydroxylase Inhibitors: A Breakthrough in the Therapy of Anemia Associated with Chronic Diseases. *J. Med. Chem.* 2018;61(16):6964–6982.

175. Pugh CW, Tan CC, Jones RW, Ratcliffe PJ. Functional analysis of an oxygen-regulated transcriptional enhancer lying 3’ to the mouse erythropoietin gene. *Proc. Natl. Acad. Sci. U. S. A.* 1991;88(23):10553–7.

176. Semenza GL, Nejfelt MK, Chi SM, Antonarakis SE. Hypoxia-inducible nuclear factors bind to an enhancer element located 3’ to the human erythropoietin gene. *Proc. Natl. Acad. Sci. U. S. A.* 1991;88(13):5680–4.

177. Beck I, Ramirez S, Weinmann R, Caro J. Enhancer element at the 3’-flanking region controls transcriptional response to hypoxia in the human erythropoietin gene. *J. Biol. Chem.* 1991;266(24):15563–6.

178. Maxwell PH, Pugh CW. Regulation of oxygen sensing and erythropoietin production. *ESH Handb. Disord. Iron Metab.* 2009;

179. Haase VH. Regulation of erythropoiesis by hypoxia-inducible factors. *Blood Rev.* 2013;27(1):41–53.

180. Jelkmann W. Regulation of erythropoietin production. *J. Physiol.* 2011;589(Pt 6):1251–8.

181. Yang M, Su H, Soga T, Kranc KR, Pollard PJ. Prolyl hydroxylase domain enzymes: important regulators of cancer metabolism. *Hypoxia (Auckland, N.Z.)*. 2014;2:127–142.

182. Fong G-H, Takeda K. Role and regulation of prolyl hydroxylase domain proteins. *Cell Death Differ.* 2008;15(4):635–641.

183. Maxwell PH, Wiesener MS, Chang GW, et al. The tumour suppressor protein VHL targets hypoxia-inducible factors for oxygen-dependent proteolysis. *Nature*. 1999;399(6733):271–5.

184. Lando D, Peet DJ, Gorman JJ, et al. FIH-1 is an asparaginyl hydroxylase enzyme that regulates the transcriptional activity of hypoxia-inducible factor. *Genes Dev.* 2002;16(12):1466–71.

185. Appelhoff RJ, Tian Y-M, Raval RR, et al. Differential Function of the Prolyl Hydroxylases PHD1, PHD2, and PHD3 in the Regulation of Hypoxia-inducible Factor. *J. Biol. Chem.* 2004;279(37):38458–38465.

186. Minamishima YA, Moslehi J, Bardeesy N, et al. Somatic inactivation of the PHD2 prolyl hydroxylase causes polycythemia and congestive heart failure. *Blood*. 2008;111(6):3236–3244.

187. Berra E, Ginouvès A, Pouysségur J. The hypoxia-inducible-factor hydroxylases bring fresh air into hypoxia signalling. *EMBO Rep.* 2006;7(1):41–5.

188. Berra E, Ginouvès A, Pouysségur J. The hypoxia-inducible-factor hydroxylases bring fresh air into hypoxia signalling. *EMBO Rep.* 2006;7(1):41–5.

189. Bruegge K, Jelkmann W, Metzen E. Hydroxylation of hypoxia-inducible transcription factors and chemical compounds targeting the HIF-alpha hydroxylases. *Curr. Med. Chem.* 2007;14(17):1853–62.

190. Kling PJ, Dragsten PR, Roberts RA, et al. Iron deprivation increases erythropoietin production in vitro, in normal subjects and patients with malignancy. *Br. J. Haematol.* 1996;95(2):241–8.

191. Paliege A, Rosenberger C, Bondke A, et al. Hypoxia-inducible factor-2α-expressing interstitial fibroblasts are the only renal cells that express erythropoietin under hypoxia-inducible factor stabilization. *Kidney Int.* 2010;77(4):312–318.

192. Lieb ME, Menzies K, Moschella MC, Ni R, Taubman MB. Mammalian EGLN genes have distinct patterns of mRNA expression and regulation. *Biochem. Cell Biol.* 2002;80(4):421–6.

193. Oehme F, Ellinghaus P, Kolkhof P, et al. Overexpression of PH-4, a novel putative proline 4-hydroxylase, modulates activity of hypoxia-inducible transcription factors. *Biochem. Biophys. Res. Commun.* 2002;296(2):343–349.

194. Cioffi CL, Qin Liu X, Kosinski PA, Garay M, Bowen BR. Differential regulation of HIF-1α prolyl-4-hydroxylase genes by hypoxia in human cardiovascular cells. *Biochem. Biophys. Res. Commun.* 2003;303(3):947–953.

195. Erez N, Milyavsky M, Goldfinger N, et al. Falkor, a novel cell growth regulator isolated by a functional genetic screen. *Oncogene*. 2002;21(44):6713–6721.

196. Dupuy D, Aubert I, Dupérat VG, et al. Mapping, Characterization, and Expression

Analysis of the SM-20 Human Homologue, C1orf12, and Identification of a Novel Related Gene, SCAND2. *Genomics*. 2000;69(3):348–354.

197. Metzen E, Berchner-Pfannschmidt U, Stengel P, et al. Intracellular localisation of human HIF-1 alpha hydroxylases: implications for oxygen sensing. *J. Cell Sci.* 2003;116(Pt 7):1319–26.

198. Yasumoto K, Kowata Y, Yoshida A, Torii S, Sogawa K. Role of the intracellular localization of HIF-prolyl hydroxylases. *Biochim. Biophys. Acta - Mol. Cell Res.* 2009;1793(5):792–797.

199. Percy MJ, Zhao Q, Flores A, et al. A family with erythrocytosis establishes a role for prolyl hydroxylase domain protein 2 in oxygen homeostasis. *Proc. Natl. Acad. Sci.* 2006;103(3):654–659.

200. Erez N, Milyavsky M, Eilam R, et al. Expression of prolyl-hydroxylase-1 (PHD1/EGLN2) suppresses hypoxia inducible factor-1alpha activation and inhibits tumor growth. *Cancer Res.* 2003;63(24):8777–83.

201. Takeda K, Aguila HL, Parikh NS, et al. Regulation of adult erythropoiesis by prolyl hydroxylase domain proteins. *Blood*. 2008;111(6):3229–3235.

202. Frei C, Edgar BA. Drosophila cyclin D/Cdk4 requires Hif-1 prolyl hydroxylase to drive cell growth. *Dev. Cell*. 2004;6(2):241–51.

203. Wax SD, Rosenfield CL, Taubman MB. Identification of a novel growth factor-responsive gene in vascular smooth muscle cells. *J. Biol. Chem.* 1994;269(17):13041–7.

204. Xie X, Xiao H, Ding F, et al. Over-expression of prolyl hydroxylase-1 blocks NF-κB-mediated cyclin D1 expression and proliferation in lung carcinoma cells. *Cancer Genet.* 2014;207(5):188–194.

205. Scholz CC, Cavadas MAS, Tambuwala MM, et al. Regulation of IL-1β-induced NF-κB by hydroxylases links key hypoxic and inflammatory signaling pathways. *Proc. Natl. Acad. Sci. U. S. A.* 2013;110(46):18490–5.

206. Wang J, Zhang J, Zhou C, Chen L, Yu Q. An Insertion/Deletion Polymorphism Within the Proximal Promoter of *EGLN2* Is Associated With Susceptibility for Gastric Cancer in the Chinese Population. *Genet. Test. Mol. Biomarkers*. 2014;18(4):269–273.

207. Che J, Jiang D, Zheng Y, et al. Polymorphism in PHD1 gene and risk of non-small cell lung cancer in a Chinese population. *Tumor Biol.* 2014;35(9):8921–8925.

208. Epstein AC, Gleadle JM, McNeill LA, et al. C. elegans EGL-9 and mammalian homologs define a family of dioxygenases that regulate HIF by prolyl hydroxylation. *Cell*. 2001;107(1):43–54.

209. Seth P, Krop I, Porter D, Polyak K. Novel estrogen and tamoxifen induced genes

identified by SAGE (Serial Analysis of Gene Expression). *Oncogene*. 2002;21(5):836–843.

210. Jares P, Campo E. Advances in the understanding of mantle cell lymphoma. *Br. J. Haematol.* 2008;142(2):149–65.

211. Shah BD, Martin P, Sotomayor EM. Mantle cell lymphoma: a clinically heterogeneous disease in need of tailored approaches. *Cancer Control*. 2012;19(3):227–35.

212. Erales J, Coffino P. Ubiquitin-independent proteasomal degradation. *Biochim. Biophys. Acta - Mol. Cell Res.* 2014;1843(1):216–221.

213. Baugh JM, Viktorova EG, Pilipenko E V. Proteasomes Can Degrade a Significant Proportion of Cellular Proteins Independent of Ubiquitination. *J. Mol. Biol.* 2009;386(3):814–827.

214. Mangold U. The antizyme family: Polyamines and beyond. *IUBMB Life (International Union Biochem. Mol. Biol. Life)*. 2005;57(10):671–676.

215. Murai N, Murakami Y, Tajima A, Matsufuji S. Novel ubiquitin-independent nucleolar c-Myc degradation pathway mediated by antizyme 2. *Sci. Rep.* 2018;8(1):3005.

216. Murakami Y, Matsufuji S, Kameji T, et al. Ornithine decarboxylase is degraded by the 26S proteasome without ubiquitination. *Nature*. 1992;360(6404):597–599.

217. Asher G, Bercovich Z, Tsvetkov P, Shaul Y, Kahana C. 20S Proteasomal Degradation of Ornithine Decarboxylase Is Regulated by NQO1. *Mol. Cell*. 2005;17(5):645–655.

218. Tsvetkov P, Asher G, Reiss V, et al. Inhibition of NAD(P)H:quinone oxidoreductase 1 activity and induction of p53 degradation by the natural phenolic compound curcumin. *Proc. Natl. Acad. Sci. U. S. A.* 2005;102(15):5535–40.

219. Newman RM, Mobascher A, Mangold U, et al. Antizyme targets cyclin D1 for degradation. A novel mechanism for cell growth repression. *J. Biol. Chem.* 2004;279(40):41504–11.

220. Murakami Y, Hayashi S. Role of antizyme in degradation of ornithine decarboxylase in HTC cells. *Biochem. J.* 1985;226(3):893–6.

221. Fu D, Richardson DR. Iron chelation and regulation of the cell cycle: 2 mechanisms of posttranscriptional regulation of the universal cyclin-dependent kinase inhibitor p21CIP1/WAF1 by iron depletion. *Blood*. 2007;110(2):752–761.

222. Le NT V, Richardson DR. Potent iron chelators increase the mRNA levels of the universal cyclin-dependent kinase inhibitor p21(CIP1/WAF1), but paradoxically inhibit its translation: a potential mechanism of cell cycle dysregulation. *Carcinogenesis*. 2003;24(6):1045–58.

223. Brunet A, Bonni A, Zigmond MJ, et al. Akt promotes cell survival by phosphorylating

and inhibiting a Forkhead transcription factor. *Cell*. 1999;96(6):857–68.

224. Stahl M, Dijkers PF, Kops GJPL, et al. The forkhead transcription factor FoxO regulates transcription of p27Kip1 and Bim in response to IL-2. *J. Immunol.* 2002;168(10):5024–31.

225. Ekoff M, Kaufmann T, Engström M, et al. The BH3-only protein Puma plays an essential role in cytokine deprivation induced apoptosis of mast cells. *Blood*. 2007;110(9):3209–17.

226. Nho RS, Hergert P. FoxO3a and disease progression. *World J. Biol. Chem.* 2014;5(3):346.

227. Zhang X, Tang N, Hadden TJ, Rishi AK. Akt, FoxO and regulation of apoptosis. *Biochim. Biophys. Acta - Mol. Cell Res.* 2011;1813(11):1978–1986.

228. Schmidt M, Fernandez de Mattos S, van der Horst A, et al. Cell cycle inhibition by FoxO forkhead transcription factors involves downregulation of cyclin D. *Mol. Cell. Biol.* 2002;22(22):7842–52.

229. Zheng X, Zhai B, Koivunen P, et al. Prolyl hydroxylation by EglN2 destabilizes FOXO3a by blocking its interaction with the USP9x deubiquitinase. *Genes Dev.* 2014;28(13):1429–1444.

230. Constantinescu SN, Liu X, Beyer W, et al. Activation of the erythropoietin receptor by the gp55-P viral envelope protein is determined by a single amino acid in its transmembrane domain. *EMBO J.* 1999;18(12):3334–47.

231. Liu X, Constantinescu SN, Sun Y, et al. Generation of mammalian cells stably expressing multiple genes at predetermined levels. *Anal. Biochem.* 2000;280(1):20–8.

232. Kasparek P, Krausova M, Haneckova R, et al. Efficient gene targeting of the Rosa26 locus in mouse zygotes using TALE nucleases. *FEBS Lett.* 2014;588(21):3982–8.

233. Pearse RN, Feinman R, Ravetch J V. Characterization of the promoter of the human gene encoding the high-affinity IgG receptor: transcriptional induction by gamma-interferon is mediated through common DNA response elements. *Proc. Natl. Acad. Sci. U. S. A.* 1991;88(24):11305–9.

234. Kumar P, Henikoff S, Ng PC. Predicting the effects of coding non-synonymous variants on protein function using the SIFT algorithm. *Nat. Protoc.* 2009;4(7):1073–81.

235. Tavtigian S V, Deffenbaugh AM, Yin L, et al. Comprehensive statistical study of 452 BRCA1 missense substitutions with classification of eight recurrent substitutions as neutral. *J. Med. Genet.* 2006;43(4):295–305.

236. Ramensky V, Bork P, Sunyaev S. Human non-synonymous SNPs: server and survey.

Nucleic Acids Res. 2002;30(17):3894–900.

237. Schwarz JM, Cooper DN, Schuelke M, Seelow D. MutationTaster2: mutation prediction for the deep-sequencing age. *Nat. Methods*. 2014;11(4):361–2.

238. Witzig TE, Price-Troska TL, Stenson MJ, Gupta M. Lack of JAK2 activating non-synonymous mutations in diffuse large B-cell tumors: JAK2 deregulation still unexplained. *Leuk. Lymphoma*. 2013;54(2):397–9.

239. Hudson AM, Yates T, Li Y, et al. Discrepancies in cancer genomic sequencing highlight opportunities for driver mutation discovery. *Cancer Res.* 2014;74(22):6390–6396.

240. Lek M, Karczewski KJ, Minikel E V, et al. Analysis of protein-coding genetic variation in 60,706 humans. *Nature*. 2016;536(7616):285–91.

241. Arber DA, Orazi A, Hasserjian R, et al. The 2016 revision to the World Health Organization (WHO) classification of myeloid neoplasms and acute leukemia. *Blood*. 2016;127(20):2391–405.

242. Lee E-J, Dykas DJ, Leavitt AD, et al. Whole-exome sequencing in evaluation of patients with venous thromboembolism. *Blood Adv.* 2017;1(16):1224–1237.

243. van den Akker EB, Pitts SJ, Deelen J, et al. Uncompromised 10-year survival of oldest old carrying somatic mutations in DNMT3A and TET2. *Blood*. 2016;127(11):1512–5.

244. Hahn CN, Babic M, Schreiber AW, et al. Rare and Common Germline Variants Contribute to Occurrence of Myelodysplastic Syndrome. *Blood*. 2015;126(23):.

245. Lundberg P, Karow A, Nienhold R, et al. Clonal evolution and clinical correlates of somatic mutations in myeloproliferative neoplasms. *Blood*. 2014;123(14):2220–8.

246. Leroy E, Dusa A, Colau D, et al. Uncoupling JAK2 V617F activation from cytokine-induced signalling by modulation of JH2 αC helix. *Biochem. J.* 2016;473(11):1579–91.

247. Campbell PJ, Scott LM, Buck G, et al. Definition of subtypes of essential thrombocythaemia and relation to polycythaemia vera based on JAK2 V617F mutation status: a prospective study. *Lancet (London, England)*. 2005;366(9501):1945–53.

248. Meier C, Hoeller S, Bourgau C, et al. Recurrent numerical aberrations of JAK2 and deregulation of the JAK2-STAT cascade in lymphomas. *Mod. Pathol.* 2009;22(3):476–87.

249. Sharma S V, Settleman J. Oncogene addiction: setting the stage for molecularly targeted cancer therapy. *Genes Dev.* 2007;21(24):3214–31.

250. Weinstein IB. Cancer. Addiction to oncogenes--the Achilles heal of cancer. *Science*. 2002;297(5578):63–4.

251. Klier M, Anastasov N, Hermann A, et al. Specific lentiviral shRNA-mediated knockdown of cyclin D1 in mantle cell lymphoma has minimal effects on cell survival and reveals a regulatory circuit with cyclin D2. *Leukemia*. 2008;22(11):2097–105.

252. Asher G, Tsvetkov P, Kahana C, Shaul Y. A mechanism of ubiquitin-independent proteasomal degradation of the tumor suppressors p53 and p73. *Genes Dev.* 2005;19(3):316–21.

253. Asher G, Tsvetkov P, Kahana C, Shaul Y. A mechanism of ubiquitin-independent proteasomal degradation of the tumor suppressors p53 and p73. *Genes Dev.* 2005;19(3):316–321.

254. Hosoda S, Nakamura W, Hayashi K. Properties and reaction mechanism of DT diaphorase from rat liver. *J. Biol. Chem.* 1974;249(20):6416–23.

255. Rodriguez J, Herrero A, Li S, et al. PHD3 Regulates p53 Protein Stability by Hydroxylating Proline 359. *Cell Rep.* 2018;24(5):1316–1329.

8 Publications

8.1 List of publications

In order of occurrence in the thesis:

Lanikova, L., **O. Babosova**, S. Swierczek, L. Wang, D.A. Wheeler, V. Divoky, V. Korinek, and J.T. Prchal. 2016. "Coexistence of Gain-of-Function JAK2 Germ Line Mutations with JAK2V617F in Polycythemia Vera." *Blood* 128 (18).

O. Babosova*, Mambet*, C., J. P. Defour*, E. Leroy, L. Necula, O. Stanca, A. Tatic, N. Berbec, D. Coriu, M. Belickova, B. Kralova, L. Lanikova, J. Vesela, C. Pecquet, P. Saussoy, V. Havelange, C. C. Diaconu, V. Divoky and S. N. Constantinescu. 2018. ''Co-Occurring JAK2 V617F and R1063H Mutations Increase JAK2 Signaling and Neutrophilia in MPN Patients.'' *Blood* – accepted, pre-print version included in the thesis

Babosova, O., K. Kapralova, V. Korinek, V. Divoky, J. T. Prchal and L. Lanikova. 2018. ''Cyclin D1 in Mantle Cell Lymphoma Escapes EGLN2/PHD1 Proline Hydroxylase and Its Hydroxylation Target FOXO3A Regulation.'' - manuscript

Additionally, during the first year of my studies I focused solely on the project entitled '*Cross-talk of the Wnt and YAP/TAZ signaling pathways'*. I thus became involved in other projects, which were focusing on the topic of Wnt signaling in colorectal cancer.

Other work:

Hrckulak, D., L. Janeckova, L. Lanikova, V. Kriz, M. Horazna, **O. Babosova**, M. Vojtechova, K. Galuskova, E. Sloncova, and V. Korinek. 2018. "Wnt Effector TCF4 Is Dispensable for Wnt Signaling in Human Cancer Cells." *Genes* 9 (9): 439.

Kriz, V., M. Krausova, P. Buresova, J. Dobes, D. Hrckulak, **O. Babosova**, J. Svec, and V. Korinek. 2017. "Establishment of a Tagged Variant of Lgr4 Receptor Suitable for Functional and Expression Studies in the Mouse." *Transgenic Research* 26 (5).